UNIVERSITÄTSKLINIKUM HAMBURG-EPPENDORF

Institute of Experimental Cardiovascular Research

Prof. Dr. Viacheslav Nikolaev

Inhibition of acute Angiotensin II-induced cAMP signaling and aldosterone secretion by atrial natriuretic peptide

Dissertation

zur Erlangung des Doktorgrades PhD

an der Medizinischen Fakultät der Universität Hamburg.

vorgelegt von:

Sanika Mohagaonkar

von Nasik, India

Hamburg 2025

Angenommen von der
Medizinischen Fakultät der Universität Hamburg am: 01 December 2025

Veröffentlicht mit Genehmigung der
Medizinischen Fakultät der Universität Hamburg.

Prüfungsausschuss, der/die Vorsitzende: Prof. Dr. Viacheslav Nikolaev

Prüfungsausschuss, zweite/r Gutachter/in: Prof.Dr.med. Ulrich Wenzel

Prüfungsausschuss, dritte/r Gutachter/in: Prof. Dr. Friederike Cuello

Datum der Disputation: 26 January 2026

Table of Contents

List of Figures

List of Tables

List of equations

1 Introduction

1.1 Adrenal glands

1.1.1 Morphology and physiology of Adrenal Glands

The adrenal glands are a pair of triangular/crescentic organs responsible for producing steroid hormones, noradrenaline and adrenaline. They are also known as suprarenal glands due to their presence on top of each kidney. The adrenal glands, surrounded by thick capsule, are composed of outer cortex and inner medullary region each responsible for producing different hormones as seen in Figure 1.1.

Adrenal medulla, present in the center of adrenal gland produces catecholamines; adrenaline and noradrenaline in response to stress or the fight-or-flight response. It is more reddish-brown in color due to ample supply of blood vessels.

Adrenal cortex, fattier and yellowish in appearance, has three distinct zones. The outermost *zona glomerulosa* (ZG), attached to the capsule is response for the synthesis of mineralocorticoid hormone, aldosterone. The middle, *zona fasciculata* (ZF) produces glucocorticoids such as cortisol to regulate metabolism and modulate immune system. The innermost, *zona reticularis* (ZR) produces androgens and is responsible for the development of secondary sexual characteristics (Dutt *et al.*, 2023; Megha *et al.*, 2022).

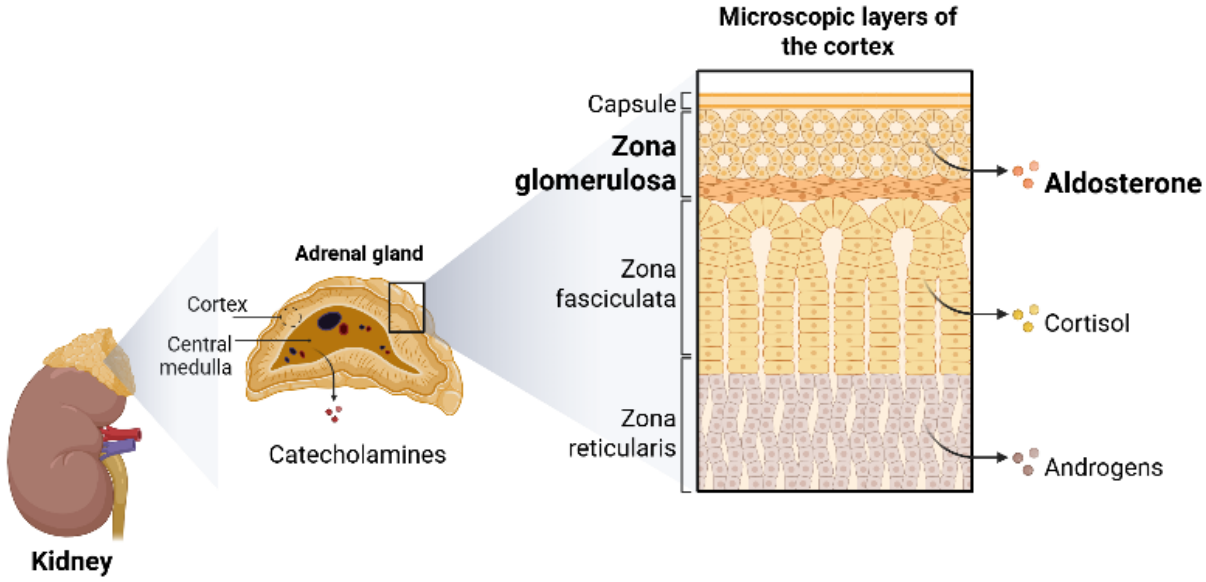

Figure 1.1. Adrenal Gland

Depicted is an adrenal gland located on top of kidneys with visible adrenal cortex and medulla. Three layers of adrenal cortex: *Zona glomerulosa*, *zona fasciculata* and *zona reticularis* (top-bottom) along with their respective hormones. Created using Biorender.

1.2 Zona Glomerulosa cells

ZG are located on the outermost layer of adrenal cortex beneath the capsule and characterized by their cluster or rosette arrangement. They are responsible for producing mineralocorticoid aldosterone, that will be the focus of this study.

1.2.1 Aldosterone

1.2.1.1 Structure and function of aldosterone

Aldosterone, an endogenous steroid hormone ($C_{21}H_{28}O_5$) (Figure 1.2) is responsible for maintaining salt and water balance in the body to regulate the blood pressure and blood volume. The mitochondria of ZG cells express aldosterone synthase (CYP11B2) which is the final enzyme in aldosterone biosynthesis. Cholesterol is a precursor of all steroid hormones and aldosterone. Free cholesterol is transported from outer mitochondrial membrane to inner mitochondrial membrane to produce aldosterone. This side chain cleavage of cholesterol in mitochondria is regulated by Steroidogenic Acute Regulatory (StAR) protein. Phosphorylation

of StAR protein acts as a rate limiting step in aldosterone biosynthesis(Arakane *et al.*, 1997; Funder, 2007; Furman, 2007; Gambaryan *et al.*, 2023).

Aldosterone acts on the mineralocorticoid receptor of epithelial cells in the kidney. Upon activation, this receptor can translocate from the cytosol to the nucleus, thereby facilitating gene transcription response for regulating sodium and water reabsorption. This mechanism is classified under the genomic response, a slower physiological response. For non-genomic effects, aldosterone acts acutely via rapid increase in intracellular calcium (Ca^{2+}) activating protein kinases and secondary messengers (Verhovez *et al.*, 2012).

Furthermore, aldosterone receptors are expressed on a large variety of cells, ranging from cardiomyocytes to immune cells, where they regulate multiple physiological and pathophysiological functions/processes such as cardiac hypertrophy, inflammation and hypertension (van der Heijden *et al.*, 2022; Nakagawa *et al.*, 2014).

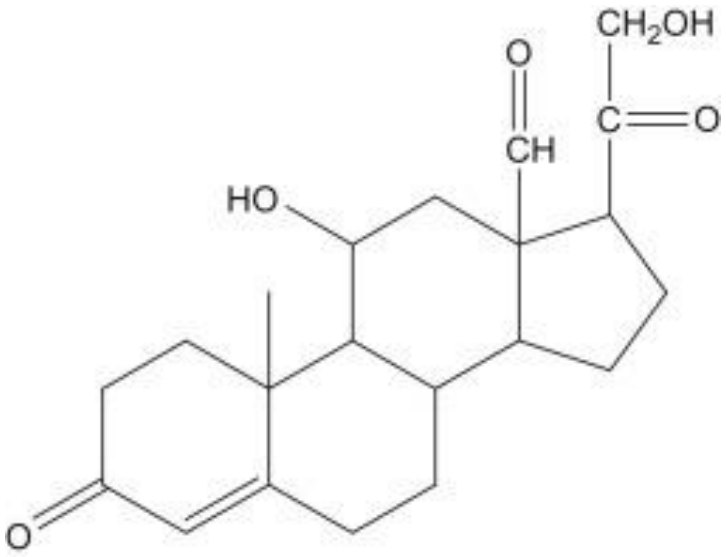

Figure 1.2. Structure of Aldosterone

Structure of Aldosterone. Steroid ring structure with chemical formula ($C_{21}H_{28}O_5$). Adapted from (“Aldosterone - an overview | ScienceDirect Topics”, n.d.)

1.2.1.2 Diseases associated with aldosterone

Dysregulation of aldosterone can cause electrophysiological imbalances leading to cardiovascular and renal diseases such as hypertension, hypokalemia or alkalosis. Increase in aldosterone or hyperaldosteronism can be classified as primary or secondary. Primary aldosteronism (PA) is essentially high blood pressure or hypertension with reduced renin production. Two common subtypes of primary aldosteronism are aldosterone-producing adenomas and bilateral idiopathic hyperaldosteronism. Patients with PA have a high risk of cardiovascular comorbidities due to inevitable hypertension (Stowasser and Gordon, 2004; Young and Bancos, 2023). Secondary aldosteronism occurs because of electrolyte imbalance in the serum. This can be caused by heart failure or liver cirrhosis or even because of diarrhea (Corry and Tuck, 1995; Mories Álvarez, 2008).

Deficiency of cortisol or aldosterone can cause severe damage to the adrenal glands and cause primary adrenal insufficiency or Addison's disease. Reduced production of these hormones can also result from autoimmune adrenalitis or destroyed adrenal cortexes causing life threatening adrenal shock or hypotension (MICHELS and MICHELS, 2014; Nieman and Chanco Turner, 2006).

1.3 Renin-angiotensin-aldosterone system

Aldosterone is produced as a part of renin-angiotensin-aldosterone system (RAAS) though a cascade of proteolytic enzyme cleavages. The RAAS is a complex series of hormonal system. Circulating angiotensinogen, produced by the liver, is cleaved by renin to produce angiotensin I (AngI). Renin is released from juxtaglomerular cells of kidneys responsible for sodium reabsorption. AngI is then converted to angiotensin II (AngII) by angiotensin converting enzyme (ACE) that is secreted by the lungs. Angiotensinogen is the biological precursor for all angiotensin peptides circulating and active in the body as seen briefly Figure 1.3 (Carey and Padia, 2018; Gambaryan *et al.*, 2023; Lu *et al.*, 2016).

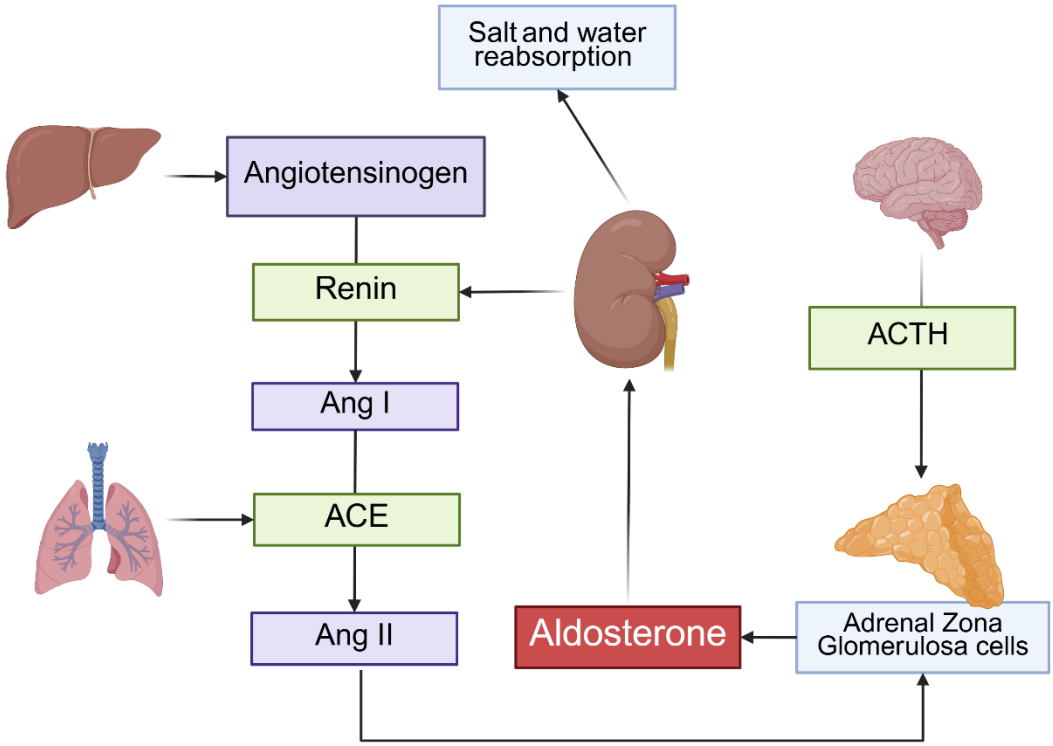

Figure 1.3. Overview of Renin-angiotensin-aldosterone system (RAAS)

Briefly, Adrenocorticotropin hormone (ACTH) secreted from the brain stimulates *zona glomerulosa* (ZG) cells of adrenal gland to produce aldosterone. Renin from kidney converts angiotensinogen to angiotensin II (AngII) to stimulate the production of aldosterone that gives feedback to kidneys for salt and water reabsorption. Created using Biorender. Modified from (Gambaryan *et al.*, 2023).

1.4 Heart

1.4.1 Cardiovascular diseases

Cardiovascular diseases are one of the leading causes of mortality around the world. In section 1.2.1.2, I discussed diseases related to aldosterone dysregulation, but aldosterone can also affect other organs drastically. Hyperaldosteronism causes cardiac and vascular remodeling, further adding to the risk of this disease leading to pulmonary or arterial hypertension, cardiac inflammation, heart failure and even associated with diabetes mellitus and chronic kidney disease (Buffolo *et al.*, 2022; Parksook and Williams, 2023). So far, mineralocorticoid receptor antagonists are the recommended treatment, but the exact molecular pathways underlying

aldosterone induced cardiac disease and remodeling are not completely clear (Alfarano *et al.*, 2025).

1.4.2 Atrial Natriuretic peptide

Cardiac atria produce and secrete atrial natriuretic peptides (ANP) in response to hypervolemia and hypertension as a cardioprotective mechanism. Studies have reported that ANP inhibits sodium and water reabsorption by increasing glomerular filtration rate. This leads to vasodilation, regulates RAAS and natriuresis (Hedner *et al.*, 1987; Hodgson-Zingman *et al.*, 2008).

1.5 ANP/GC-A: Crosstalk between heart and adrenal glands

ANP endogenously inhibits aldosterone secretion by increasing intracellular secondary messenger 3',5' cyclic guanosine monophosphate (cGMP). It acts via guanylyl cyclase A receptor (GC-A) present on ZG cell membrane (Gambaryan *et al.*, 2005; Ganguly, 1992).

GC-A mediates endocrine effects in response to cardiac volume or pressure overload and moderates the sympathetic salt, water and appetite balance, regulates RAAS, protects lung and endothelial barrier, increases lipolysis and other metabolic actions as summarized in Figure 1.4 (Kuhn, 2016).

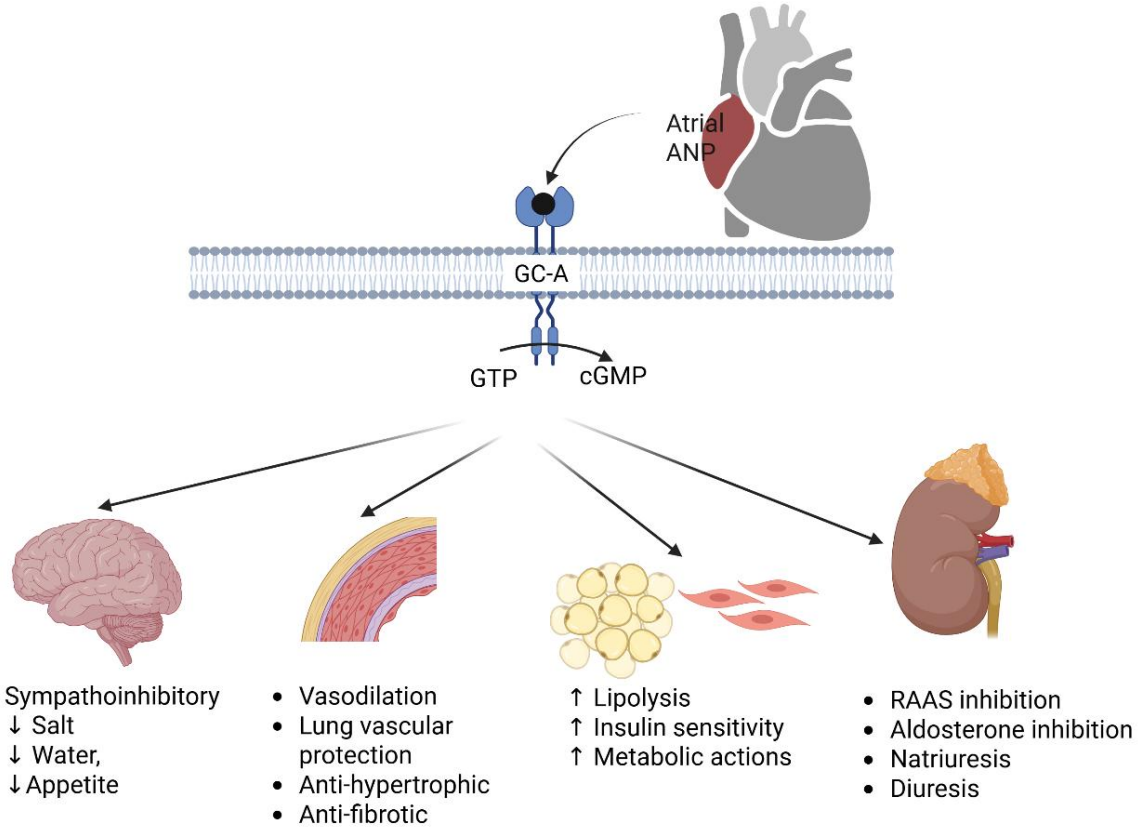

Figure 1.4. GC-A mediated cardiovascular and metabolic actions by ANP

GC-A mediated cardiovascular and metabolic actions by ANP in response to cardiac volume or pressure overload. ANP acts via GC-A/cGMP pathway acts on the lungs, adrenals, kidneys to increase insulin sensitivity, reduces salt and water intake, vasodilation and has anti-hypertrophic and anti-fibrotic effects. Created using Biorender. Adapted from (Kuhn, 2016).

1.6 Cyclic nucleotides and phosphodiesterases in ZG cells

1.6.1 Aldosterone regulation by cyclic nucleotide signaling pathway

cAMP and cGMP are universal secondary messengers that drive the intracellular signaling pathways.

In ZG cells, aldosterone synthesis is stimulated by adrenocorticotropic hormone (ACTH), AngII, Forskolin (Fsk) and potassium (K^+) and is inhibited by ANP via the GC-A/cGMP pathway. ACTH, secreted from the pituitary gland, directly acts on the melanocortin-2 receptor

(MC_2R), a G-protein coupled receptor (GPCR) on ZG cell membrane. MC_2R is $G\alpha_s$-coupled and facilitates the 3',5'-cyclic adenosine monophosphate (cAMP) / protein kinase-A (PKA) pathway to control the levels of aldosterone. cAMP producing enzyme, adenylyl cyclase (AC) are modulated by GPCRs that facilitate the conversion of adenosine triphosphate (ATP) to cAMP (El Ghorayeb *et al.*, 2016; KAPLAN and BARTER, 1962). Forskolin (Fsk), a direct adenylyl cyclase (AC) activator, induces cAMP increase in ZG cells followed by aldosterone production (Nikolaev *et al.*, 2005).

AngII, acting via its G-protein coupled angiotensin type 1 receptor (AT_1R) is an octapeptide responsible for aldosterone production. AT_1R is $G_{q/11}$ coupled and when stimulated by AngII, activates phospholipase C (PLC) leading to increase intracellular Ca^{2+} in the cell. This leads to upregulation of StAR protein to further facilitate aldosterone biosynthesis. Elevated levels of K^+ or hyperkalemia stimulate the production of aldosterone from the adrenal cortex along with AngII via the elevation of intracellular Ca^{2+} levels (Lymperopoulos *et al.*, 2024; Mulrow, 1999).

Downstream of cAMP are three effectors namely PKA, exchange protein activated by cAMP (EPAC) and cyclic nucleotide gated channels. PKA, a symmetrical tetrameric complex consisting of two regulatory subunits and two catalytic subunits, is activated when cAMP binds to its regulatory subunits. PKA phosphorylates multiple enzymes to regulate aldosterone levels in ZG cells (Sassone-Corsi, 2012; Taylor *et al.*, 1992). Activation of PKA via cAMP is an important step in aldosterone biosynthesis which further phosphorylates cholesterol ester hydrolase (CEH), StAR and cAMP Response Element-Binding protein (CREB). Apart from PKA, EPAC also relays downstream actions of cAMP. Both PKA and EPAC have different mechanisms of action to facilitate aldosterone production (Lewis *et al.*, 2016).

1.6.2 Role of phosphodiesterase in aldosterone regulation

Phosphodiesterase (PDEs) hydrolyze the 3' phosphate bonds of cyclic nucleotides in the presence of water (H_2O) and magnesium (Mg^{2+}) producing hydrogen ion (H^+). PDEs, by rapidly degrading cAMP and cGMP to respective mononucleotides AMP and GMP, control their intracellular levels and inactivate them. There are eleven PDE families with more than 20 genes encoding around 50 distinct PDE isoforms. PDE superfamily is classified into 11 families based on the C-terminal catalytic domain. Every family may contain several subfamilies and

isoforms which differ in their N-terminal domains responsible for subcellular localization. This allows PDEs to act at diverse cellular and subcellular locations. In this regard, they are considered as having specific therapeutic potential which can be leveraged for precise disease treatments without adverse effects (Baillie *et al.*, 2019; Kelly *et al.*, 2025; Lugnier, 2006).

In ZG cells, cGMP activated PDE2A subfamily has been shown to be engaged by ANP treatment to facilitate the hydrolysis of cAMP to inhibit aldosterone production. PDE2A is a dual specific PDE. The N-terminus of PDE2A has two regulatory domains called GAF-A and GAF-B. GAF-A is responsible for PDE2 dimerization and GAF-B allosterically binds to cGMP (Kelly *et al.*, 2025; MacFarland *et al.*, 1991).

Studies have reported that ANP/GC-A/cGMP pathway activates PDE2A in ZG cells to degrade cAMP stimulated by Fsk and ACTH, thereby reducing aldosterone production. The rate of cAMP degradation is faster than the rate of cAMP synthesis making this rapid PDE2 response control the downstream actions of cAMP (Nikolaev *et al.*, 2005) . A schematic representation of this ANP/GC-A/cGMP mediated cAMP degradation via PDE2A is shown in Figure 1.5.

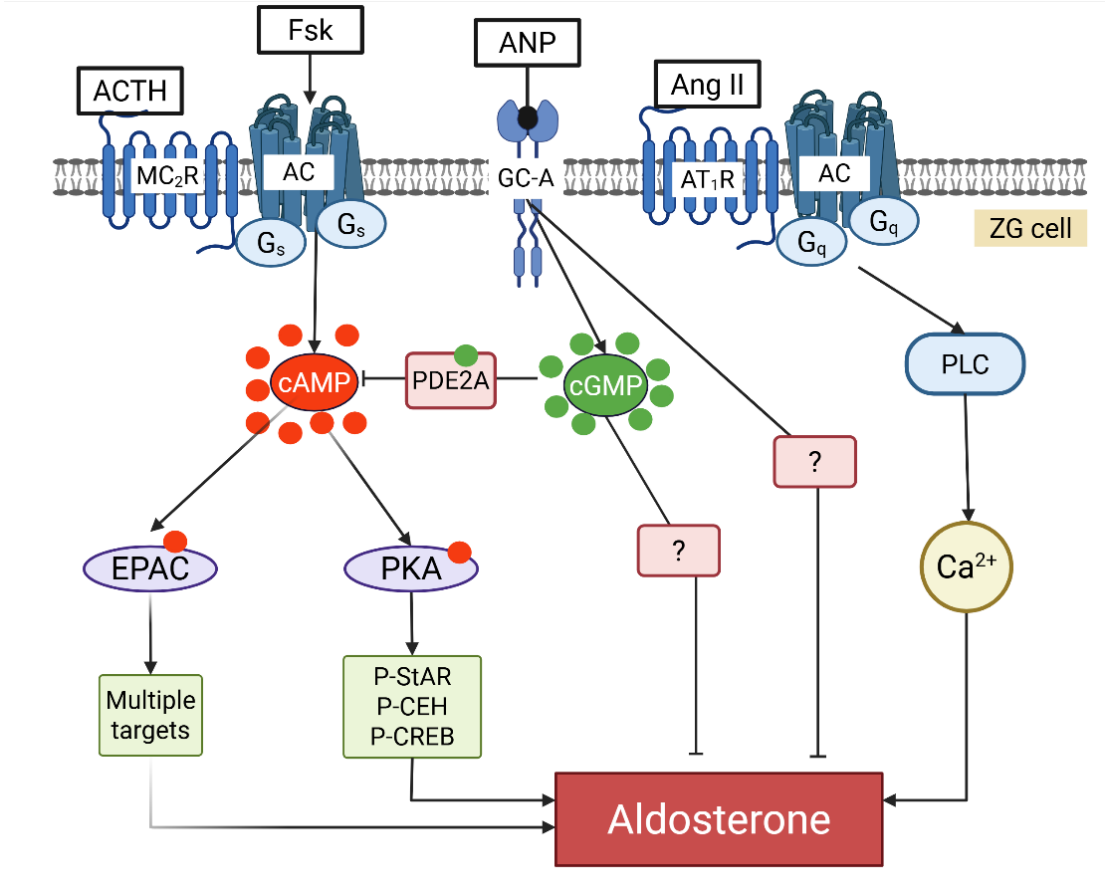

Figure 1.5. Regulation of aldosterone by cyclic nucleotides and phosphodiesterase

ACTH via its MC_2R and Fsk directly via AC by cAMP/PKA or EPAC pathway to stimulate aldosterone production. AngII via its AT_1 receptor stimulates aldosterone production via G_q coupled AC by increasing PLC and intracellular Ca^{2+}. ANP acting on GC-A via cGMP activate PDE2A to hydrolyze cAMP and inhibit aldosterone production. It is not yet known how ANP inhibits aldosterone produced by AngII. Created using Biorender. Adapted from (Gambaryan *et al.*, 2023; Nikolaev *et al.*, 2005).

1.6.3 Role of cGMP-dependent protein kinases and regulatory proteins

The role of ANP in AngII stimulated adrenal steroidogenesis in RAAS and acute aldosterone inhibition via PDE2A is well documented, but the detailed molecular mechanism by which it occurs is unexplored. One hypothesis as to why this happens could be due to the activation of cGMP-dependent protein kinases (PKG). PKG phosphorylates serine and threonine, and modifications of these proteins regulate calcium homeostasis (Francis *et al.*, 2010; Gambaryan *et al.*, 1998). It is known from literature that PKG II is expressed in the adrenal cortex and more

specifically in the ZG cells. Activation of PKG II leads to phosphorylation of proteins such as StAR for aldosterone production (Gambaryan *et al.*, 2003; MacFarland *et al.*, 1991).

PKG can also phosphorylate regulators of G-protein signaling (RGS) proteins. RGS proteins inactivate the G-proteins by binding to the activated alpha subunit of G-proteins (G_α) including the ones activated by AngII receptors (Lymperopoulos *et al.*, 2023). Ca^{2+} dependent aldosterone secretion can not only be regulated by AT_1R, but also by RGS proteins mainly RGS2 and RGS4 (Currie, 2010). A study on cardiomyocytes reported that the selective interaction of PKG and RGS2 modulates the AngII/AT_1R signaling driven by ANP/GC-a/cGMP pathway (Klaiber *et al.*, 2010). Another study reported that upregulation of RGS2 proteins acts as negative feedback for AngII stimulated aldosterone production (Romero *et al.*, 2006). RGS4, by regulating Ca^{2+}/calmodulin (CaMK) and protein kinase C also moderate AngII/AT_1R signaling pathway for aldosterone production in H295R cells (Ariyeloye *et al.*, 2024). Even though RGS2 and RGS4 proteins have similar inhibitory effect on AngII induced aldosterone production, they are not sole inhibitors of this signaling pathway.

1.6.4 Role of calcium in aldosterone secretion

Extracellular stimuli such as ACTH, AngII or K^+ lead to the production of aldosterone from adrenal ZG cells. These then converge into two major intracellular signaling pathways. First one being increase in cAMP production and second being mobilization of intracellular Ca^{2+} as shown in Figure 1.5.

When AngII/AT_1R pathway is activated, active PLC cleaves phosphatidylinositol-4,5-bisphosphate (PIP_2) to inositol triphosphate (IP_3) and diacylglycerol (DAG). This leads to depolarization of the voltage-gated calcium channels (VGCC) present on the ZG membrane. This leads to Ca^{2+} influx or transients triggered by IP_3 which ultimately leads to aldosterone production. This is because ZG cells at rest have negative resting membrane potential and activation of AT_1R by AngII led to this calcium oscillation (Dinh *et al.*, 2024; Guagliardo *et al.*, 2020). VGCCs have been reported to play an important role in regulation of aldosterone production (Barrett *et al.*, 2016).

It has been established that Ca^{2+} activates some isoforms for adenylyl cyclase (AC) via calmodulin either directly or indirectly. AC isoforms AC1, AC3 and AC8 are Ca^{2+} activated which provides a mechanism for a positive crosstalk between Ca^{2+} and cAMP levels (Cooper *et al.*, 1995; Eckel-Mahan and Storm, 2007). It has also been reported that capacitive Ca^{2+} influx activated by AngII have an effect on bovine adrenal glands by the action of Ca^{2+} on Ca^{2+} activated AC type 3 (Burnay *et al.*, 1998). This resulted in an augmented ACTH-induced aldosterone synthesis in the presence of AngII. Ca^{2+} also plays an important role in aldosterone production by regulating transcription of aldosterone synthase gene, *Cyp11b2* (Yang *et al.*, 2020). Aldosterone production is regulated by several isoforms of Ca^{2+}/calmodulin complexes and their dependent protein kinase (CaMKs) that are expressed in ZG cells (Gambaryan *et al.*, 2006).

1.7 Use of CRISPR/Cas9 system to generate knockouts in eukaryotic cells

Clustered regularly interspaces short palindromic repeats (CRISPR), a tool used to cut and modify DNA is widely used in scientific research. CRISPR was identified from the prokaryotic system as part of an adaptive immune response in providing protection from viruses. CRISPR system refers to a recurrent motif of 24-50 nucleotides regularly spaces naturally occurring in many prokaryotic genomes. CRISPR system refers to a recurrent motif of 24-40 nucleotides regularly spaces naturally occurring in many prokaryotic genomes. They also found CRISPR associated protein (Cas9) enzyme in the vicinity of CRISPR genes having properties of nucleases and helicases and thus commonly known as “molecular scissors”. Cas9 is an endonuclease that can cleave DNA at target sites guided by specific RNAs (Gostimskaya, 2022; Lander, 2016; Mojica *et al.*, 1995) .

In recent years, CRISPR/Cas9 gene editing techniques have been applied to eukaryotic cells. Briefly, a singe guide RNA (sgRNA) ~20-22 base pairs oligonucleotide, targeting specific DNA sequence guides the Cas9 enzyme to a protospacer-adjacent motif (PAM) sequence. Guide RNAs serve as a template for the specific site where double stranded breaks are required. The PAM sequence is present in near the target DNA sequence that ensures correct sequence is cut by Cas9. Once the double strand breaks are made by Cas9, the DNA is repaired by cells natural repair mechanism.

Commonly it is done by two methods:

A. Non-homologous end joining method
B. Homology directed repair

The non-homologous end joining method (NHEJ), is an error-prone mechanism leading to rapid ligation of the two strand breaks introduced in the DNA. It is commonly used to knockout (KO) a gene *in vitro.* This method leads to small insertions or deletions (indels) that interrupt the reading frame. NHEJ method is highly efficient and maintains genome stability. For this project, NHEJ method of CRISPR/Cas9 is used to generate *in vitro* PDE2A KO in primary bovine ZG cells.

In homology directed repair (HDR), donor strand of DNA is introduced after creating double-strand breaks by Cas9. This allows for knocking in gene of interest. HDR occurs during the active S and G2 phase of cell cycle where single-stranded DNA oligonucleotide serves as a template either on the sense or antisense strand (Gostimskaya, 2022; Ran *et al.*, 2013). A schematic representation of CRISPR/Cas9 gene editing system is depicted in Figure 1.6

Recently, our group has established for the first time functional knockouts of PDE2A and PDE3A isoforms in neonatal and adult rat cardiomyocytes but adenoviral gene transfer of Cas9 and specific gRNAs. This is an attractive and efficient strategy which can be used to knockout various genes directly in primary cells cultures, bypassing the generation of transgenic organisms or stable cell lines such as those of pluripotent cells, as commonly established in the field (Skryabin *et al.*, 2023).

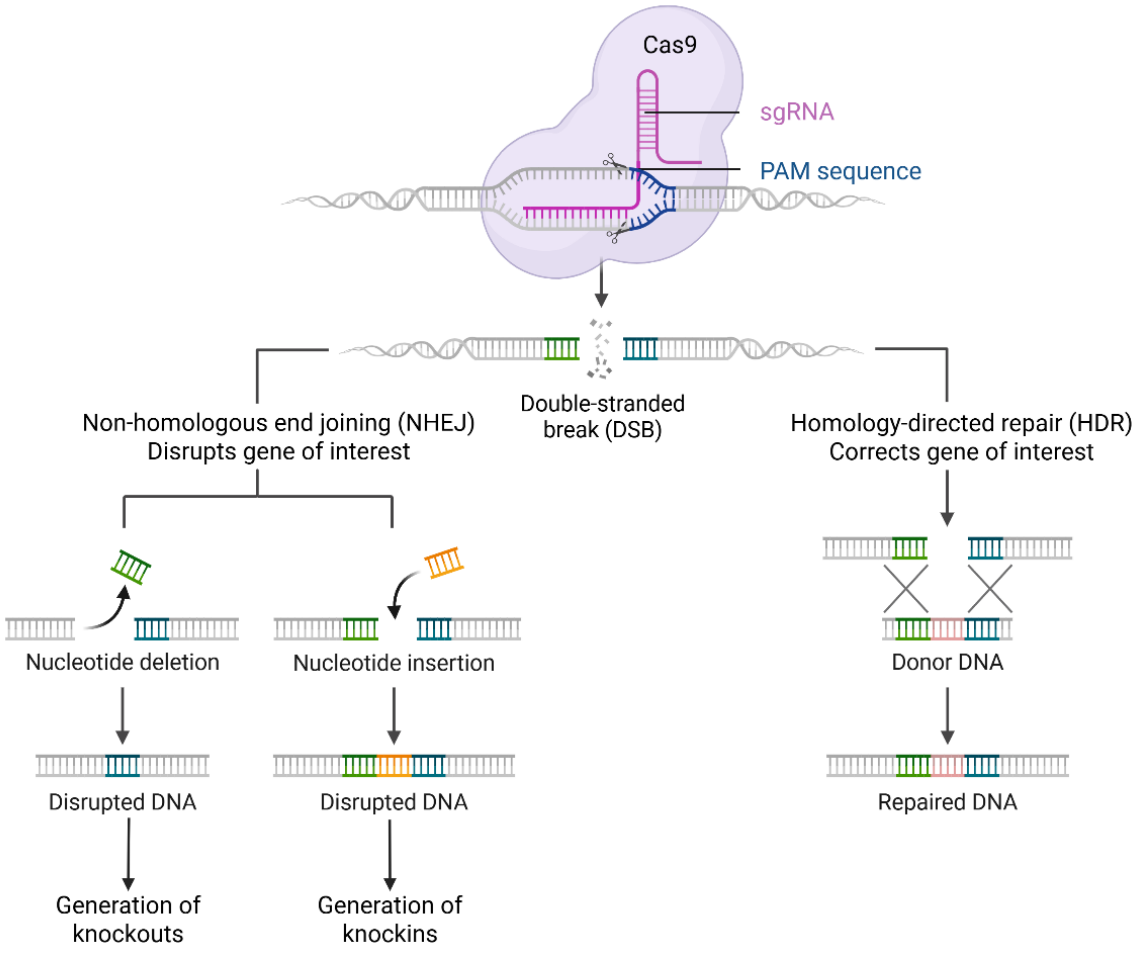

Figure 1.6. Schematic representation of CRISPR/Cas9 genome editing

CRISPR/Cas9 is a gene editing technique to insert, delete or correct gene of interest in DNA. Cas9 is an enzyme that introduces double strand breaks (DSB) in the DNA at the target site using guide RNA (sgRNA). The DNA is then repaired using NHEJ or HDR mechanisms to ligate the DSB. PAM sequence is used as a guide for the Cas9 to bind. Created using Biorender. Adapted from ("Addgene: CRISPR Guide", n.d.).

1.8 Tools for live cell imaging: Förster resonance energy transfer

Intracellular effects of cyclic nucleotides (cAMP and cGMP) are often compartmentalized to discrete subcellular microdomains. The same cell can have different responses triggered by cyclic nucleotides depending on the extracellular stimuli and stimulated receptor. Each microdomain is governed by specific GPCR, protein kinases and PDEs. To analyze these

second messenger dynamics, live cell imaging techniques are used to monitor real time changes with high spatial and temporal resolution. Although various radioactive (Radioimmunoassay) and non-radioactive (ELISA, immunoblot) methods exist to measure *in vitro* cyclic nucleotide content or activity in cells, they have some drawbacks such as requiring large numbers of cells and tissues, disruption of subcellular microdomains etc. It is therefore necessary to use live cell imaging techniques for visualization of cyclic nucleotides real time (Sprenger and Nikolaev, 2013).

Förster resonance energy transfer (FRET) is a non-radioactive energy transfer phenomenon. Biosensors specific to cyclic nucleotides are generated with a donor and acceptor fluorophore.

The FRET mechanism was discovered in 1948 by Theodor Förster and is based on the principle of resonance energy transfer as shown in the Jablonski diagram (Figure 1.7A). When the donor and acceptor fluorophores are in close proximity (~5-10 nm) along with favorable spatial orientation, and upon excitation of the donor at a certain wavelength, energy is transferred from donor to the acceptor without its direct excitation due to dipole-dipole interaction. The emission spectrum of the donor must also overlap with the acceptor excitation spectrum by ~30% for FRET to occur as shown in Figure 1.7B (Förster, 1948; Förster and Forster, 1960). In attoseconds (as) the donor photon is excited to its lowest subshell from ground state (S_0) to excited state (S_1).

In the vicinity of suitable acceptor, upon relaxation (within picoseconds (ps)) of the donor photon, coupling occurs, and energy is transferred to the acceptor molecule. This phenomenon is known as FRET (total time: nanoseconds (ns)). This process leads to a decrease in donor and increase in acceptor fluorescence intensity (Szabó *et al.*, 2022).

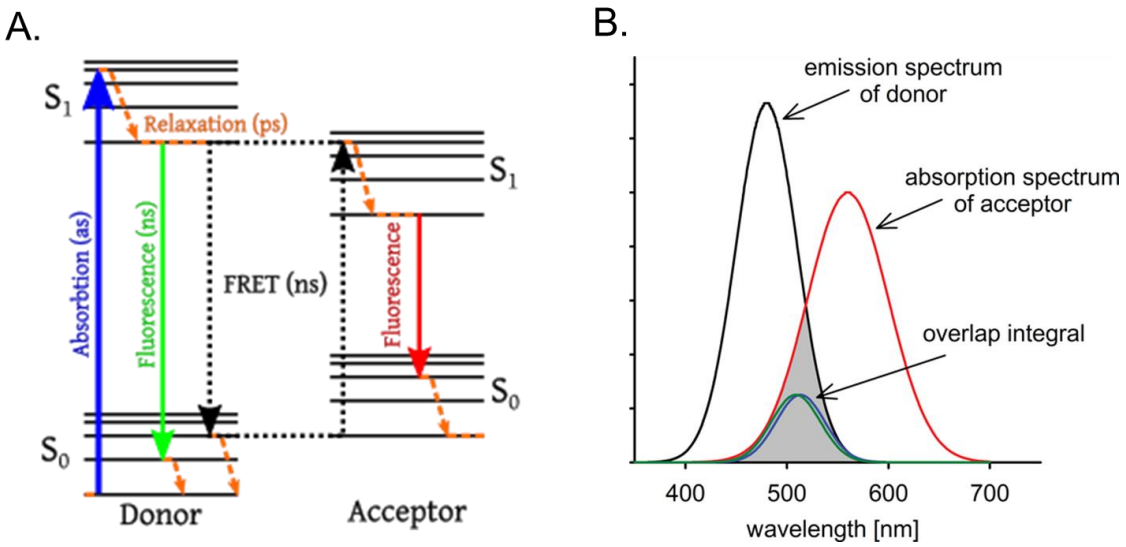

Figure 1.7. Principles of Förster resonance energy transfer (FRET)

(A) The Jablonski diagram shows the principle of FRET. Energy transfer between donor and acceptor fluorophores where S_0 is the ground state, S_1 is the excited state. (ns-nanoseconds, ps-picoseconds, as-attoseconds) (B) Spectral overlap of emission and donor spectrum essential for energy transfer. Adapted from (Jabłoństski, 1933; Szabó *et al.*, 2022).

1.9 Aim of thesis

It is well established that ANP inhibits aldosterone production stimulated by AngII in ZG cells. However, the exact molecular pathway is unknown.

The aim of this thesis was to elucidate molecular mechanisms by which ANP/cGMP pathway can acutely moderate AngII stimulated aldosterone production. This was done using various molecular biology and live cell imagining techniques.

Primary bovine ZG cells were used to answer the following questions:

a. Is the acute ANP inhibition of AngII stimulated aldosterone cGMP-dependent?
b. Does calcium play a role in ANP inhibition of AngII stimulated aldosterone?
c. Does PDE2A play a role in aldosterone inhibition by ANP stimulated by AngII?
d. Is there a role of AngII stimulated calcium in activating cAMP/PKA pathway? And does this affect aldosterone production?

2 Materials and Methods

2.1 Materials

2.1.1 Chemicals

Table 2.1 List of all the chemicals used

Chemical	Manufacturer	Catalogue No.
2-(4-(2-Hydroxyethly) piperazin-1-yl) ethanesulfonic acid (HEPES)	Sigma Aldrich	H4034
3-Isobutyl-1-Methylxanthine (IBMX)	AppliChem	A0695-0001
4',6-diamidino-2-phenylindole (DAPI)	Sigma Aldrich	D9542
Acrylamide (Rotiphorese gel)	Carl Roth	3029.1
Ammonium persulfate (APS)	Sigma Aldrich	A3678
Ampuwa water	Fresenius Kabi	40676.00.00
Angiotensin II (AngII), Human	Bachem	4006473
Atrial natriuretic peptide (ANP), human	Calbiochem	05-23-0300
BAY 60-7550	Santa Cruz	Sc396772
Bromophenol blue salt	Carl Roth	A512.1
Calbryte 520 AM	AAT Bioquest	20650
Calcium Chloride ($CaCl_2$)	Sigma Aldrich	C8106
Collagenase NB 4G	Nordmark	S1746503
Dulbecco's Modified Eagle's Medium (DMEM)	Sigma Aldrich	D6546

Dulbecco's Phosphate buffered saline (PBS)	Sigma Aldrich (Gibco)	D8537
Ethanol >99%	Carl Roth	9065.2
Ethanol, 70%	Th. Geyer	2202
Fetal Bovine Serum (FBS)	Sigma Aldrich	F4135
Forskolin	Cayman Chemicals	11018
Glycerol	Millipore	356350
Hydrochloric acid (HCl), 37%	Carl Roth	9277.1
Immersion liquid type F	Leica	11515859
L-Glutamine solution	Sigma Aldrich	G7513
Magnesium chloride ($MgCl_2$)	Signa Aldrich	M2670
Methanol, 99%	ThermoFischer Scientific	L13255.0F
Milk powder	Carl Roth	T145.1
Myristoylated protein kinase inhibitor (myrPKI 14-22 amide)	Tocris biosciences	2546
N-(cis-2-phenyl-cyclopentyl) azacyclotridecan-2-imine-hydrochloride (MDL-12,330A)	Merck	M182
N, N, N', N'-Tetramethylethylenediamine (TEMED)	Sigma Aldrich	T9281
Penicillin/streptomycin (10000 U/mL, 10000 µg/mL)	Sigma Aldrich	P0781
Ponceau S	Sigma Aldrich	P3504

Potassium chloride (KCl)	Sigma Aldrich	P9541
RNase-Free DNase	Qiagen	79254
Sodium chloride (NaCl)	Carl Roth	9265.1
Sodium dodecyl sulfate (SDS)	Sigma Aldrich	05030
Sodium dodecyl sulfate (SDS) solution, 20%	AppliChem	A0675.0500
Sodium hydroxide (NaOH)	Carl Roth	6771.1
Tris-(hydroxymethly)-aminomethane (TRIS)	Carl Roth	4855.2
Triton X-100 solution	AppliChem	A1287,0100
Tween 20	Sigma Aldrich	P1379
β-Mercaptoethanol	Sigma Aldrich	M6250

2.1.2 Consumables and kits

Table 2.2 List of all the consumables and kits used

Consumables	**Manufacturer**	**Catalogue No.**
12-well plate, Standard flat base (Cell culture)	Sarstedt	83.3921
35 mm Dish, 14 mm Glass diameter, No. 1.5 coverslip	MatTek	P35G-1.5-14-C
4% Formaldehyde	Biognost	F4
Aldosterone ELISA kit	DRG	EIA-5298
Amersham Protran 0.45 µM nitrocellulose membrane	Cytiva	10600002

Aspiration pipette 2 mL	Sarstedt	86.1252.011
Combi-tips advanced, 10 mL	Eppendorf	0030089464
Falcon tube, 15 mL	Sarstedt	62.554.016
Falcon tube, 50 mL	Sarstedt	62.559.004
Filter paper Type 598	Hahnemühle	5984657
Gloves XS (Latex free, powder free)	Braun	7144543
Kimtech wipes	Kimberly Clark	P502.1
Microcentrifuge tube 1.5 mL	Sarstedt	72.690.001
Microcentrifuge tube 2 mL	Sarstedt	72.691
Pipette tips, 10 µL	Sarstedt	70.1130.600
Pipette tips, 1000 µL	Sarstedt	70.3050.100
Pipette tips, 200 µL	Sarstedt	70.760.502
PluriStrainer cell strainer, PET mesh, Sterile 70 µm	pluriSelect	43-50070-51
Protein ladder (10-250 kDa)	ThermoFischer Scientific	26619
Safe Seal reaction tubes 2 mL	Sarstedt	72.695.500
Safe Seal reaction tubes, 1.5 mL	Sarstedt	72.706.400
Serological pipette 10 mL	Sarstedt	86.1254.001
Serological pipette 25 mL	Sarstedt	86.1685.001
Serological pipette 2mL	Sarstedt	86.1252.001

Serological pipette 50 mL	Sarstedt	86.1256.001
Serological pipette 5mL	Sarstedt	86.1253.001
Soft-man acute	Braun	19114
Sterile container with screw cap, 100 mL, 57 x 75 mm	Sarstedt	75.562.105
Sterile disposable Scalpel 22	Braun	BA822SU
Sterile Tissce culture dish, TC-Schale, 150 cell+	Sarstedt	83.3903.300
Sterile Tissue culture dish, TC-Schale, 100 cell+	Sarstedt	83.3902.300
Steritop 0.22 µM filter	Merck	SCGPT10RE
SuperSignal West Pico PLUS	ThermoFischer Scientific	34580
X-ray films (Super Rx)	Fujifilm	741019230

2.1.3 Antibodies

In this thesis, primary and secondary antibodies were used for western blot analysis and immunofluorescence of isolated primary bovine ZG cells.

2.1.3.1 Primary antibodies for western blot analysis

All primary antibodies were incubated at +4°C on shaker overnight in non-fat milk.

Table 2.3 List of primary antibodies for western blot analysis

Primary antibody	Dilution	Source	Manufacturer	Catalogue No.
Anti- Phospho-(Ser/Thr) PKA substrate	1:1000 in 0.1% milk	Rabbit	Cell signaling technology	9621
Anti-Glyceraldehyde-3-phosphate Dehydrogenase (GAPDH)	1:1000 in 5% milk	Rabbit	Cell signaling technology	3683S (14C10)
Anti-PDE2A	1:750 in 5% milk	Rabbit	Fabgennix	101AP
Anti-PDE4B	1:1000 in 5% milk	Rabbit	Abcam	ERP11830

2.1.3.2 Primary antibodies for immunofluorescence analysis

All primary antibodies for immunofluorescence were incubated at +4°C overnight and diluted in blocking buffer.

Table 2.4 List of primary antibodies for immunofluorescence analysis

Primary antibody	Dilution	Source	Manufacturer	Catalogue No.
Aldosterone synthase (CYP11B2)	1:1000	Rabbit	Gift from Dr. Celso Gomez-Sanchez	(Gomez-Sanchez *et al.*, 2013)
Disabled-2 (*Dab2*)	1:1000	Mouse	BD biosciences	610464

4',6'-Diamidino-2-phenylindole (DAPI)	1:20	Sigma-Aldrich	D9542

2.1.3.3 Secondary antibodies for western blot analysis

All secondary antibodies for western blot analysis were horseradish peroxidase (HRP) conjugated.1:5000 dilution in 5% non-fat milk was used to prepare the secondary antibodies. The incubation time was 1 h at room temperature (RT)

Table 2.5. List of secondary antibodies for western blot analysis

Primary antibody	**Source**	**Manufacturer**	**Catalogue No.**
Anti-mouse	Goat	Bio-Rad	170-5047
Anti-rabbit	Goat	Bio-Rad	170-5046

2.1.3.4 Secondary antibodies for immunofluorescence analysis

Secondary antibodies for immunofluorescence were prepared in blocking buffer in 1:500 dilution. Incubation time was 1 h at RT.

Table 2.6. List of secondary antibodies used for immunofluorescence analysis

Primary antibody	**Source**	**Manufacturer**	**Catalogue No.**
Anti-Mouse IgG (H+L) Cross-absorbed Alexa Fluor 488	Goat	ThermoFischer scientific	A-11001
Anti-Rabbit IgG (H+L) Cross-absorbed Alexa Fluor 633	Goat	ThermoFischer scientific	A-21070

2.1.4 General Instruments and devices

Table 2.7 List of general devices and instruments

Instrument/Device	**Manufacturer**
Accujet pro pipette controller	Brand
Balance	Precisa
Biosafety cabinet (BSL-3)	Ibs technomara
Centrifuge 5810R	Eppendorf
CO_2 incubator MCO-5AC	Sanyo
FlexStation3 Multi-mode microplate reader	Modular devices
Freezer	Leibherr
Fridge	Liebherr
Magnetic stirrer	IKA
Microcentrifuge	VWR
Microwave	Panasonic
pH meter	inolab
Power Pac basic power supply	Bio-Rad
Scanner LiDE 220	Cannon
Thermomixer comfort	Eppendorf
Vortex genie 2	Scientific industries

Water bath	GFL
Western blot equipment (comb, glass plates, transfer and running chambers)	Bio-Rad
X-ray Flim processor SRX-101A	Konica Minolta

2.1.5 Microscope devices

Table 2.8 List of all microscope devices

Microscope device	**Manufacturer**
CMOS camera (OptiMOS)	QImaging
Digital to analog input-output board	Arduino
DMI 3000B inverted fluorescent microscope	Leica
DV2 DualView containing CUBE 05-EM (505 dcxr, D480/30m, D535/40m) emission filter	Photometrics
LSM800 confocal microscope	Zeiss
Oil-immersion 63x/1.40 objective	Leica
pE-100 Fluorescent light source LED, 440 nm	CoolLED

2.1.6 Software

Table 2.9 List of software's used

Software	**Manufacturer**
GraphPad Prism 10.6.1	GraphPad software inc
ImageJ-win64	National Institutes of Health
Mendeley	Mendeley referencing software
Micro-Manager 1.4.22	Open source microscopy software
Microsoft office package	Microsoft office 365
ICY software	Open source, Bioimage analysis
MultiFRET software (Java plugin)	(Ramuz *et al.*, 2019)
SoftMax Pro software	Molecular devices

2.2 Methods

Figure 2.1 represents the workflow summary post isolation and culture of primary bovine ZG cells. Detailed methods mentioned in further sections.

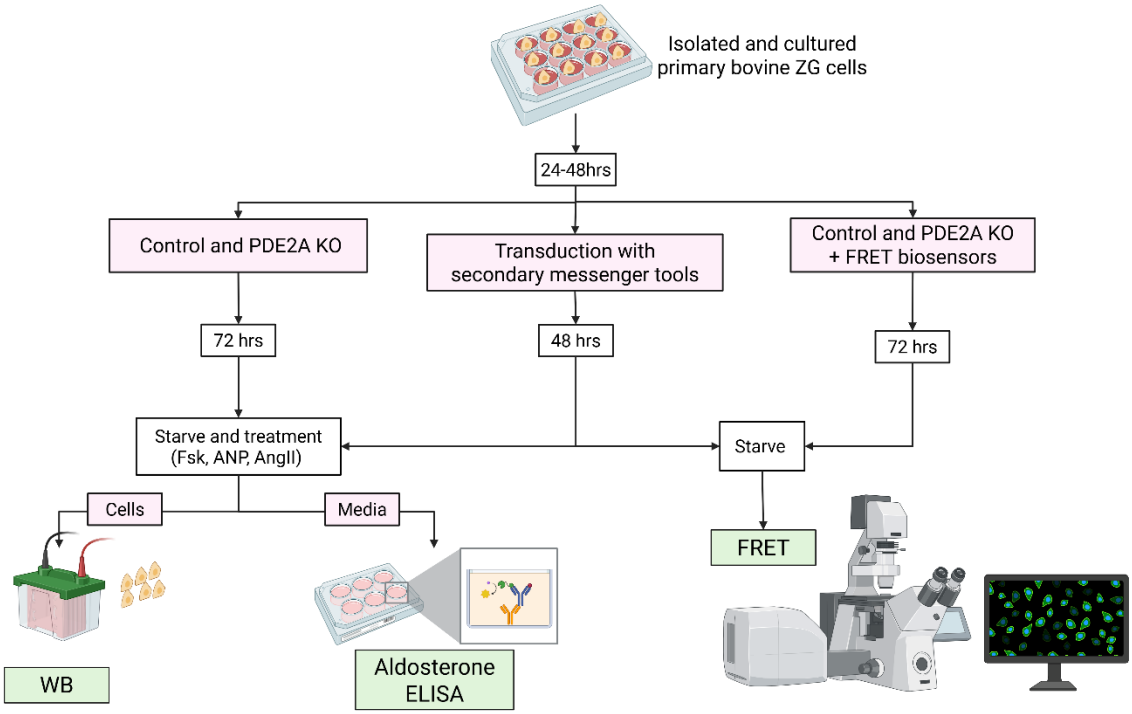

Figure 2.1 Workflow summary

Workflow summary of isolation and culture of primary bovine ZG cells. After 24-48 h of cell recovery, experiments like western blot, aldosterone ELISA and FRET were performed along with different treatment conditions. Created using Biorender.

2.2.1 Isolation and culture of bovine ZG cells

Male and female bovine adrenal glands were obtained from local a slaughterhouse/abattoir (Seestermühe, Germany) and transported in cold PBS in containers. Excess fat was then removed from adrenal glands. Using 22-blade, the adrenal glands were cut in half. Medullary tissue was carefully removed by mechanical disintegration. ZG cells attached to the capsule were collected in 50 mL flacon with 15 mL serum free media. 300 µL HEPES, 20 µL RNase free DNase-I and 30 mg collagenase NB 4G were added and incubated in water bath at 37°C

for 20 mins with intermittent mixing. The media was then filtered using a 70 µM filter and to obtain single cells, centrifuged in 15 mL falcon at 850 RPM for 5 min.

Isolated primary ZG cells were plated in 12-well standard cell culture plate for adherent cells in DMEM (Table 2.10) and cultured at 37°C in 5% CO_2 incubator. Media was changed every day. Protocol previously described (Nikolaev *et al.*, 2005).

Table 2.10 DMEM cell culture media composition

DMEM prepared sterile and stored at +4°C

Chemical	**Final volume/concentration**
Dulbecco's Modified Eagle's Medium (DMEM)	500 mL
Fetal bovine serum (FBS)	10%
L-Glutamine solution	5% (100 U/mL)
Penicillin/Streptomycin solution	5% (100 µg/mL)

All isolation procedures were done in biosafety cabinet 3 in sterile environment using sterile instruments and media. A workflow of isolation and culture is depicted in Figure 2.2.

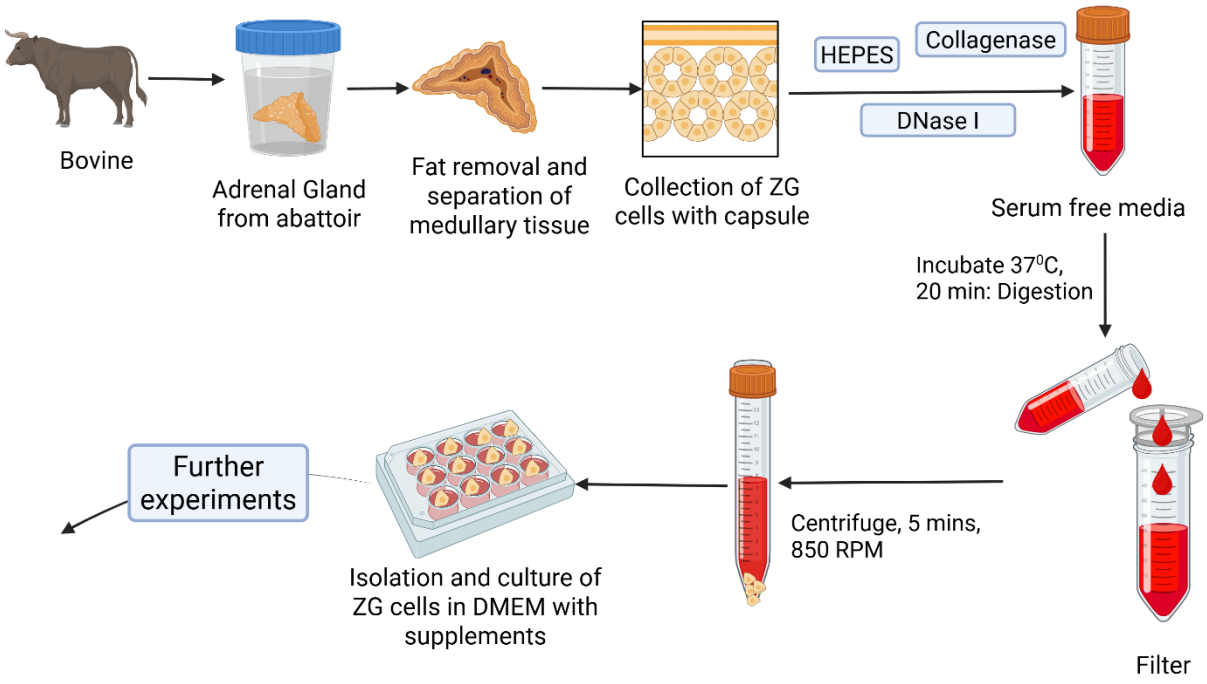

Figure 2.2 Isolation and culture of primary bovine ZG cell

Bovine adrenal glands were transported in PBS from local abattoir. External fat was removed and ZG cells with capsule were collected. They were further digested in serum free DMEM media and cells were pelleted and plated on a 12-well plate. Further experiments were carried out. Created using Biorender.

2.2.2 Confocal Imaging

Freshly isolated bovine ZG cells were plated on 35 mm glass bottomed dishes and fixed with 4% formaldehyde. Washed three times with PBS and incubated for 2 h at RT in blocking buffer (Table 2.11). Incubated with primary antibodies against aldosterone synthase (CYP11B2) (Gomez-Sanchez *et al.*, 2013) and disabled 2 (*Dab2*) as mentioned in Table 2.4 overnight at +4°C. Washed thrice with cold PBS and corresponding secondary antibodies as mentioned in Table 2.6 were incubated for 1 h at RT in dark. Cells were washed thrice with PBS and incubated with DAPI (nuclear stain marker) for 10 min at RT before confocal imaging.

Table 2.11 Blocking buffer composition

Prepared in Ampuwa water. Stored at +4°C

Chemical	Final volume
FBS	10% (v/v)
Triton X-100%	0.3% (v/v)

Confocal imaging was performed using Zeiss LSM800 microscope.

2.2.3 Aldosterone measurements by ELISA

Aldosterone was measured using commercially available aldosterone ELISA kit as per manufacturers protocol. This kit is based on competitive principles and is a solid enzyme linked immunosorbent assay (ELISA) as shown in Figure 2.3.

The 96 microtiter wells provided in the kit are pre-coated with polyclonal secondary antibody raised against analyte (aldosterone) and are immobilized to solid phase. The sample and enzyme-conjugate or aldosterone horseradish peroxidase (HRP) is added which competes for the antibody binding site that is specific towards the antigenic site of aldosterone molecules. After washing, where unbound conjugate is washed off, the substrate solution catalyzed by the enzyme produces color. The color of substrate is inversely proportional to aldosterone concentration in sample (“Competitive ELISA - Creative Diagnostics”, n.d.; “DRG Diagnostics GmbH | DRG Aldosterone ELISA”, n.d.).

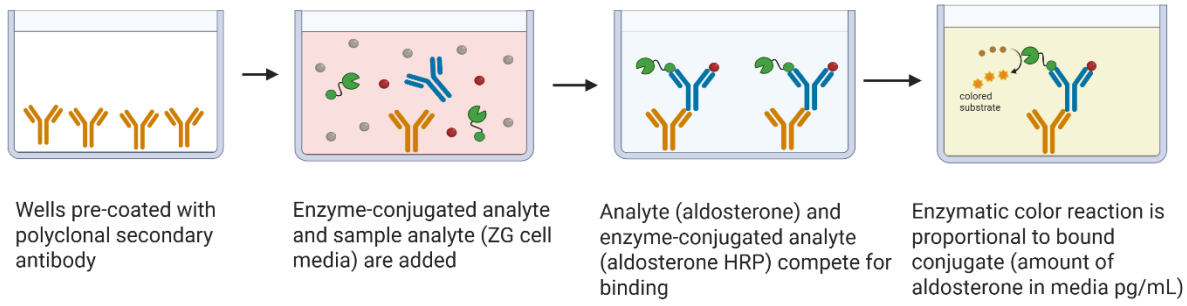

Figure 2.3 Principle of competitive aldosterone ELISA

Wells are precoated with polyclonal secondary antibody against aldosterone. Once samples and enzyme-conjugate analyte are added they compete for the antibody binding site. In the final step, the enzymatic conjugate catalyzes the reaction producing color proportional to the amount of bound conjugate. Created using Biorender. Adapted from ("Which Controls to Use in ELISA Assays? - Enzo", n.d.).

For this thesis, primary cultured ZG cells were incubated for 48-72 h in 12-well plates. They were serum deprived for 2 h and then stimulated for 1 h with different combinations of drugs to be tested. The different drugs used were: 5 µM Fsk, 100 nM AngII, 100 nM ANP, 30 µM PKI and 100 µM MDL. 30 min pre-incubation was done with ANP, myrPKI and MDL before adding stimulating compounds.

The ELISA protocol was done at RT. 100 µL of cell media, controls (low and high) and standard were added to the pre-coated 96-well plate provided in kit and incubated for 30 min. 100 µL enzyme conjugate was added and mixed thoroughly and incubated for 1 h. Wells were then washed with 300 µL 1x wash buffer manually three times. 100 µL substrate solution was added and incubated for 30 min. Finally, 50 µL stop solution was added. Optical density (OD) was measured using microplate reader at 450 nm and 630 nm (background).

Final optical density was calculated using the formula: OD_{630}-OD_{450} = OD_F

Aldosterone concentration (X pg/mL) was calculated using the obtained OD_F in GraphPad prism using sigmoidal, four parameter logistic function to interpolate the X concentration (log).

Sigmoidal S-shaped graph was obtained from standards against which sample and control aldosterone concentrations were calculated.

Aldosterone concentrations (pg/mL) were further normalized to basal aldosterone levels and represented results as fold basal.

2.2.4 Calcium imaging

In this thesis, to measure calcium transients, calcium imaging technique was applied using green, fluorescent dye, Calbryte 520 AM. To allow the dye to cross cell membrane in living cells, an acetoxymethyl ester (AM) is attached. The AM bond is cleaved by intracellular esterases activate the product. Once Ca^{2+} is bound to this hydrolyzed product, Calbryte 520 generates a bright fluorescent signal. As opposed to popular Fluo-4 AM that requires a probenecid, Calbryte 520 AM was developed with improved properties such as:

a. Improved intracellular retention
b. Improved brightness
c. Superior fluorescent intensity ratio F (Intensity after stimulation)/F_0 (Intensity basal)

Studies show Calbryte 520 AM, a non-ratiometric dye, generated five-fold better signal for Ca^{2+} measurements as compared to ratiometric dyes. This method is still a relative measure of intracellular Ca^{2+} concentrations and even with quantitative analysis absolute values cannot be calculated (“CalbryteTM 520 AM | AAT Bioquest”, n.d.; Dinh et al., 2024; Liao et al., 2021).

Freshly isolated ZG cells were plated on 35 mm glass bottomed dishes for 48 h in DMEM for Ca^{2+} measurements. Calbryte 520 AM was dissolved in imaging buffer without calcium (Table 2.12).

Table 2.12 Calcium imaging buffer without calcium

Prepared in Ampuwa water and stored at RT. pH 7.3

Chemical	**Final volume**
KCl	5 mM
NaCl	144 mM
$MgCl_2.6H_2O$	1 mM
HEPES	20 mM

The cells were first incubated in 37 µmol/L Calbryte 520 AM in imaging buffer with 2 mM $CaCl_2$. To perform Ca^{2+} measurements, the imaging buffer was replaced with 0.1 mM $CaCl_2$.

Ca^{2+} sparks were then measured with 100 nM AngII with and without 100 nM ANP pre-stimulation. Ca^{2+} peak signal (F) was normalized to basal intensity (F_0) represented as ratio (F/F_0)

2.2.5 Generation of *in vitro* PDE2A KO of bovine ZG cells by CRISPR/Cas9

CRISPR/Cas9 technology was used to generate PDE2A KO in cultured primary bovine ZG cells. Target region of bovine PDE2A was selected using UniProt. Once amino acid sequence of target domain was identified, gRNAs were made using the University of California Santa Cruz (UCSC) genome browser (https://genome.ucsc.edu/).

pDNR221_U6gRNA vector was used to clone two guide RNAs (gRNA) that target exon 18 of PDE2A bovine gene. pDNR221 vector encoding Cas9 was cloned using the same backbone. The cloned gRNAs (Table 2.13) and Cas9 were recombined into adenoviral vector (pAd) using gateway system cloning (LR gateway cloning) as per manufacturer's protocol. Viral transfection using lipofectamine 2000 and amplification was done in HEK293A cells. The purification was done using CsCl gradient as described in (Skryabin *et al.*, 2023). The generated viruses for gRNA 1, gRNA 2 and Cas9 were stored at -80°C. and represented as

plaque forming unit (Pfu). The viruses generated for gRNA 1, gRNA 2 and Cas9 (physical Pfu/mL: 1.60E+10) were stored at -80°C.

Table 2.13 Sequence of two gRNAs

gRNA	Sequence	Physical Pfu/mL	MOI
gRNA1	GCGGGUCAUGUGGCGACCAC	5.56E+10	10
gRNA2	GCCUACACGCAUUCGUAGA	2.80E+10	10

Primary bovine ZG cells were cultured for 48 -72 h and transduced with gRNAs and Cas9. The multiplicity of infection (MOI) was 10 for gRNAs and 5 for Cas9 decided on trial-and-error method. ZG cells were transduced for 72 h with media change every 24 h. The control ZG cells used were only transduced with Cas9 virus without gRNAs.

2.2.6 Western blot and analysis

Western blot or immunoblotting is a common technique to determine protein expression of target protein in specific samples. The technique works on the principle of gel electrophoresis and separates proteins in samples based on molecular weight expressed in kilo Dalton (kDa).

In this work, primary bovine ZG cells from 12-well plates were lysed directly with 100 µL 4x Laemmli buffer composition in Table 2.14.

Table 2.14 4x Laemmli buffer

Stored at RT.

Chemical	Final volume/concentration
Tris, 1M (pH 6.8)	250 mM
SDS solution	8% (v/v)

100% Glycerol	40% (v/v)
Bromophenol blue salt	0.02% (w/v)
β-Mercaptoethanol	10% (v/v)

Once the samples were lysed and transferred to microcentrifuge tubes, they were boiled to denaturalize and linearize proteins at 95°C for 5 min in thermomixer. These samples can either be used directly or stored at -20°C for future use.

Next step was to prepare stacking and separating gels. Using the Bio-Rad western blotting equipment, 10% separating gels (Table 2.19) and stacking gel (Table 2.20) with 10-well, 1.0 mm comb were made. Samples were then loaded in desired order. Protein ladder was loaded in first well and run along with the samples at 100 V for 30 min, then 130 V for 60 min using powerpack in 1x SDS running buffer (prepared in Ampuwa water from 10x SDS running buffer Table 2.18).

Table 2.15 4x Tris/SDS, pH 8.8

Prepared in Ampuwa water. Stored at RT

Chemical	**Final volume/concentration**
Tris	1.5 mM
SDS solution	0.4% (v/v)

Table 2.16 4x Tris/SDS, pH 6.8

Prepared in Ampuwa water. Stored at RT

Chemical	**Final volume/concentration**

Tris	500 mM
SDS solution	0.4% (v/v)

Table 2.17 APS Solution

Prepared weekly. Stored at +4°C

Chemical	**Final volume/concentration**
Tris	500 mM
SDS solution	0.4% (v/v)

Table 2.18 10x SDS Running buffer, pH 8.3

Prepared in Ampuwa water. Stored at RT

Chemical	**Final volume/concentration**
Tris	250 mM
SDS solution	1% (v/v)
Glycine	1.9 M

Table 2.19 Separating gel

Composition for two-10% gels. Composition is adjusted based on number of gels required and gel pore size.

Chemical	**Final volume/concentration**

Double distilled water	5 mL
Acrylamide	4 mL
4x Tris/SDS, pH 8.8	3 mL
10% APS	48 µL
TEMED	18 µL

Table 2.20 Stacking gel

Chemical	**Final volume/concentration**
Double distilled water	2.31 mL
Acrylamide	500 µL
4x Tris/SDS, pH 6.8	940 µL
10% APS	18.8 µL
TEMED	7.5 µL

After proteins were separated on gel, they were transferred onto nitrocellulose membrane with sandwich method for transfer. Transfer is done in chilled 1x transfer buffer (Table 2.21 and Table 2.22) with ice pack inside the transfer chamber for 90 min at 100 V.

Table 2.21 10x Transfer Buffer

Prepared in Ampuwa water. Stored at RT

Chemical	**Final volume/concentration**
Tris	325 mM

Glycine	1.9 M

Table 2.22 1x Transfer Buffer

Prepared from 10x transfer buffer and prepared in Ampuwa water. Stored at +4°C

Chemical	**Final volume/concentration**
10x transfer buffer	1x
Methanol	10% (v/v)

The nitrocellulose membrane after transfer is cut at desired size for protein identification. The membranes were blocked with 5% milk prepared in TBS-T (Table 2.23 and **Table** 2.24) for 20 min with constant shaking. Primary antibodies prepared in milk (dilutions and milk percentage in Table 2.3) were added to the membranes which were kept at +4°C with constant shaking, overnight. Secondary antibodies (dilutions and milk percentage in Table 2.5) were added for 1 h at RT with constant shaking. Membranes were washed after primary and secondary antibody incubation three times for 10 min.

Table 2.23 10x Tris-Buffered Saline (TBS), pH 7.5

Chemical	**Final volume/concentration**
Tris	100 mM
Sodium chloride (NaCl)	1.5 M

Table 2.24 1x TBS-Tween (TBS-T) buffer

To ensure complete dissolution of tween, stir the buffer with magnetic stirrer for 20 min.

Chemical	Final volume/concentration
10x TBS buffer	1x
Tween 20	0.1% (v/v)

The membranes were then incubated with chemiluminescent reagents (SuperSignal West Pico PLUS kit) for protein detection for 1 min. The membranes were developed using the developing machine (30 s – 10 min exposure time) and signal detected on X-ray films. Densitometry analysis was performed using ImageJ software on scanned blots/films. GAPDH was used as housekeeping protein to ensure equal loading and to normalize other proteins.

2.2.7 FRET measurement and live cell imaging

2.2.7.1 FRET microscope and setup

In this thesis, Leica inverted microscope was used to perform all measurements in bovine ZG cells. The schematics of the microscope set up can be seen in Figure 2.4 which has a microscope stage, image splitter, camera and computer with ICY software with MultiFRET to record measurements. 63x/1.5 oil immersion objective was used for all experiments (Börner *et al.*, 2011).

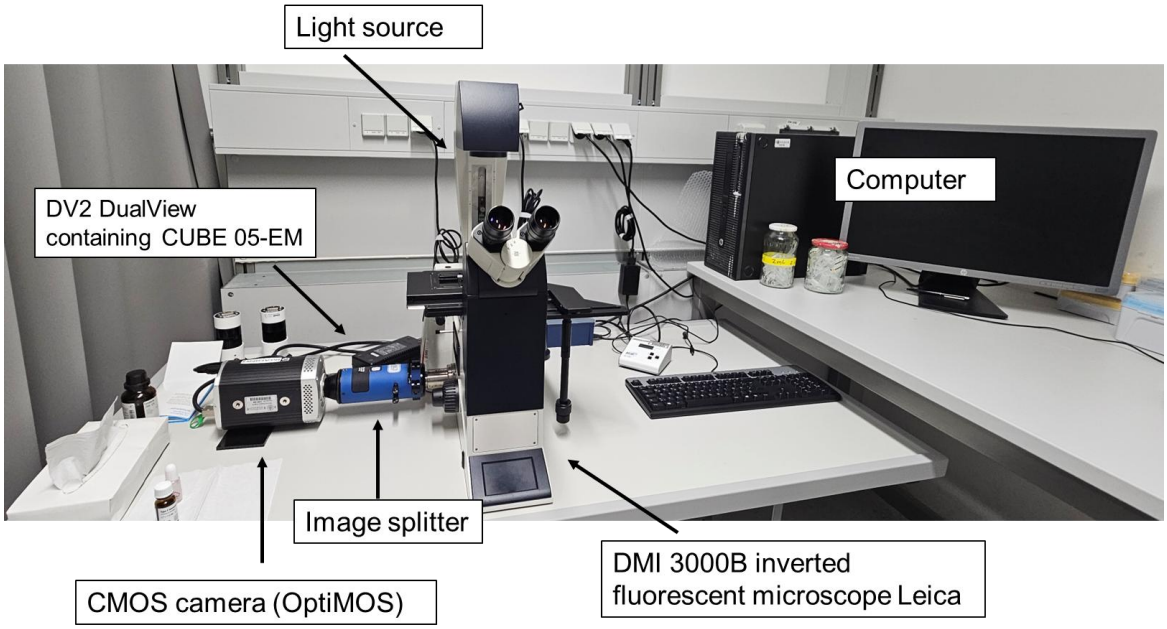

Figure 2.4 FRET microscope set up for cAMP measurements in bovine ZG cells

Experimental setup of inverted microscope (Leica) for FRET imaging. It consists of microscope stage, image splitter to divide emission light into donor and acceptor channels, light source and camera to detect emitted intensities.

2.2.7.2 Real-time FRET measurements in bovine ZG cells

Real-time FRET measurements were conducted in live bovine ZG cells after 48-72 h adenoviral transduction. DMEM was replaced by 1 mL FRET buffer (Table 2.25) after one wash to remove any dead cells. One drop of immersion oil was placed on the objective, and the glass bottom dish was placed on a holding frame of the microscope stage and secured tightly. Using the above-mentioned software and pharmacological modulators, experiments were recorded. Stable baseline was first recorded followed by drug treatments. The different drugs were: 10 µM Fsk, 100 nM AngII, 100 nM BAY 60-7550, 100 nM ANP and 100 µM IBMX. A brief workflow is shown in Figure 2.5.

Table 2.25 FRET Buffer

Prepared in Ampuwa water. Stored at RT.

Chemical	Final volume
KCl	5.5 mM
NaCl	144 mM
$MgCl_2.6H_2O$	1 mM
HEPES	10 mM
$CaCl_2$	1 mM

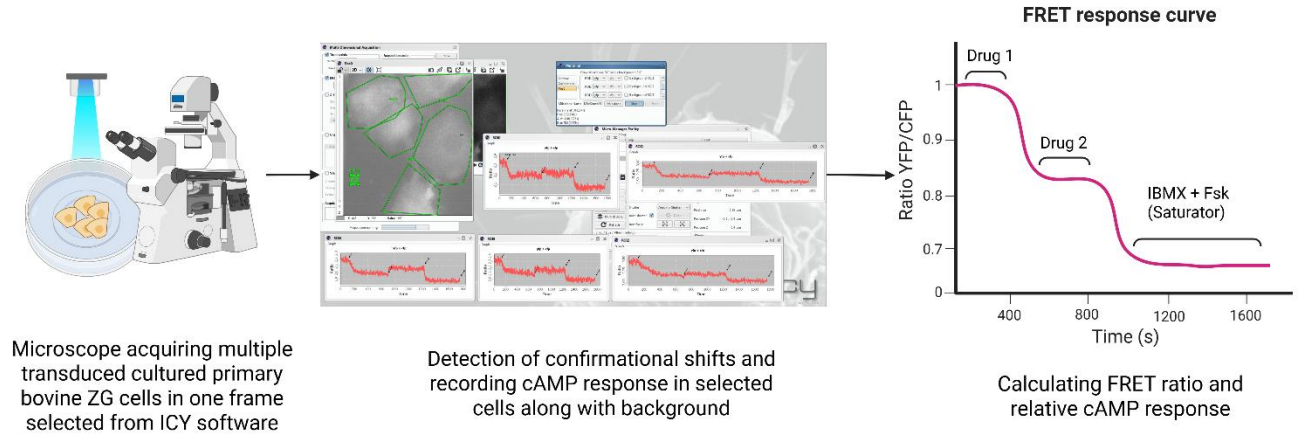

Figure 2.5 Schematic representation of FRET workflow

Transduced bovine ZG cells in glass bottom dish were placed on FRET microscope setup. ICY and MultiFRET software's were used to measure multiple cells in single frame along with background intensity. FRET response is recorded in Microsoft Excel. YFP/CFP ratios were calculated for measuring relative biosensor response. Created using Biorender. Adapted from (Ramuz *et al.*, 2019).

Epac2-camps cAMP biosensor (Nikolaev *et al.*, 2005) and AKAR3 (A-kinase activity reporter PKA)(Jones-Tabah *et al.*, 2020) were used in this project to measure relative cAMP and PKA

activity. Both biosensors use an acceptor (Yellow fluorescent protein YFP) and donor (Cyan fluorescent protein CFP).

2.2.7.3 Epac2-camps and AKAR3 biosensors

In Epac2-camps biosensor (Figure 2.6A), upon cAMP binding to the cyclic nucleotide binding domain (CNBD), there is change in conformation and distance between CFP and YFP increases, leading to decrease in FRET. Therefore, a decrease in YFP/CFP ratio represents increase in intracellular cAMP concentrations (Börner *et al.*, 2011; Nikolaev *et al.*, 2005).

The AKAR3 biosensor (Figure 2.6B) has FHA ligand (forehead-associated ligand) (pThr/pSer) binding domain (LBD) and PKA substrate sequence (pSite). Increase in PKA activity (as a result of increased intracellular cAMP) leads to PKA mediated phosphorylation of the pSite in the AKAR3 biosensor. Interaction of phosphorylated substrate sequence with FHA ligand binding domain leads to a conformational change, bringing the CFP and YFP closer together and causing FRET to increase (measured as YFP/CFP ratio) (Jones-Tabah *et al.*, 2020). Thus, increase in YFP/CFP ratio represents increase in cAMP/PKA activity.

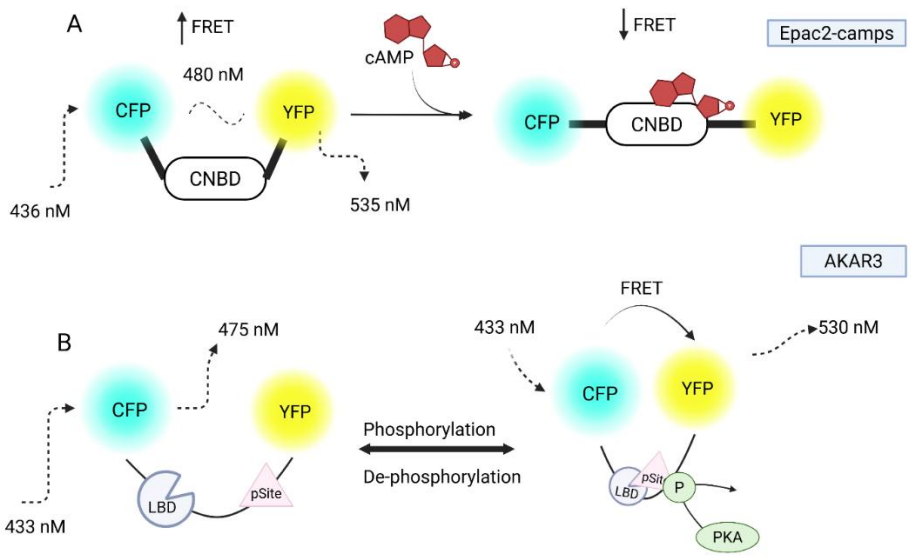

Figure 2.6. Principle of Epac2-camps and AKAR3 FRET biosensors

(A) Epac2-camps biosensor showing high FRET before and low FRET after cAMP binds to cyclic nucleotide binding domain (CNBD). Increase in cAMP results in decrease in FRET and this YFP/CFP

ratio decreases. (B) AKAR3 biosensor with ligand binding domain (LBD) and PKA binding site (pSite). When the sensor is phosphorylated by PKA, it binds to pSite of the biosensor leading to increase in FRET and YFP/CFP ratio. Created using Biorender. Adapted from (Jones-Tabah *et al.*, 2020; Nikolaev *et al.*, 2005).

2.2.7.4 FRET analysis and calculations

Raw YFP, CFP and background values were obtained from the raw images and exported into Excel file. To calculate mean FRET intensity, see Equation 1

Equation 1 Mean intensity (FRET)

$$FRET\ mean\ intensitiy\ = \frac{YFP\ raw\ - YFP\ background}{CFP\ raw - CFP\ background}$$

Once the mean intensity is calculated, the mean FRET intensity was corrected for bleedthrough factor. It is important to correct for bleedthrough due to overlapping spectrum of YFP and CFP. The resulting corrected values were normalized with baseline to get relative FRET see Equation 2

Equation 2 Relative FRET

$$Relative\ FRET\ = \frac{Average\ baseline\ FRET\ ratio}{Corrected\ FRET\ ratio}$$

Results are also represented by change in FRET (%) see Equation 3

Equation 3 Change in FRET (%)

$$Change\ in\ FRET\ (\%) = \frac{Average\ baseline\ FRET\ ratio - average\ treatment\ FRET\ ratio}{Average\ baseline\ FRET\ ratio} \times 100$$

2.3 Statistical Analysis

All statistical analysis was done using GraphPad Prism 10.6.1 software and Microsoft Excel. Data represented as mean ± standard error of mean (SEM). Two-tailed, unpaired *t*-tests were used to compare two groups. Grouped data were analyzed by two-way ANOVA with multiple comparisons. Non-parametric Friedman test was used for data not normally distributed. Normally distributed data was compared with ordinary one-way ANOVA with Geisser-greenhouse correction. Standalone comparisons were done using Fischer's test. Multiple comparison was done using Tukey's test.

3 Results

3.1 Validation of isolated ZG cells by immunofluorescence

To validate the isolation, cultured primary bovine ZG cells were stained with aldosterone synthase (CYP11B1), final enzyme in aldosterone biosynthesis (Gomez-Sanchez *et al.*, 2013) and Disabled-2 (*Dab-2*), a ZG specific marker (Romero *et al.*, 2007) and DAPI, a nuclear staining marker.

From Figure 3.1, it can be observed that virtually all DAPI stained cells express CYP11B2 and *Dab2*. This confirms the validity of isolation protocol and that correct cells are being cultured and used for further experiments.

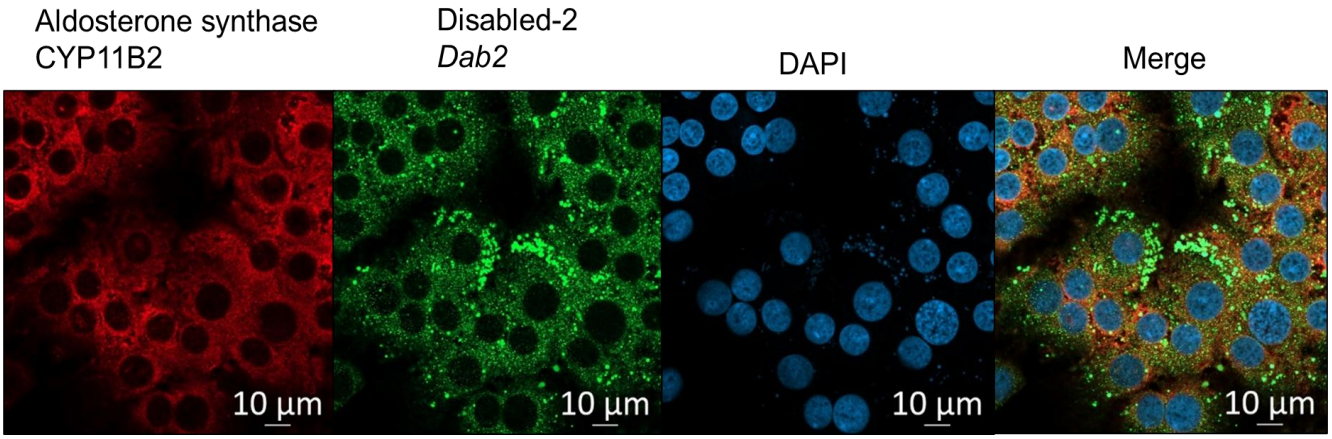

Figure 3.1 Immunofluorescence staining of bovine adrenal ZG cells

Confocal images of primary cultured bovine ZG cells. Immunostaining done for aldosterone synthase (CYP11B2), Disabled-2 (*Dab-2*) and DAPI, a nuclear stain. Merge image shows the overlay of all three antibodies as an outline of ZG cells. Scale bar: 10 µm.

3.2 Acute inhibitory effect of ANP is cGMP-dependent

It has been previously shown that AngII induces aldosterone production via AT_1R (Gambaryan *et al.*, 2006). ANP inhibits this aldosterone stimulated by AngII/AT_1R. To answer the question whether this inhibitory effect of ANP is cGMP-dependent cells were transduced with SponGee.

SponGee is a genetically encoded cGMP scavenger tool. It is known that ANP/GC-A/cGMP pathway has many downstream effects in ZG cells. SponGee encodes for the cGMP binding domains of the PKG (fused to a red fluorescent protein called mApple) which can bind cGMP and render it inactive (Ros *et al.*, 2019). This tool provided useful information on the further role of cGMP and cGMP-dependent downstream pathways in bovine ZG cell *in vitro*. This is a unique tool that binds only cGMP and does not interfere with other nucleotides such as cAMP. Therefore, experiments with and without ANP stimulation prior to AngII treatment were performed. Figure 3.2 shows the mechanism of action of SponGee.

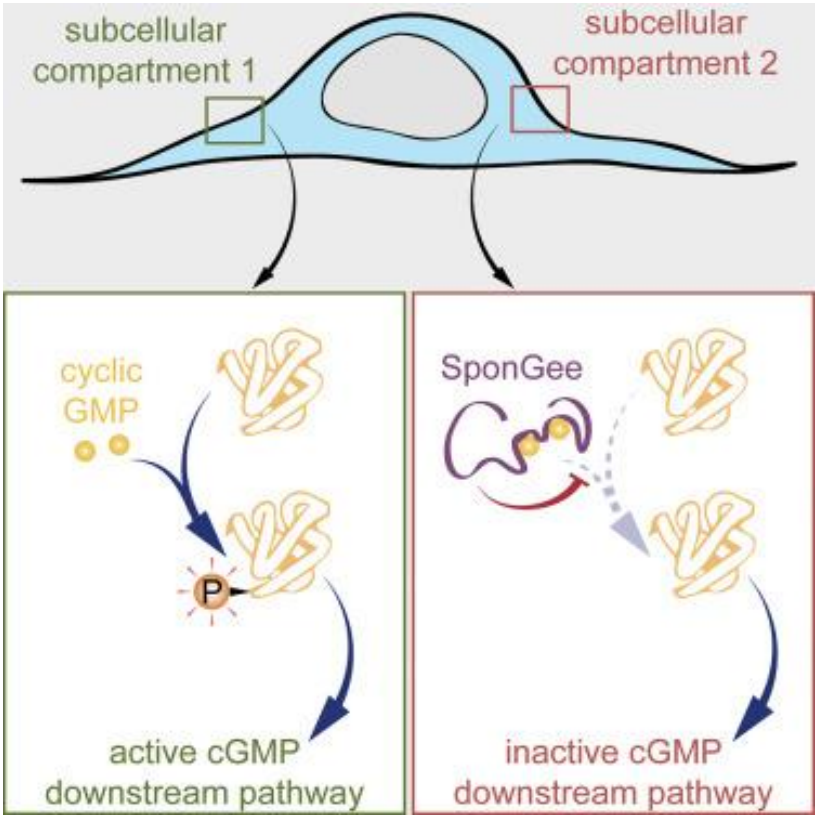

Figure 3.2 Mechanism of action by SponGee

SponGee binds to intracellular cGMP, rendering it inactive. Inactivation of cGMP by SponGee also inactivates cGMP-dependent downstream pathways, making it a useful tool to study the ANP/cGMP pathway. From (Ros et al., 2019).

To study inhibitory effects of ANP by cGMP, primary bovine ZG cells were transduced with a control gRNA vector and SponGee with MOI: 15. Figure 3.3 shows the successful visualization of SponGee by mApple fluorescence.

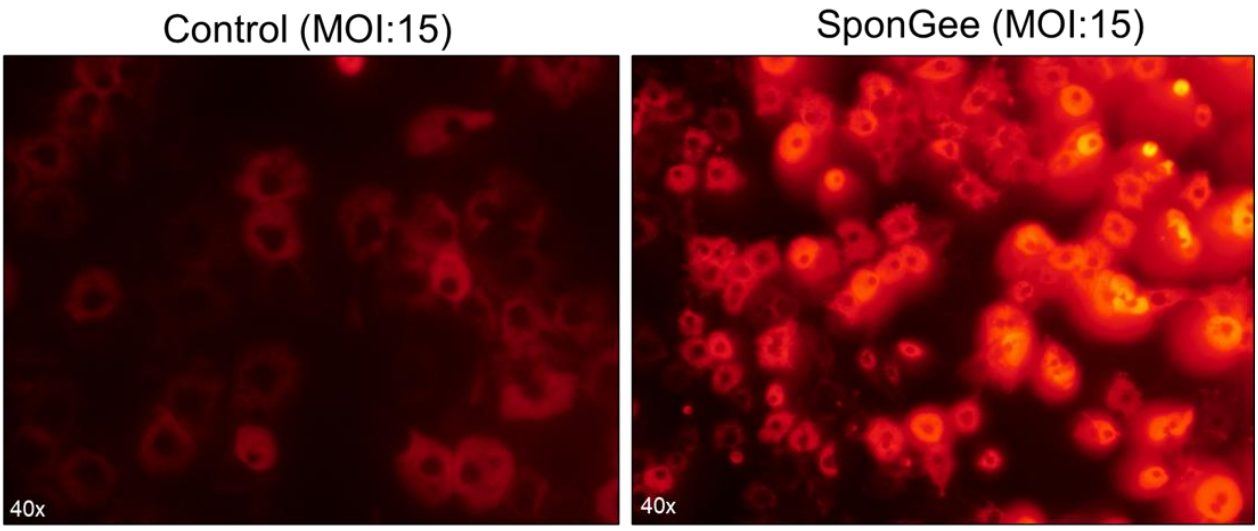

Figure 3.3 Expression and visualization of SponGee

In bovine ZG cells, gRNA (left, gRNA 1, MOI: 15) was transduced as control and SponGee (right, MOI: 15) was transduced. Visualization of successful SponGee expression was observed by mApple fluorescence encoded by SponGee construct. Image from 40x microscope magnification.

Aldosterone levels were measured in supernatants from control and SponGee transduced cells treated with or without 100 nM ANP pre-incubation with 100 nM AngII.

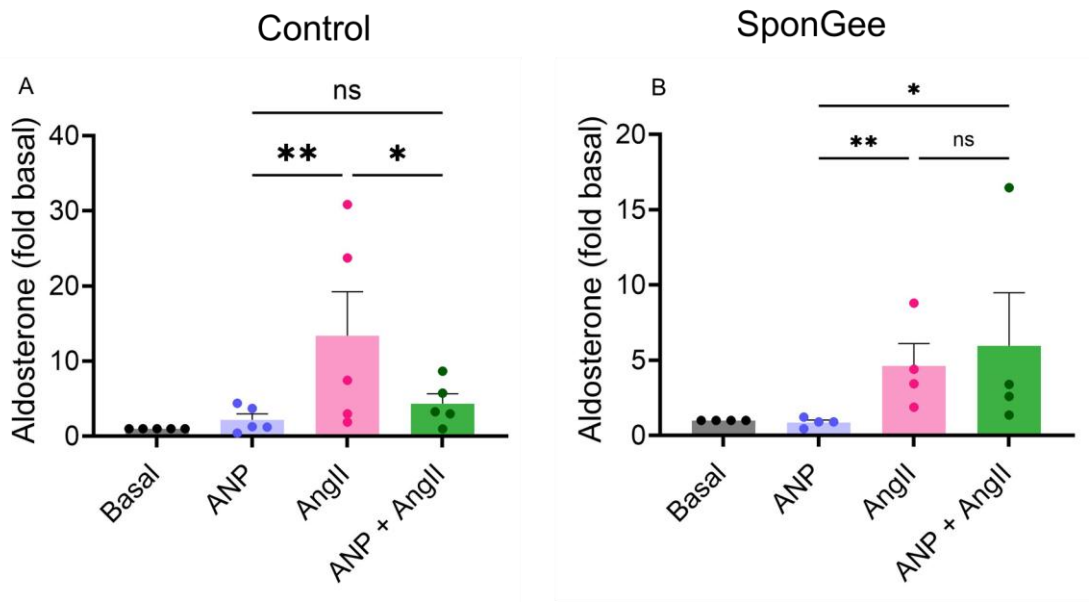

Figure 3.4 Inhibition by ANP of AngII stimulated aldosterone production is cGMP-dependent

In control cells (A), 100 nM ANP inhibits 100 nM AngII stimulated aldosterone production. 10 min pre-incubation of bovine ZG cells with ANP resulted in complete abolished ANP response in SponGee transduced cells (B). Aldosterone values were calculated as fold change of basal. Data represented as mean ± SEM. n=5 control and n = 4 SponGee from independent experiments. Ordinary one-way ANOVA with multiple comparisons and Friedmans test. *p<0.05, **p<0.01

From Figure 3.4 A and B, it can be seen that when normalized to basal (basal = 1), there is a significant ~ 5-10-fold increase in aldosterone production by AngII. ANP, as we know from the literature and observed here, did not stimulate aldosterone production when given alone. Pre-stimulating ZG cells with ANP for 10 min, led to inhibition of AngII induced aldosterone production by ~10-fold as expected in control cells.

In SponGee transduced cells, pre-stimulating ZG cells with ANP for 10 min did not inhibit aldosterone production induced by AngII. The acute inhibitory effect of ANP was completely abolished. There is also a significant difference between ANP alone and ANP + AngII stimulated cell ~6-fold. This indicated that inhibition by ANP of AngII-stimulated aldosterone production is cGMP-dependent and cGMP downstream pathways play an important role in moderating aldosterone levels.

3.3 Acute inhibition by ANP is not Ca^{2+} dependent

Studies have shown that AngII/AT_1R pathway also stimulated the increase of intracellular Ca^{2+} and Ca^{2+}-dependent pathways as mentioned in 1.6.4. Once established that inhibitory effect of ANP is cGMP-dependent, the next question was to see whether Ca^{2+} plays any role in this inhibitory pathway. As mentioned in 1.6.3, one possibility could be the phosphorylation of RGS2 or RGS4 proteins by PKG. This cGMP/PKG dependent pathway could interact rapidly with AngII/ Ca^{2+} signaling pathway to inhibit aldosterone production.

Calcium imaging using Calbryte 520 AM (2.2.4) was done to observe calcium transients as shown in Figure 3.5.

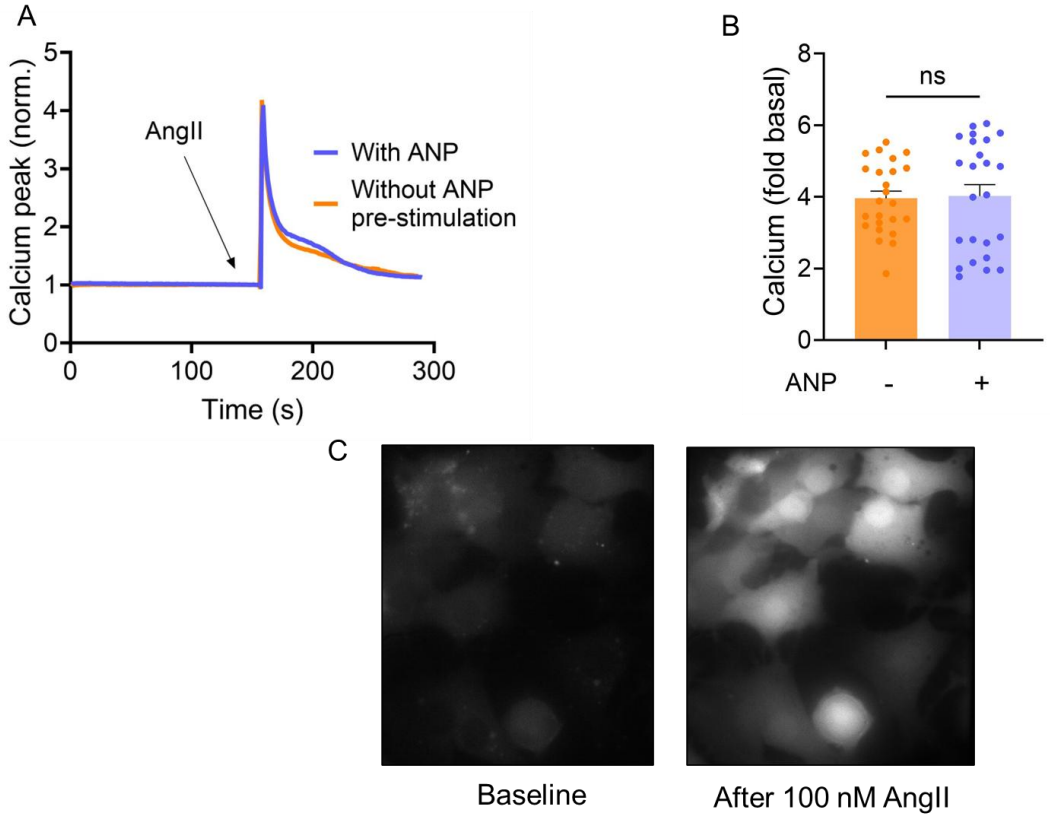

Figure 3.5 Inhibitory effect of ANP on AngII stimulated cells is not calcium dependent: Calcium imaging study

(A) Calcium transients measured in ZG cells with Calbryte 520 AM. ZG cells pre-treated with and without ANP have no effect on Ca^{2+} peak stimulated by a 100 nM AngII. (B) Quantification of calcium peaks represented as fold basal for individual experiments shows no significant difference (n.s). (C) Snippet

from Calbryte 520AM treated bovine ZG cells at baseline and after 100 nM AngII-stimulation. Data represented as mean ± SEM. n= 24, unpaired *t*-test, two-tailed. p=0.8713.

AngII induced a ~4-fold increase in Ca^{2+} signal from basal as shown in Figure 3.5A. However, Ca^{2+} peaks after 100 nM AngII-stimulation showed no difference with and without 10 min, 100 nM ANP pre-stimulation. There was no change in Ca^{2+} amplitude with ANP pre-incubation as shown after quantification in Figure 3.5B. Increase in intracellular Ca^{2+} was seen in snippet (Figure 3.5C) at baseline and after AngII-stimulation. This indicates that ANP/cGMP pathway does not inhibit or affect AngII-stimulated Ca^{2+} increase in bovine ZG cells and other mechanism/s exist for aldosterone inhibited by ANP.

Polyclonal antibody raised against phosphorylates PKA substrate sequence can potentially detect both PKA and PKG substrates due to identical kinase consensus motif. To check for PKA/PKG substrates activated or inhibited by ANP/cGMP pathway western blot analysis was done with ZG cell lysates prepared after stimulation with 100 nM ANP or 100 nM AngII for 1 h.

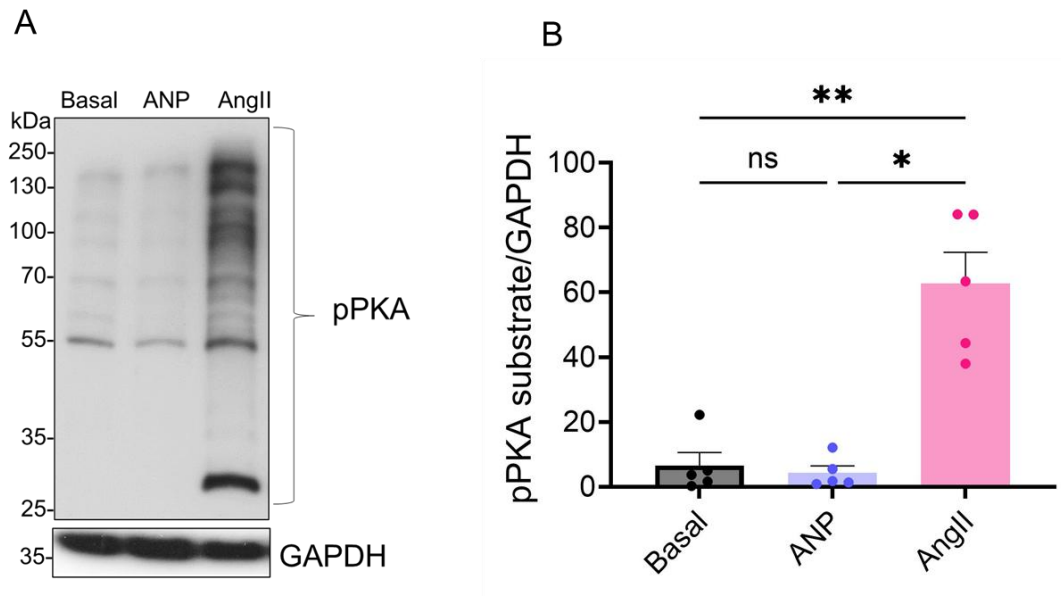

Figure 3.6 PKA substrate phosphorylation by ANP and AngII

(A) Representative western blot and (B) quantification of 4-5 independent experiments performed to probe for phosphorylated PKA/PKG substrates shows strong phosphorylation by 100 nM AngII and

negligible effect by 100 nM ANP. GAPDH was used as loading control. Data represented as mean ± SEM. One-way ANOVA with multiple comparison by Tukey's test. ns; not-significant, *p<0.05, **p<0.01.

ANP stimulation had negligible effect on PKA/PKG substrate phosphorylation as compared to AngII that showed strong activation of PKA/PKG substrates (see Figure 3.6) suggesting the involvement of other pathways in acute AngII-inhibition by ANP.

3.4 CRISPR/Cas9 generated *in vitro* PDE2A KO

3.4.1 PDE2A expression in PDE2A KO ZG cells

PDE2A is a dual specific PDE that is activated by cGMP and hydrolyzes cAMP as elaborated in 1.6.2. The cGMP-activated PDE2A is hypothesized to play a role in ANP mediated inhibition of aldosterone. For this reason, PDE2A KO cells were generated using CRISPR/Cas9 system as described in Figure 3.7.

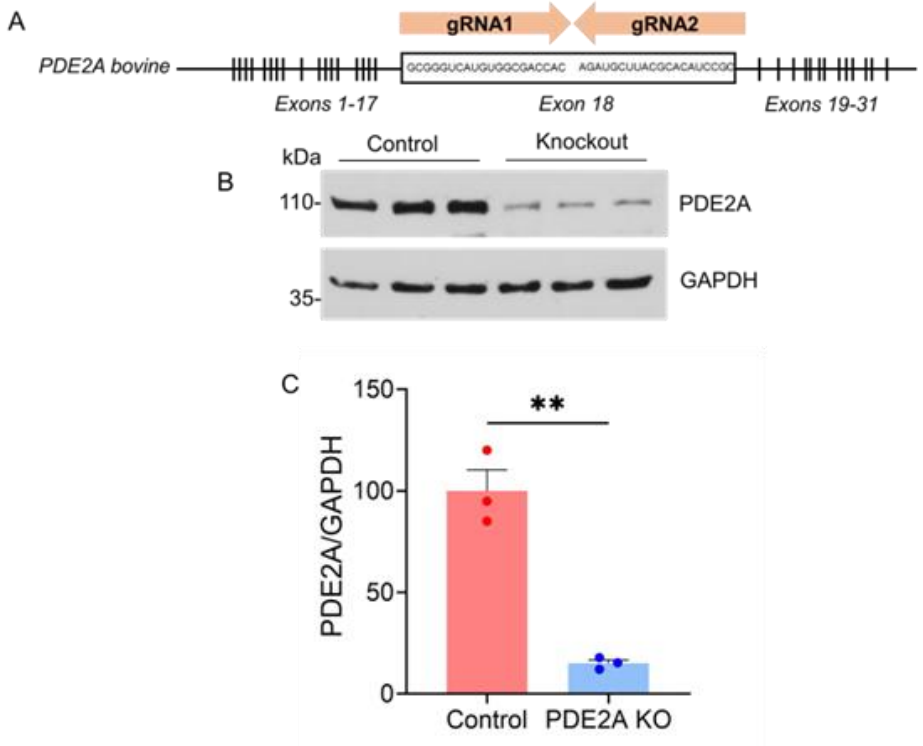

Figure 3.7 CRISPR/Cas9 generated PDE2A KO in bovine ZG cells

(A) Bovine PDE2A gene with gRNAs targeting exon 18 to generate PDE2A KO. (B) and (C) show representative western blot and quantification of PDE2A protein levels in control and PDE2A KO ZG

cells normalized to GAPDH (loading control). n=3 for each group (independent isolations). Data represented as mean ± SEM. **p<0.001, unpaired *t*-test, two-tailed.

Figure 3.7A shows the sequence of gRNAs used to target exon 18 of bovine PDE2A gene. Figure 3.7B shows western blot of PDE2A protein in control (first three lanes) and KO (last three lanes) cells. GAPDH was used as loading control and to normalize the protein expression quantified in Figure 3.7C. ~80% loss of PDE2A protein expression in cultured primary bovine ZG cells was observed with this CRISPR/Cas9 model using two gRNAs.

3.4.2 Functional validation of PDE2A KO using FRET

Live cell imaging using Epac2-camps biosensor (2.2.7.3) was performed on primary cultured bovine ZG cells to functionally validate the CRISPR/Cas9 PDE2A KO model. ZG cells were transduced for 72 h with cAMP biosensors adenovirus along with gRNAs and Cas9 to generate PDE2A KO cells. Control and KO cells were stimulated with 100 nM Bay 60-7550 (PDE2 inhibitor) followed by 100 µM IBMX (non-selective PDE inhibitor) and finally 10 µM Fsk (direct AC/cAMP activator). (Figure 3.8)

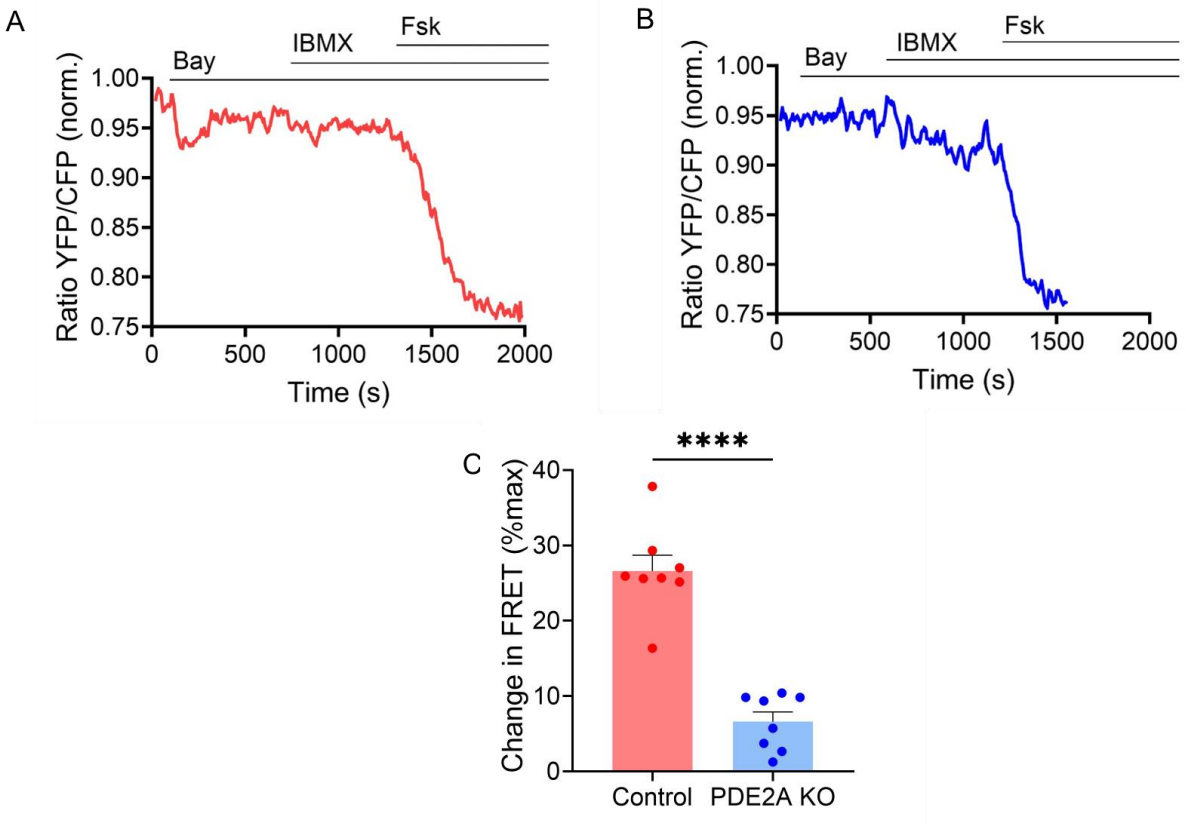

Figure 3.8 Functional validation of PDE2A KO using FRET

Representative FRET traces of control (A) and PDE2A KO (B). In control ZG cells, we can observe Bay 60-7550 (Bay) response but in PDE2A KO cells, this response is abolished. 100 µM IBMX and 10 µM Fsk were used to achieve maximal cAMP response of the Epac2-camps biosensor. (C) shows quantification of FRET measurements. ~25% of Bay response is seen in control ZG cells as compared to negligible Bay response in PDE2A KO cells. n=3 for each group (independent isolations). Data represented as mean ± SEM. ****p<0.0001, unpaired *t*-test, two-tailed.

In control ZG cells, Bay 60-7550 results in ~25% decrease in FRET signals indicative of increase in cAMP. In PDE2A KO ZG cells, Bay 60-7550 response is abolished confirming the validity of CRISPR/Cas9 generated PDE2A KO in primary bovine ZG cells. Effective deletion of PDE2A KO opened the opportunity to explore the role of ANP-PDE2A led inhibition of aldosterone.

3.5 Acute inhibitory effect of ANP on AngII-stimulated aldosterone is mediated by PDE2A

3.5.1 Rapid degradation of cAMP by PDE2A: live cell imaging finding

Previous studies have shown that Forskolin increases intracellular cAMP levels by directly acting on adenylyl cyclase. Subsequent co-treatment with ANP activates the ANP/cGMP pathway to activate PDE2 which rapidly hydrolyzes cAMP (Nikolaev *et al.*, 2005).

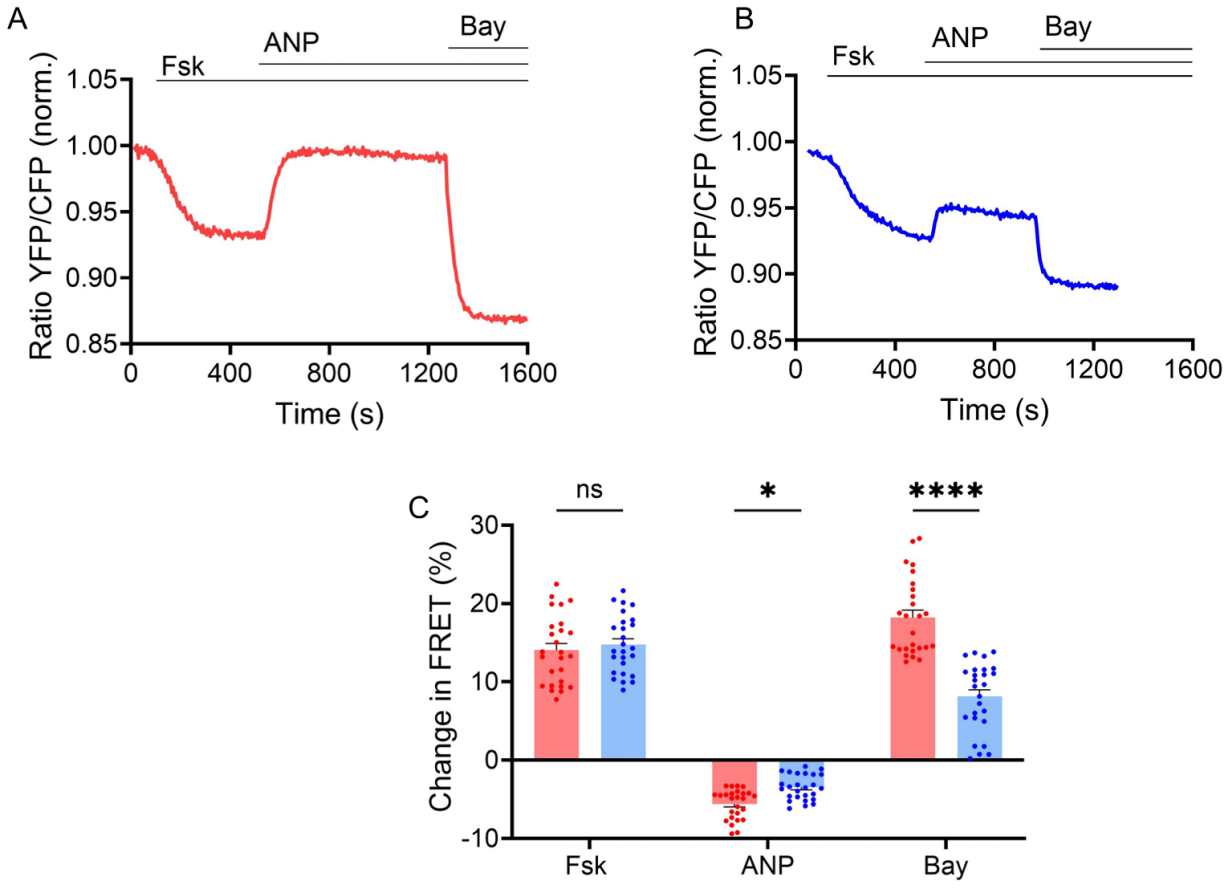

Figure 3.9 Rapid degradation of cAMP by PDE2A

cAMP activated by 10 μM Fsk in control (A) and PDE2A KO (B) ZG cells, is rapidly degraded by 100 nM ANP in control but not in PDE2A KO cells. Rapid degradation of cAMP by ANP activated PDE2A is seen in control and not in KO ZG cells. 100 nM bay 60-7550 effect is also attenuated in PDE2A KO cells. Quantification of relative cAMP levels represented as change in FRET (C). Data represented as mean ± SEM. Each individual data point represents separate experiment from at least 3 independent

isolations. 2-way ANOVA performed on grouped data in control and KO cells. n.s; not significant, *p<0.05, ****p<0.0001.

For this thesis, the same experiment was repeated with Epac2-camps biosensor in control and PDE2A KO cells (generated as per 2.2.5). As seen in Figure 3.9 PDE2A KO cells blunted the ANP response which was also confirmed with subsequent 100 nM Bay 60-7550 addition.

3.5.2 Rapid degradation of cAMP by PDE2A: Aldosterone ELISA

Bovine ZG cells secrete aldosterone into serum free media upon stimulation. After 72 h of CRISPR/Cas9 transduction used to generate PDE2A KO bovine ZG cells, they were stimulated for 1 h under different conditions. Cell lysates were then used for western blot analysis (2.2.6) and media was used to measure aldosterone concentration (2.2.3).

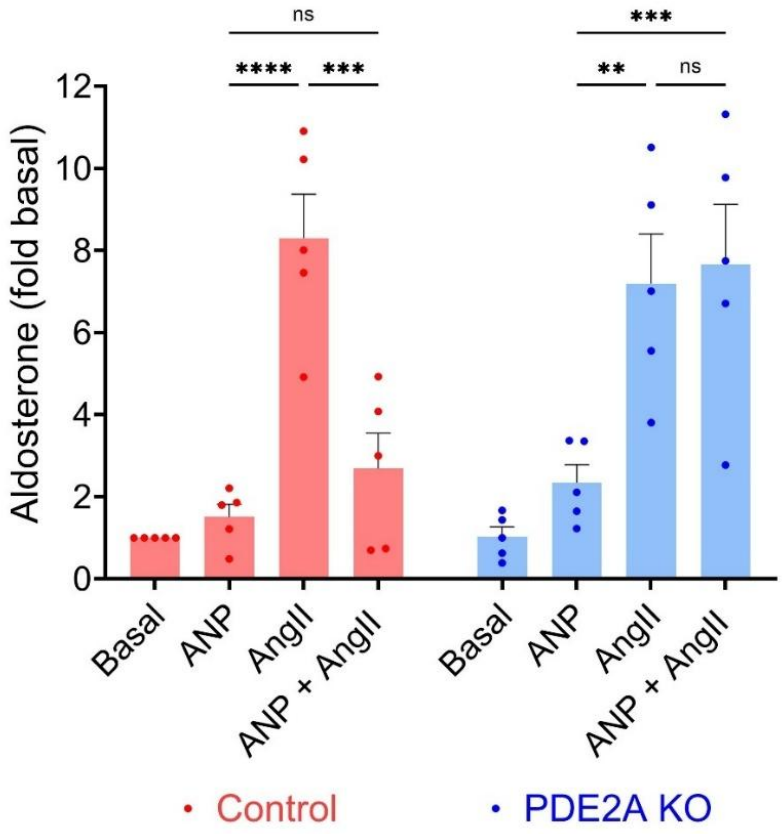

Figure 3.10 Aldosterone ELISA measurements

Aldosterone ELISA measurements in control and PDE2A KO ZG cells showed ~8-fold increase in 100 nM AngII-stimulated aldosterone production as compared with basal. 100 nM ANP inhibits this

aldosterone produced by ~5-fold in control cells, but in PDE2A KO cells there is no inhibition by ANP suggesting PDE2A dependent mechanism. Data represented as mean ± SEM. Mixed model analysis with multiple comparisons using Tukey's test. n.s; not significant, **p<0.01, ***p<0.0001, ****p<0.0001.

To measure the effect of ANP inhibition by PDE2A, cultured ZG cells were treated with and without 100 nM ANP pre-stimulation for 30 min, 100 nM AngII and 100 nM ANP. Unstimulated ZG cells were used as basal/ control. Aldosterone represented as fold basal in Figure 3.10, showed that AngII-stimulated aldosterone production is inhibited by ANP, and in PDE2A KO cells, this effect is abolished. This suggested that ANP/cGMP mediated inhibition of AngII-stimulated aldosterone is PDE2A dependent. Both FRET and aldosterone ELISA data correlate well and support the finding that effect of ANP is PDE2A dependent.

3.6 AngII activates cAMP synthesis that is inhibited by ANP

In the pervious experiments, it was established that PDE2A is responsible for aldosterone degradation by hydrolyzing cAMP in ZG cells as one of the mechanisms. The next question was whether AngII-stimulation can led to increase in intracellular cAMP and PKA activity. AngII is hypothesized to do so via Ca^{2+} stimulated adenylyl cyclase type 3, which has been reported to be expressed in bovine ZG cells (Burnay *et al.*, 1998).

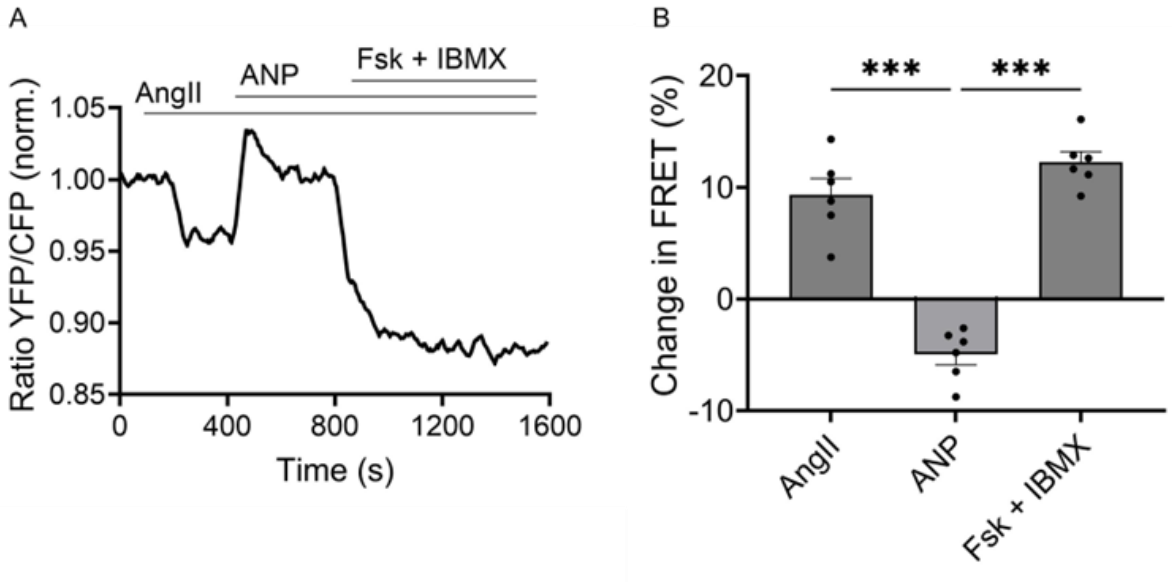

Figure 3.11 Activation of cAMP by AngII using Epac2-camps biosensor

Stimulation of ZG cells transduced with Epac2-camps biosensor with 100 nM AngII led to increase in cAMP production as represented by the FRET trace (A). Subsequent stimulation wit 100 nM ANP led to degradation of this cAMP by rapid action of PDE2A. 10µM Fsk and 100 µM IBMX were used for maximal sensor response. Quantitative analysis of relative cAMP levels normalized to baseline as presented by change in FRET (%) is shown in (B). Data represented as mean ± SEM. n=6 cells, from at least 3 independent isolations. One-way ANOVA and multiple comparison with Tukey's test. ***p<0.001.

Bovine ZG cells transduced with Epac2-camps biosensor were stimulated with 100 nM AngII that led to increase in intracellular cAMP response. Subsequent stimulation with 100 nM ANP led to increase in FRET signal (YFP/CFP) indication decrease in cAMP. This indicated that ANP via PDE2A degrades AngII stimulated cAMP in bovine ZG cells. Fsk and IBMX were used to saturate the biosensor to produce maximal cAMP response Figure 3.11

The question that came up next was, how important is this AngII stimulated cAMP for aldosterone production.

3.7 Role of AngII-stimulated cAMP in aldosterone production

cAMP plays a major role in aldosterone production as described in 1.6.1. It is also known from literature that cyclic nucleotides and their protein kinases act in compartments and microdomains. To first understand whether the increase in intracellular cAMP stimulated by AngII affects aldosterone levels, PDE4B was overexpressed in bovine ZG cells. PDE4B is a highly active and cAMP specific phosphodiesterase that degrades this second messenger and inhibits its downstream pathways.

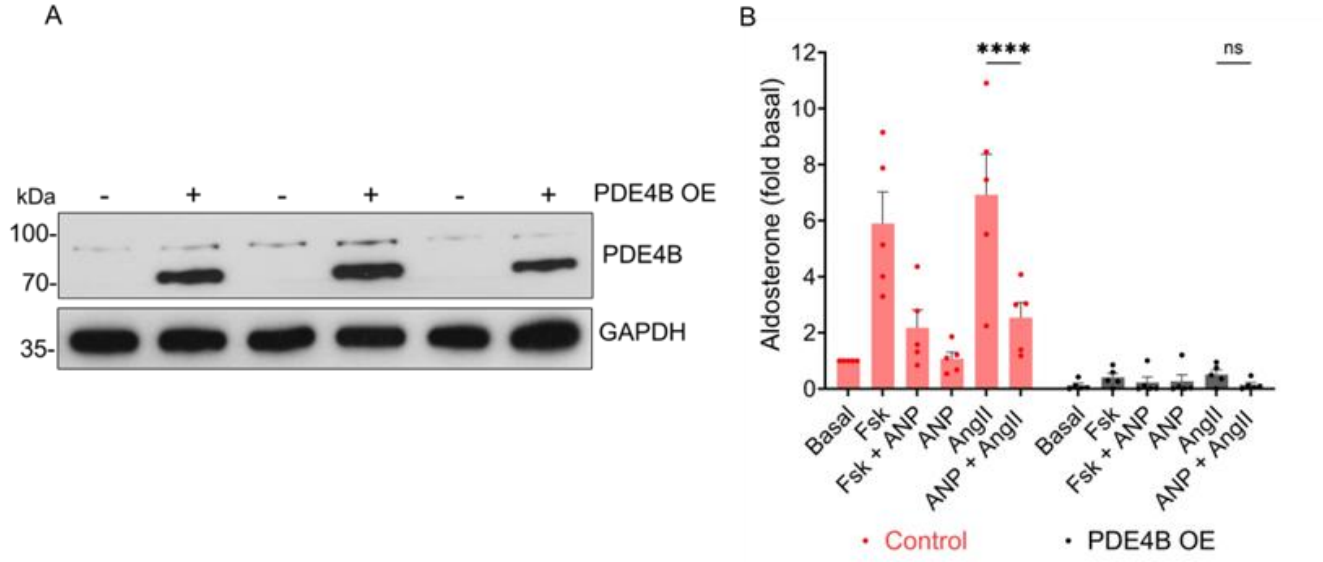

Figure 3.12 Role of AngII stimulated cAMP in aldosterone production

Western blot (A) showing control vs PDE4B overexpressed bovine ZG cells. GAPDH was used as loading control. (B) Aldosterone measured in these cells showed that PDE4B overexpression in bovine ZG cells leads to inhibition of Fsk and AngII induced response. Aldosterone represented as fold change of basal. Data represented as mean ± SEM. two-way ANOVA with multiple comparisons with Tukey's test. ****p<0.0001, n.s; not significant.

PDE4B was overexpressed in bovine ZG cells. Cell lysates were used for western blot as shown in Figure 3.12A and equal loading was confirmed by GAPDH. Media of the same cell lysates was used to produce aldosterone ELISA data as shown in Figure 3.12B. ZG cells cultured in 12-well plate were treated with 5 µM Fsk, 100 nM ANP and 100 nM AngII. 30 min pre-treatment with ANP was done before adding the stimulants alone or in combination. As

expected, Fsk and AngII stimulated aldosterone production (~6-8-fold) which was inhibited by ANP by (~4-6-fold) pre-incubation in control bovine ZG cells. In PDE4B overexpressed cells, aldosterone production is blunted in Fsk and AngII stimulated cell. This experiment led to the conclusion that AngII/cAMP pathway led to increased aldosterone production.

3.8 Activation of cAMP/PKA pathway by AngII-stimulation

As mentioned in section 1.6, increase in intracellular cAMP activates PKA activity and downstream phosphorylation processes. To investigate whether cAMP activated by AngII-stimulation also translates into higher PKA activity, bovine ZG cells were transduced with AKAR3 biosensor (2.2.7.3).

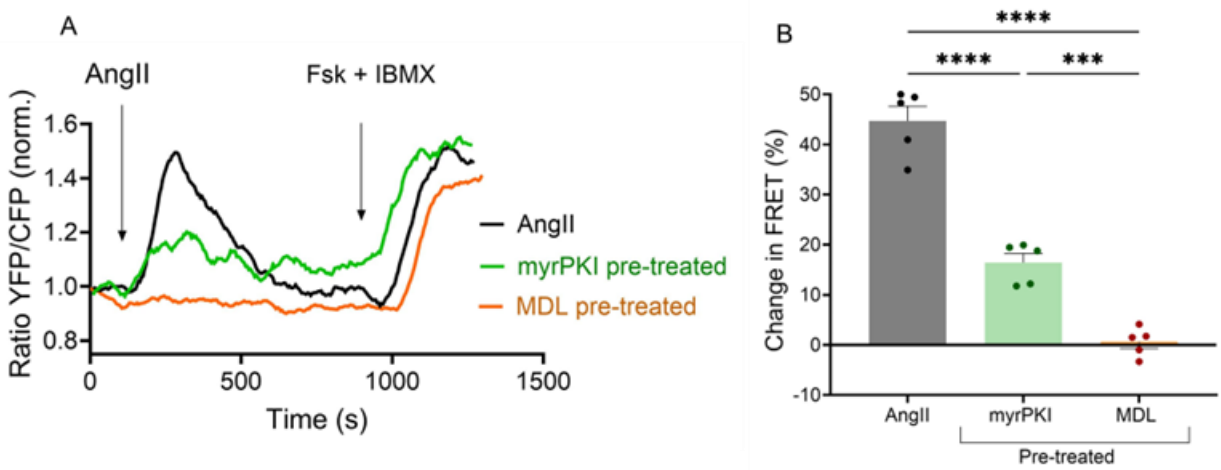

Figure 3.13 Activation of cAMP/PKA pathway by AngII

(A) Bovine ZG cells transduced with AKAR3 biosensor were stimulated with 100 nM AngII followed by 10 µM Fsk and 100 µM IBMX (maximal sensor response). In ZG cells pre-treated with 30 µM myrPKI, a PKA inhibitor or 100 µM MDL, an adenylyl cyclase inhibitor, the AngII response is diminished. (B) Quantification of change in FRET responses (%). AngII treatment alone showed ~45% relative increase in PKA activity. This effect was abolished by myrPKI (down to ~15%) and MDL pre-treatment which led to negligible AngII stimulated PKA activity. Data represented as mean ± SEM. One-way ANOVA by multiple comparison with Tukey's test. ***p<0.001, ****p<0.0001.

When bovine ZG cells were transduced with adenovirus expressing AKAR3 biosensor, AngII-stimulation showed an increase in PKA activity as represented by YFP/CFP ratio in Figure

3.13A. Here, increase in FRET represented an increase in PKA activity. When ZG cells were pre-treated for 30 min with 30 µM myrPKI (PKA inhibitor) and 100 µM MDL (adenylyl cyclase inhibitor), the PKA activity after AngII-stimulation was reduced by ~30% and ~90%, respectively Figure 3.13B.

To investigate if AngII stimulated PKA activity translates into aldosterone levels, bovine ZG cells were pre-treated for 30 min with 30 µM myrPKI and 100 µM MDL before adding AngII for 1 h.

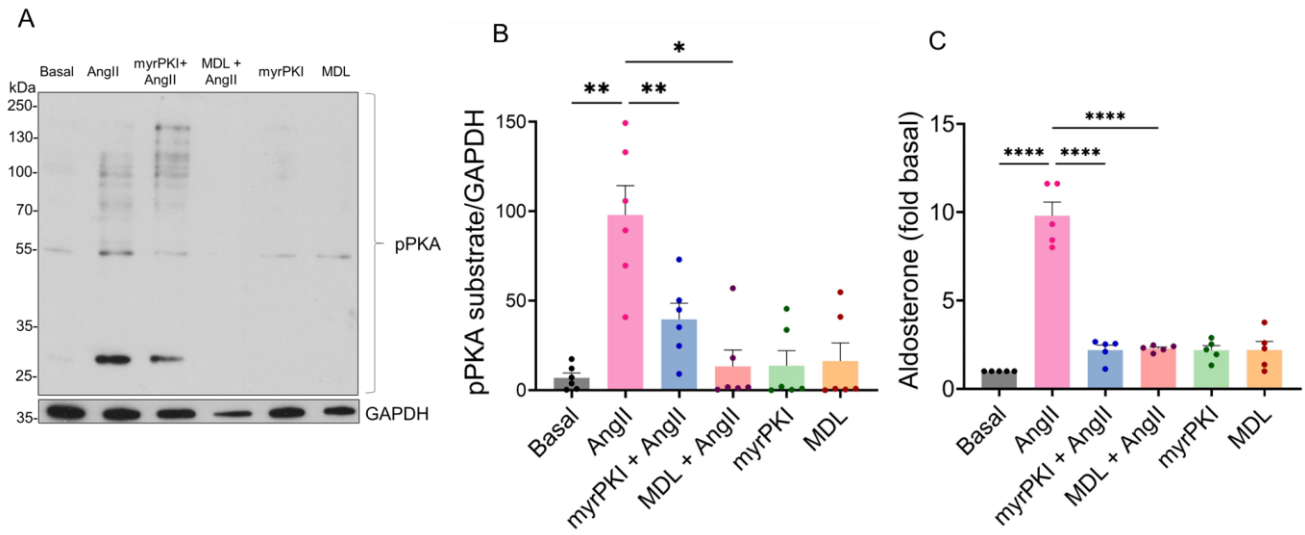

Figure 3.14 Inhibition of AngII activated cAMP/PKA pathway

(A) Western blot analysis of phosphorylated PKA (pPKA) substrates with GAPDH as loading control. (B) Quantification of western blot showed inhibition of AngII stimulated pPKA substrates by 30µM myrPKI and 100 µM MDL after 100 nM AngII-stimulation. (C) AngII stimulated aldosterone production is significantly decreased when inhibited by myrPKI or MDL. Data represented as mean ± SEM. ordinary one-way ANOVA (B) and non-parametric Friedman test (C) followed by multiple comparison test. *p<0.05, **p<0.01, ****p< 0.0001.

Bovine ZG cell lysates were used for western blot Figure 3.14A and quantification Figure 3.14B. Media was used for aldosterone ELISA Figure 3.14C. By blocking PKA with PKA inhibitor/ myrPKI or AC with MDL, AngII stimulated PKA substrates and aldosterone production

were strongly attenuated. This showed that AngII/AT_1R stimulation activated cAMP/PKA pathway to further phosphorylate substrates leading to aldosterone production.

Collectively, these findings suggest that Ca^{2+}, via Ca^{2+}-activated adenylyl cyclase and cAMP synthesis, engages cAMP/PKA pathway to stimulate aldosterone production.

4 Discussion

Aldosterone is one of the key hormones under the regulation of renin-angiotensin-aldosterone system or RAAS to modulate blood pressure and blood volume. Dysregulation of RAAS and mainly aldosterone can lead to cardiovascular, metabolic and renal diseases. Patho-physiology of RAAS is complex as well as crucial in maintaining homeostasis. Factors such as low sodium, potassium or reduced blood volume can trigger the RAAS cascade leading to vasoconstriction, natriuresis or diuresis.

The classical RAAS pathway is outlined as renin-ACE-AngII-AT_1R (0). Around 1990s, AT_2R was discovered along with Mas receptors acting via the ACE2-Ang (1-7)-Mas axis known as protective RAAS mechanism. Protective RAAS counters classical AT_1R RAAS mechanism by having vasodilatory effects (Ruan *et al.*, 2024; Villela *et al.*, 2015). Since it is an endocrine, autocrine and paracrine system, inhibitors and blockers act directly on the pathway as well as receptors of affecting organs. Aldosterone binds to the mineralocorticoid receptor in target cells to facilitate sodium and water reabsorption and potassium excretion.

Different inhibitors and approved drugs are:

- ACE inhibitors: block the conversion of AngI to AngII (e.g. ramipril, enalapril).
- Direct renin inhibitors: inhibit renin which is the first enzyme of RAAS (e.g aliskiren, remikiren).
- Angiotensin receptor blockers (ARBs): prevents biding of AngII to its receptor (e.g. losartan, telmisartan)
- Mineralocorticoid receptor antagonists or aldosterone antagonists: block the action of aldosterone (e.g. spironolactone, eplerenone)

Given its complexity and intricate networks of peptides, enzymes and receptors, drug development for RAAS is an active research area since the mechanisms are still being uncovered (Thatcher, 2017).

The aim of this thesis was to elucidate potential molecular mechanism/s of acute AngII-inhibition by ANP in ZG cells. For this, bovine adrenal ZG cells were cultured for 24-48 h followed by CRISPR/Cas9 PDE2A KO generation for live-cell imaging using FRET technique and aldosterone measurements using ELISA.

4.1 Validation of isolation by immunohistochemistry

Adrenal bovine ZG cell isolation protocol has been previously established (Nikolaev *et al.*, 2005) and elaborated in Figure 2.2. To validate it in this project, ZG cells were stained with aldosterone synthase (CYP11B2) (Gomez-Sanchez *et al.*, 2013) and *Dab2* (Romero *et al.*, 2007). CYP11B2 is the final enzyme in aldosterone biosynthesis pathway. The development of such staining antibodies against human adrenals allowed the visualization of aldosterone synthase in normal vs aldosterone producing adenomas (APAs). APAs testing positive for CYP11B2 clusters were found in patients with PA not only in ZG cells but also surrounding tissue highlighting the importance of such antibodies to identify mutations from patients' samples with hyperaldosteronism (Fernandes-Rosa *et al.*, 2015). *Dab2* is a phosphoprotein that co-localizes with CYP11B2 and loses its expression when ZG cells trans-differentiate to ZF cells. It has been shown in some patients that in APA cells, *dab2* expression is absent and could act as a differential marker for ZG cells and APAs. It has been shown in some patients that in APA cells, dab2 expression is absent and could act as a differential marker for ZG cells and APAs (Boulkroun *et al.*, 2010; Seccia *et al.*, 2017).

Antibodies against CYP11B2 and *Dab2* are ZG specific and as seen from Figure 2.2, both markers were expressed in virtually all primary culture of bovine adrenal ZG cells isolated for the purpose of this thesis.

4.2 Acute AngII-stimulated aldosterone production inhibited by ANP is cGMP-dependent but not Ca^{2+}-dependent

Several signaling pathways are known to regulate aldosterone production. ACTH, K^+ and AngII are widely known stimulants of aldosterone production. Their mechanism of action includes but is not limited to cAMP-dependent PKA activation, increase in Ca^{2+} oscillation and activation of protein kinase C (Gambaryan *et al.*, 2003) . Aldosterone production is controlled by natriuretic peptides and nitric oxide (NO). Steroidogenesis can also be regulated by nitric oxide. It has been well established that nitric oxide inhibits ACTH and AngII-induced aldosterone production (Hanke *et al.*, 2000; Natarajan *et al.*, 1997). Although the NO-cGMP pathway is well established in vascular and endothelial cells, few studies report that inhibition of aldosterone by nitric oxide is a GC-A independent effect (Ichiki *et al.*, 1998; Kreklau *et al.*, 1999; Sainz *et*

al., 2004). One study in bovine adrenal ZG cells reported that AngII stimulated aldosterone production was inhibited by deta nonoate (Diethylamine NONOate), a NO donor, without increasing intracellular cGMP concentrations (Hanke *et al.*, 1998) .

It is also known that acute aldosterone stimulated by AngII is inhibited by cardiac peptide hormone ANP by acting on GC-A receptor of ZG cells. This leads to increase in cGMP that activates PDE2 to further hydrolyze cAMP. This ANP/GC-A/cGMP pathway is established and known to inhibit ACTH/cAMP induced aldosterone production (Schieblnger *et al.*, 1988). The exact mechanism for ANP inhibition of aldosterone stimulated by AngII is ambiguous.

Here, in control ZG cells, the inhibition by ANP is first shown by aldosterone ELISA. Primary cultured bovine ZG cells were pre-incubated with ANP for 30 min followed by AngII-stimulation for 1 h. Aldosterone was produced in serum free media and as seen before, ANP inhibits AngII-stimulated aldosterone production. When ZG cells were transduced with SponGee to render intracellular cGMP and related downstream pathways inactive, the AngII-stimulated inhibition by ANP was blunted, see Figure 3.4. This led to the conclusion that inhibition by ANP is cGMP-dependent.

Studies in rat ZG cells showed the importance of cGMP-dependent PKG. One study showed that RAAS activation by low sodium diet in rats upregulated PKG II expression but not PKG I. This was based on the fact that PKG II is expressed in ZG cells whereas PKG I is restricted to blood vessels and capsule of adrenal gland.(Gambaryan *et al.*, 2003) Plasma aldosterone levels were enhanced in rats overexpressing PKG II in ZG cells. Activation or inhibition of PKG II showed direct synergetic effects on AngII or ACTH induced aldosterone production. These PKG II activators or inhibitors used do not affect phosphodiesterase. Although this was not observed in H295R cells as they do not express PKG II (Butt *et al.*, 1992). Gene regulation of StAR protein in isolated ZG cells from rats was shown to be unaffected by PKG II activation indicating that PKG II could be important for moderating basal aldosterone production. This further elaborated on the fact that StAR protein is phosphorylated by PKGII and hence is necessary for aldosterone production (MacFarland *et al.*, 1991). On the contrary, a study in PKG II knockout mice reported that negligible changes were detected in basal, ACTH or AngII-stimulated plasma aldosterone levels. Inhibition by ANP was also not significantly different between ACTH stimulated and basal aldosterone levels in PKG II knockout mice *in vivo* (Spießberger *et al.*, 2009). Both studies in rats and mice showed activation of PDE2 lead to a

decrease in ACTH-stimulated aldosterone production by decreasing cAMP levels. Given the differences between above rats and mice studies (*In vitro* vs *in vivo*) the role of PKG II in aldosterone production needs further elaboration. It is also acknowledged that rat and mice adrenal are small in size and yield low number of ZG cells and hinder direct results. For this reason, bovine adrenal ZG cells were used for the purpose of this thesis.

PKG also phosphorylates RGS proteins that act as GTPase-activating proteins (GAPs). RGS proteins are responsible for deactivating G-proteins and their downstream pathways. Mainly, RGS2 and RGS4 that are expressed in ZG cells, play a role in inactivating AngII/AT_1R pathways including the ones responsible for increasing intracellular Ca^{2+} for aldosterone production. RGS proteins via GAPs promote vasodilation to regulate blood pressure in the body by regulating aldosterone production (Lymperopoulos and Stoicovy, 2024; Romero *et al.*, 2006).

Role of RGS2 proteins has also been previously shown in cardiomyocytes in modulating Ca^{2+} inhibition. ANP inhibition in mice cardiac myocytes deficient in RGS2 showed no response to AngII (Klaiber *et al.*, 2010). RGS4 has also been reported to affect AngII-stimulated aldosterone production by regulating Ca^{2+}/CaMKs and protein kinase C in H295R cells. H295R cells are AngII-responsive steroid producing adrenocortical cell line. Using an ANP-analogue M-atrial natriuretic peptide (MANP), the authors demonstrated inhibition of Ca^{2+} response induced by AngII (Chen *et al.*, 2021; Chen, Iyer, *et al.*, 2022). Although there are drawbacks of using cell lines. These cells are devoid of ANP receptor and PKG II essential for studying aldosterone production. They tend to lose cellular receptors and cell signaling pathways during prolonged passages. Receptors are transfected or transduced into these cells making them artificial as cell lines usually lose most of their natural cell properties. The current work used primary bovine adrenal ZG cells cultured for a maximum of 72-96 h. Primary cells also allow us to study cross-talk between signaling pathways (such as cAMP-cGMP cross-talk relevant in this study) that are otherwise lost in cell lines.

Primary bovine ZG cells were incubated with Calbryte dye followed by AngII-stimulation to generate Ca^{2+} sparks. Using Calbryte 520 AM, fluorescent changes in ZG cells were seen in terms of AngII-induced Ca^{2+} oscillations represented by Ca^{2+} peaks from baseline. From Figure 3.5, it was seen that ANP/cGMP effect does not affect AngII induced Ca^{2+} transients. Calbryte

is a chemical dye that has a brighter signal and response upon Ca^{2+} binding as compared to commonly used Fluo-4 dyes (Dinh *et al.*, 2024). This argues that PKG/RGS dependent mechanisms do not play considerable role under in bovine ZG cells under our experimental conditions. ANP stimulation also had negligible effect on PKA/PKG substrate phosphorylation as compared to AngII that showed strong activation of PKA/PKG substrates as shown by western blot (Figure 3.6) suggesting the involvement of other pathways in acute AngII-inhibition by ANP.

4.3 Inhibition of AngII-stimulated aldosterone by ANP is PDE2A dependent

Since ANP/GC-A/cGMP pathway hydrolyze cAMP via PDE2, primary bovine ZG cells were transduced with gRNAs and Cas9 to generate PDE2A knockouts. Non-homologous end joining method was used to generate CRISPR/Cas9 knockouts as the gRNAs guide the Cas9 to the target region followed by double strand breaks in the DNA. CRISPR/Cas9 technique is inspired by natural defense mechanism of bacteria that has been modified into a powerful gene editing method using one or two guide RNAs that direct Cas9 enzyme to make cuts in the DNA at a target site. The DNA is then repaired using the cells natural mechanism. For generating *in vitro* CRISPR/Cas9 PDE2A knockouts, exon 18 of bovine PDE2A gene was targeted using two gRNAs as described in 1.7.

Since *in vitro* knockout generation is a precision based technique, it was important to validate PDE2A knockout both at protein level and on the basis of its functionality as seen in 3.4. Using western blot technique, it was shown that there was ~80% loss of PDE2A activity in ZG KO cells as compared to control. Anti-GAPDH primary antibody was used as loading control and to normalize PDE2A. For functional validation of PDE2A KO, ZG cells transduced with Epac2-camps biosensors were stimulated with Bay 60-7550. Bay 60-7550, a PDE2 inhibitor that led to increase in cAMP activity by ~25% represented by a decrease in FRET in control cells. In PDE2A KO cells, Bay response was blunted confirming the CRISPR/Cas9 model functionally. Live-cell imaging using FRET microscopy technique is a useful method in monitoring cyclic nucleotide and protein kinase activity real time using biosensors. The distance between two fluorophores YFP and CFP determines the energy transferred upon stimulation and based on the structure of the biosensor depicts an increase or decrease in FRET signal. The FRET signal can then be normalized to a baseline signal before adding simulants or to the maximal sensor response. IBMX, a non-selective phosphodiesterase inhibitor was used to generate

maximal sensor response. These biosensors can be localized to nuclear membrane, cytoplasm, plasma membrane etc., based on experimental requirements.

By monitoring the real-time activity of cAMP, it has been reported earlier that ANP degrades Forskolin stimulated cAMP via PDE2 using Epac2-camps FRET biosensor (Nikolaev *et al.*, 2005). ANP via PDE2 also degrades ACTH activated cAMP to regulate aldosterone production (Spießberger *et al.*, 2009). Since PDE2 is highly expressed in ZG cells, and for this thesis bovine PDE2A KO were generated, FRET experiments were performed to elaborate on the mechanisms. Epac2-camps transduced bovine ZG cells showed cAMP activation ~10 fold in control and PDE2A KO cells. ANP via rapid PDE2A kinetics, degraded this cAMP in control cells but not in PDE2A KO cells after which cAMP activity was restored in control cells but was negligible in PDE2A KO cells after Bay 60-7550 stimulation. Aldosterone ELISA was performed using media of primary cultured bovine ZG control and PDE2A KO cells. Aldosterone ELISA is a quantitative tool for measuring the steroid hormone aldosterone. It is based on competitive immunoassay as mentioned in 2.2.3. Cells were pre-incubated with ANP followed by AngII-stimulation. Control and PDE2A KO cells showed ~8-fold increase in AngII-stimulated aldosterone production. ANP inhibited AngII-stimulated aldosterone in control cells but not in PDE2A KO cells. There was no significant difference between AngII-stimulated vs ANP pre-incubated AngII-stimulated aldosterone produced in PDE2A KO cells. From Figure 3.9 and Figure 3.10 it can be concluded that ANP via PDE2A modulates cAMP dynamics. This also suggests that PDE2A mediated ANP inhibition is cAMP-dependent.

Whole exome sequencing of patients from Brazilian population with bilaterial adrenal hyperplasia, which is a cause of familial primary aldosteronism was performed by (Rassi-Cruz *et al.*, 2021). Patients with rare germline mutation in PDE2A (p.Ile629Val) and PDE3B (p.Arg217Gln and pGly392Val) were identified. As expected, PDE2A and CYP11B2 staining was high in ZG cells and early onset hypertension was diagnosed in patients with PDE2A variant mutation. Patients with these mutations also showed higher PKA activity and thus higher plasma aldosterone levels as compared to patients with APAs. At molecular level, this PDE2A mutation showed lower PDE2A protein expression providing a mechanical link between PDE2A and increased hypertension in these patients. The paper concluded that PDE2A and PDE3B variants are associated with PA caused by bilateral adrenal hyperplasia.

High plasma aldosterone concentrations were detected in human patients only with PDE2A mutation highlighting its importance in acute aldosterone regulation in ZG cells.

Role of PDE2A has been shown in ANP/cGMP mechanism to inhibit aldosterone production in H295R cells (Chen *et al.*, 2021; Chen, Iyer, *et al.*, 2022). Partial inhibition by ANP was also demonstrated after acute AngII-stimulated increase in Ca^{2+} transients and aldosterone production. Although several papers have pointed out species variation between humans, rats, mice and bovine adrenal ZG cells and mechanism for aldosterone production and inhibition (Gambaryan *et al.*, 2003; Spießberger *et al.*, 2009). This thesis on bovine adrenal ZG cells and their primary culture aims to highlight the mechanisms involved in aldosterone regulation that could potentially be used for further therapeutics.

4.4 Activation of cAMP/PKA pathway by AngII-stimulation is inhibited by ANP

As highlighted earlier the role of PDE2A in degrading cAMP, it was important to investigate the role of AngII in cAMP activation as a potential pathway. Epac2-camps biosensor was used to monitor relative cAMP in bovine ZG cells after AngII stimulation. FRET experiments (Figure 3.11) showed that cAMP activated by AngII is also rapidly degraded by ANP. Forskolin and IBMX were used following ANP stimulation to generate maximal cAMP response by Epac2-camps sensor.

The importance of intracellular cAMP in regulating aldosterone production was validated using PDE4B adenoviral overexpression in primary cultured bovine ZG cells. It has been shown in other cell types such as heart that PDE4 degrades cAMP and Ca^{2+} signaling. Their study in mice reported that cardiac excitation-contraction coupling in subcellular microdomains is regulated by cAMP and varying effects of PDE4 activity can lead to arrythmias or heart failure. PDE4B and PDE4D knockout mice showed decrease in cAMP levels by live cell imaging correlating with microdomain specific PKA activity (Kraft *et al.*, 2024).

Overexpressing PDE4B in bovine ZG cells showed that aldosterone is completely inhibited as compared to control cells. Figure 3.12 showed inhibition of Forskolin and AngII-stimulated aldosterone by ANP pre-incubation in control cells as expected. In PDE4B overexpressed cells complete inhibition is shown rendering cAMP and downstream PKA pathways inactive suggesting the role of AngII-stimulated cAMP/PKA pathway.

In response to external stimuli, the second messenger cAMP regulates multiple responses in a cell as it is known to be compartmentalized in subcellular and microdomains. Studies have also shown PKA compartmentalization with A-kinase anchoring proteins (AKAPs) that are scaffolding proteins attached to PKAs at specific subcellular locations. The cAMP/PKA signaling hubs are uniquely coordinated by AKAPs based on proximity to generate distinct subcellular responses (Kovanich *et al.*, 2023). It is therefore important to target disease specific subcellular signaling locations for precise disease management. Discovering molecular pathways and signaling pools helps to bridge the translational gap between basic science and clinical application. As mentioned in several studies, combination therapy to target RAAS inhibition or non-steroidal mineralocorticoid receptor antagonist could be an approach for diseases such as heart failure, hypertension, chronic kidney disease or diabetic nephropathy (Dreher *et al.*, 2025; Li *et al.*, 2025; Weir and Bakris, 2008; Whitlock *et al.*, 2023).

PKA activity was monitored using AKAR3 biosensor that shows increase in FRET upon AngII-stimulation indicating increase in PKA activity by cAMP activation after PKA phosphorylates the AKAR3 biosensor at the pSite. Figure 3.14 showed that PKA activity as seen by transient with AngII stimulation is diminished after myrPKI (PKA inhibitor) and almost blunted after MDL (AC blocker) pre-incubation. This suggests that inhibiting PKA activity or blocking adenylyl cyclases hinder AngII-stimulated cAMP activity. Cultured bovine ZG cells were pre-incubated with myrPKI, or MDL followed by AngII stimulation. Anti-phospho-PKA substrate antibody was used to detect the phosphorylated proteins after western blot. After normalizing to GAPDH it was seen that there was a significant reduction in phosphorylated PKA substrates. This is also translated to aldosterone levels. It was seen that there was significant reduction in aldosterone production after pre-incubating with the inhibitors and as measure by ELISA.

Aldosterone levels and phosphorylated substrates inhibition by myrPKI or MDL shown in Figure 3.14. Since PKA activity is relative to cAMP levels and as concluded earlier that AngII-stimulation leads to increase in intracellular cAMP levels, these experiments led to a novel finding that AngII/AT_1R pathway is acting via cAMP/PKA pathway to regulate aldosterone production that is inhibited by ANP/GC-A/cGMP pathway.

As mentioned before, AngII/AT_1R pathway activates intracellular Ca^{2+}-oscillations to regulate aldosterone production 1.6.4. It has been reported that downstream molecular effects after

AngII or ACTH stimulation leading to increase in cAMP or Ca^{2+} are mediated by Ca^{2+}/calmodulin dependent protein kinases or CaMKs. The authors showed that aldosterone production is inhibited after AngII or ACTH stimulation using CaMKs inhibitor KN93 in rat and bovine ZG cells. They also reported that CaMK activity stimulated by cAMP is PKA independent and proposed the involvement of EPAC signaling pathway. Epac2, known to be highly expressed in ZG cell, regulates aldosterone production by activating small GTPases Rap1 and Rap2 in response to increase in cAMP levels. This signaling pathway acts independently of PKA activation although the authors acknowledge that the exact mechanism is not identified along with several unidentified cAMP mediators to regulate aldosterone production (Gambaryan *et al.*, 2006).

It has also been established that intracellular Ca^{2+} activate adenylyl cyclase (AC1, AC3 or AC8) to regulate critical mechanisms in heart, brain and in neurodevelopmental disorders which also establish a mechanism for a positive crosstalk between Ca^{2+} and cAMP levels (Chen, Ding, *et al.*, 2022; Ren *et al.*, 2021; Wong *et al.*, 1999). On the contrary studies showed that the capacitive Ca^{2+} influx activated by AngII-stimulation plays a role in bovine adenylyl cyclase activation namely AC3 (Burnay *et al.*, 1998). With the results from this thesis, it can be established that AngII stimulates Ca^{2+} activated AC to modulate cAMP/PKA pathway and thus regulate aldosterone production and can be considered as one potential molecular mechanism.

ZG cells mainly express two types of VGCC, and their subtypes vary between species. High voltage activated are L-type calcium channels with $Ca_V1.1$-1.4 subtypes and low voltage activated T-type calcium channels $Ca_V3.1$-3.3 subtypes. ACTH/cAMP/PKA mediated phosphorylation of L-type calcium channels play a role in aldosterone production via calcium activated adenylyl cyclase (Gallo-Payet *et al.*, 1996; Kojima *et al.*, 1985). Different studies in animals or cell lines have suggested that t-type calcium channels play a role in aldosterone secretion. On the other hand, clinical research in human patients with PA showed somatic mutations in L-type calcium channels. Clinical data also show that aldosterone producing adenomas can be caused by somatic mutations in L-type calcium channels. Their study showed that inhibiting T and L-type calcium channels by TTA-P2 or nifedipine respectively, inhibited basal aldosterone levels and AngII or potassium stimulated aldosterone production in human adrenal slices (Barrett et al., 201; Dinh et al., 2024). Since VGCC plays an important

role in aldosterone production and a recent study in murine ZG cells published that L-type calcium channels ($Ca_V1.2/1.3$) and not T-type calcium channels ($Ca_V3.2/3.3$) are responsible for calcium oscillations and aldosterone production, this could potentially be a pharmacological target as each subtype show a unique function required for aldosterone production in healthy or diseased patients (Barrett *et al.*, 2021).

Although VGCC and subtypes of T and L-type calcium channels are not studied in this thesis, the findings from this thesis can be used to elucidate a further role of AngII-stimulated Ca^{2+} activated AC and their role in aldosterone production.

AngII can lead to aldosterone synthesis not only via $AT_1R/G_{q/11}$ signaling pathway but also via β-arrestin-1 and 2 (βarr1 or βarr2). β-arrestins are heptahelical receptor proteins or adapter proteins that co-localize with GPCR to elicit response by activating or deactivating them triggering different signaling pathways. AngII/AT_1R/βarr results in activation of the extracellular signaling-regulated kinase (ERK) and subsequent StAR phosphorylation for aldosterone biosynthesis. Surprisingly, stimulating aldosterone with AngII analog and AT_1R agonist, SII, initiates a receptor interaction without coupling to GPCR to facilitate βarr-mediated aldosterone synthesis. The authors also reported that stimulating H295R cells with SII overexpressed with βarr1 induced StAR upregulation and aldosterone secretion. They also showed that plasma aldosterone levels were increased in rats overexpressing adrenal specific βarr1 as compared to control(Lymperopoulos et al., 2009a, 2024). Alternatively, βarrs are known to regulate GPCRs in cardiomyocytes and have cardioprotective effects (Lymperopoulos, 2018; Lymperopoulos and Aukszi, 2017; Mathieu *et al.*, 2023) and in pathogenesis of various brain disorders including Alzheimer's disease (Azam *et al.*, 2020; Ferguson *et al.*, 1996; Kee *et al.*, 2024).

Further studies on co-localization of βarr with AngII and the involvement of cardiac natriuretic peptides in adrenal ZG cells are needed for this to be a potential alternate pathway in aldosterone regulation and related diseases.

Since excessive aldosterone causes hypertension and heart failure progressions, uncovering novel pathways such as AngII/ Ca^{2+}/cAMP/PKA signaling pathway and intervening by using ANP-analogs can provide clinical significance for reducing aldosterone synthesis apart from the direct use of aldosterone synthase inhibitors. Even though new studies show that aldosterone synthase inhibitors can be used as therapy to regulate hypertension, artificial ANP

analogues such as M-atrial natriuretic peptide (MANP) could be a better choice. ANP analogues not only focus on treating hypertension but also focus on balancing negative aldosterone effects on cardiovascular and renal system making this study essential as it focuses on uncovering new pathways. Therefore, based on the findings from this thesis we can conclude that cAMP/PKA pathway activated by AngII/AT_1R could potentially be mediated via Ca^{2+} and Ca^{2+} activated adenylyl cyclase. This pathway is inhibited by the rapid kinetics of ANP activated cGMP-dependent PDE2A degradation and can be a target for the development of future generation drugs to regulate aldosterone biosynthesis.

5 Zusammenfassung/Abstract

5.1 Zusammenfassung

Aldosteron, ein Steroidhormon, das Teil des Renin-Angiotensin-Aldosteron-Systems (RAAS) ist, spielt eine entscheidende Rolle bei der Regulation des Blutdrucks und des Blutvolumens. Aldosteron wird von spezialisierten Zellen der Nebennieren, den sogenannten *Zona glomerulosa* (ZG)-Zellen, produziert, die sich in der äußersten Schicht der Nebennierenrinde befinden, die an der Kapsel befestigt ist. Eine Dysregulation von Aldosteron kann zu elektrophysiologischen Ungleichgewichten führen, die Herz-Kreislauf- und Nierenerkrankungen wie Bluthochdruck, Hypokaliämie oder Alkalose verursachen. Daher sind Inhibitoren der Aldosteronsynthase und der Aldosteronrezeptoren für die Behandlung von Bluthochdruck, Herzinsuffizienz und damit verbundenen Erkrankungen von entscheidender Bedeutung. Es ist bekannt, dass Adrenokortikotropes Hormon (ACTH), Angiotensin II (AngII) und Kalium (K+) die Aldosteronproduktion stimulieren. Die Herzvorhöfe produzieren und sezernieren als kardioprotektiven Mechanismus atriales natriuretisches Peptid (ANP) als Reaktion auf Hypervolämie und Hypertonie aufgrund von Hyperaldosteronismus. Die Expression und Aktivität von Aldosteron auf molekularer Ebene wird durch zyklische Nukleotide und Phosphodiesterasen gesteuert. ACTH stimuliert durch Erhöhung des intrazellulären cAMP die Aldosteronproduktion. K^+ induziert einen Ca^{2+}-Einstrom durch Depolarisierung spannungsgesteuerter Kalziumkanäle. AngII aktiviert über seinen Angiotensin-1-Rezeptor (AT_1R), einen G-Protein-gekoppelten Rezeptor, die Phospholipase C, um das intrazelluläre Ca^{2+} zu erhöhen und die Produktion von Aldosteron zu stimulieren. ANP führt über seinen GC-A-Rezeptor zu einer erhöhten cGMP-Konzentration, die die Phosphodiesterase Typ 2 (PDE2A) aktiviert, um ACTH-stimuliertes cAMP abzubauen und die Aldosteronproduktion zu hemmen. ANP hemmt auch die durch AngII/AT_1R stimulierte Aldosteronproduktion, und obwohl der genaue molekulare Mechanismus unbekannt ist, wurde vermutet, dass dies über PDE2A geschieht.

In dieser Arbeit wurden bovine Nebennieren-ZG-Zellen isoliert und kultiviert, um CRISPR/Cas9-in-vitro-Knockouts (KO) von PDE2A durchzuführen, um einen Funktionsverlust zu erzielen. Aus Lysaten der Primärzellkultur wurde ein Western Blot durchgeführt, um das Knockout-Modell zu validieren und weitere Proteinanalysen durchzuführen. Das Zellmedium wurde verwendet, um einen Aldosteron-ELISA durchzuführen und die Aldosteronkonzentrationen nach Vorinkubation mit ANP und Zugabe von Stimulanzien wie Forskolin und AngII zu messen. Die intrazelluläre cAMP- und PKA-Aktivität wurde ebenfalls

unter Verwendung der Förster-Resonanz-Energie-transfer-Technik (FRET) gemessen. Echtzeitänderungen der cAMP-Spiegel und der PKA-Phosphorylierung wurden unter Verwendung von Epac2-camps bzw. AKAR3-Biosensoren durch Beobachtung der Veränderungen der FRET-Signale beobachtet.

Die ersten Experimente wurden durchgeführt, um das Isolierungsprotokoll mittels Immunfärbung unter Verwendung von Aldosteronsynthase (CYP11B2)- und Disabled-2 (*Dab2*)-Antikörpern zu validieren. Aldosteron-ELISA-Messungen zeigten, dass das durch AngII stimulierte und durch ANP gehemmte akute Aldosteron cGMP-abhängig, jedoch nicht kalziumabhängig (Ca^{2+}) ist. Ca^{2+} Transienten wurden unter Verwendung des Farbstoffs Calbryte 520 AM mit und ohne ANP-Vorinkubation gefolgt von AngII-Stimulation beobachtet. Die CRISPR/Cas9-generierten PDE2A-KO-ZG-Zellen wurden etabliert und unter Verwendung der FRET-Technik validiert. Diese Ergebnisse zeigten auch, dass die inhibitorischen Effekte des ANP/GC-A/cGMP-Signalwegs in PDE2A-KO-Zellen im Vergleich zu Kontrollzellen aufgehoben waren. Dies wurde auch durch den Aldosteron-ELISA bestätigt, bei dem die Hemmung durch ANP in PDE2A-KO-Zellen aufgehoben wurde, was auf eine wichtige Rolle von PDE2A bei der ANP-gesteuerten Kinetik des cAMP-Abbaus hindeutet. ANP baute auch das durch AngII stimulierte cAMP ab, was darauf hindeutet, dass der Mechanismus cAMP-abhängig sein könnte. Bei Überexpression von PDE4B zum Abbau von cAMP zeigte sich, dass die Aldosteronproduktion vollständig unterbunden werden konnte. Unter Verwendung des AKAR3-Biosensors und des phosphorylierten PKA/PKG-Substrat-Antikörpers wurde eine Hemmung der PKA durch MyrPKI und den Adenylylcyclase-Blocker MDL beobachtet, was zu einer Abnahme der durch AngII stimulierten cAMP/PKA-Aktivität führte. Dies spiegelte sich auch in den Aldosteronspiegeln wider, was die Rolle des cAMP/PKA-vermittelten Signalwegs unterstreicht. Die neue Erkenntnis dieser Arbeit war, dass AngII den cAMP/PKA-Signalweg durch akute Stimulation von Ca^{2+} und Ca^{2+}-abhängiger Adenylylcyclase (AC) aktiviert, die nachweislich durch ANP abgebaut wird.

Da der ANP/GC-A/cGMP-Signalweg den durch AngII akut stimulierten cAMP/PKA-Signalweg für die Aldosteronproduktion über eine schnelle PDE2A-Kinetik hemmt, könnten neue therapeutische Ansatzpunkte für diesen Mechanismus bei Aldosteron-assoziierten Erkrankungen entwickelt werden.

5.2 Abstract

Aldosterone, a steroid hormone as part of the renin-angiotensin-aldosterone system plays a crucial role in regulating blood pressure and blood volume. Aldosterone is produced by specialized cells of adrenal glands known as *zona glomerulosa* (ZG) cells present on the outermost layer of adrenal cortex attached to the capsule. Dysregulation of aldosterone can cause electrophysiological imbalances leading to cardiovascular and renal diseases such as hypertension, hypokalemia or alkalosis. As such, inhibitors of aldosterone synthase and receptors are crucial for the treatment of hypertension, heart failure and associated diseases. It is established that adrenocorticotropic hormone (ACTH), angiotensin II (AngII) and potassium (K^+) stimulate aldosterone production. Cardiac atria produce and secrete atrial natriuretic peptide (ANP) in response to hypervolemia and hypertension due to hyperaldosteronism as a cardioprotective mechanism. Expression and activity of aldosterone at molecular level is controlled by cyclic nucleotides and phosphodiesterases. ACTH by increasing intracellular cAMP stimulates aldosterone production. K^+ induces an influx of Ca^{2+} by depolarizing voltage gates calcium channels. AngII via its angiotensin 1 receptor (AT_1R), a G-protein coupled receptor, activates phospholipase C to increase intracellular Ca^{2+} and stimulate the production of aldosterone. ANP via its GC-A receptor leads to increased cGMP concentration that activates phosphodiesterase type 2 (PDE2A) to degrade ACTH stimulated cAMP and inhibit aldosterone production. ANP also inhibits AngII/ AT_1R stimulated aldosterone production, and although the exact molecular mechanism is unknown, it was speculated to do so via PDE2A.

In this thesis, bovine adrenal ZG cells were isolated and cultured to perform CRISPR/Cas9 *in vitro* knockouts (KO) of PDE2A to have loss of function. From primary cell culture lysates, western blot was performed for validating the knockout model and further protein analysis. The cell media was used to perform aldosterone ELISA and measure aldosterone concentrations after pre-incubating with ANP and adding stimulants such as Forskolin (Fsk) and AngII. Intracellular cAMP and PKA activity were also measured using Förster resonance energy transfer (FRET) technique. Real time changes were shown in cAMP levels and PKA phosphorylation by using Epac2-camps and AKAR3 biosensor respectively by observing changes in FRET signals.

The first experiments were conducted to validate the isolation protocol using immunostaining using aldosterone synthase (CYP11B2) and disabled-2 (*Dab2*) antibodies. Aldosterone ELISA measurements showed that acute aldosterone stimulated by AngII, inhibited by ANP is cGMP

dependent but not calcium (Ca^{2+}). Ca^{2+} -transients were observed using Calbryte 520 AM dye with and without ANP pre-incubation followed by AngII-stimulation. The CRISPR/Cas9 generated PDE2A KO ZG cells were established and validated using FRET technique. These results also showed that the inhibitory effects of ANP/GC-A/cGMP pathway were abolished in PDE2A KO cells as compared to control cells. This was also proved by aldosterone ELISA where inhibition by ANP was abolished in PDE2A KO cells suggesting a strong role of PDE2A in ANP driven kinetics of cAMP degradation. ANP also degraded cAMP stimulated by AngII suggesting that the mechanism could be cAMP-dependent. Upon overexpressing PDE4B to degrade cAMP, it was shown that aldosterone production could be completely blunted. Using the AKAR3 biosensor and phosphorylated PKA/PKG substrate antibody, inhibition of PKA by myrPKI and adenylyl cyclase blocker, MDL a decrease in AngII stimulated cAMP/PKA activity was seen. This was also translated to aldosterone levels highlighting the role of cAMP/PKA mediated pathway. The novel finding of this thesis was that AngII activates the cAMP/PKA pathway by acutely stimulating Ca^{2+} and Ca^{2+} -dependent adenylyl cyclase (AC) which was shown to be degraded by ANP.

Since ANP/GC-A/cGMP pathway inhibits acute AngII stimulated cAMP/PKA pathway for aldosterone production mediated via rapid PDE2A kinetics, new therapeutic targets for this mechanism could be developed for aldosterone related diseases.

6 List of abbreviations

°C: Degree celsius....22

AC: Adenylyl cyclase.... 8

ACE: Angiotensin converting enzyme.... 4

ACTH: Adrenocorticotropin hormone.... 5

AM: Acetoxymethyl ester....33

AngI: Angiotensin I 4

AngII: Angiotensin II 4

ANP: Atrial natriuretic peptide.... 6

AT_1R: Angiotensin type 1 receptor.... 8

ATP: Adenosine triphosphate 8

Ca^{2+}: Calcium 3

cAMP: 3',5'-cyclic adenosine monophosphate.... 8

CEH: Cholesterol ester hydrolase 8

CFP: Cyan fluorescent protein....43

cGMP: 3',5' cyclic guanosine monophosphate 6

CNBD: Cyclic nucleotide binding domain....43

CREB: cAMP Response Element-Binding protein 8

CRISPR: Clustered regularly interspaces short palindromic repeats 12

Dab2: Disabled-2....23

DAPI: 4',6-diamidino-2-phenylindole....18

DMEM: Dulbecco's Modified Eagle's Medium 18

ELISA: Enzyme linked immunosorbent assay 31

EPAC: Exchange protein activated by cAMP.... 8

FRET: Förster resonance energy transfer 15

YFP: Yellow fluorescent protein.....43

ZF: Zona fasciculata..... 1

ZG: Zona glomerulosa..... 1

ZR: Zona reticularis..... 1

7 References

"Addgene: CRISPR Guide". (n.d.). , available at: https://www.addgene.org/guides/crispr/ (accessed 11 October 2025).

"Aldosterone - an overview | ScienceDirect Topics". (n.d.). , available at: https://www.sciencedirect.com/topics/veterinary-science-and-veterinary-medicine/aldosterone (accessed 29 September 2025).

Alfarano, M., Marchionni, G., Costantino, J., Ballatore, F., Verardo, R., Miraldi, F., Ciciarello, F.L., *et al.* (2025), "Aldosterone-Related Cardiovascular Disease and Benefits of Mineralocorticoid Receptor Antagonists in Clinical Practice", *JACC: Advances*, Elsevier, Vol. 4 No. 6, p. 101762, doi: 10.1016/J.JACADV.2025.101762.

Arakane, F., King, S.R., Du, Y., Kallen, C.B., Walsh, L.P., Watari, H., Stocco, D.M., *et al.* (1997), "Phosphorylation of steroidogenic acute regulatory protein (StAR) modulates its steroidogenic activity", *The Journal of Biological Chemistry*, J Biol Chem, Vol. 272 No. 51, pp. 32656–32662, doi: 10.1074/JBC.272.51.32656.

Ariyeloye, S., Kämmerer, S., Klapproth, E., Wielockx, B. and El-Armouche, A. (2024), "Intertwined regulators: hypoxia pathway proteins, microRNAs, and phosphodiesterases in the control of steroidogenesis", *Pflugers Archiv European Journal of Physiology*, Springer Science and Business Media Deutschland GmbH, Vol. 476 No. 9, pp. 1383–1398, doi: 10.1007/S00424-024-02921-4.

Azam, S., Haque, M.E., Jakaria, M., Jo, S.H., Kim, I.S. and Choi, D.K. (2020), "G-protein-coupled receptors in CNS: A potential therapeutic target for intervention in neurodegenerative disorders and associated cognitive deficits", *Cells*, MDPI, Vol. 9 No. 2, doi: 10.3390/CELLS9020506.

Baillie, G.S., Tejeda, G.S. and Kelly, M.P. (2019), "Therapeutic targeting of 3′,5′-cyclic nucleotide phosphodiesterases: inhibition and beyond", *Nature Reviews Drug Discovery 2019 18:10*, Nature Publishing Group, Vol. 18 No. 10, pp. 770–796, doi: 10.1038/s41573-019-0033-4.

Barrett, P.Q., Guagliardo, N.A. and Bayliss, D.A. (2021), "Ion Channel Function and Electrical Excitability in the Zona Glomerulosa: A Network Perspective on Aldosterone Regulation",

Annual Review of Physiology, NIH Public Access, Vol. 83, p. 451, doi: 10.1146/ANNUREV-PHYSIOL-030220-113038.

Barrett, P.Q., Guagliardo, N.A., Klein, P.M., Hu, C., Breault, D.T. and Beenhakker, M.P. (2016), "Role of voltage-gated calcium channels in the regulation of aldosterone production from zona glomerulosa cells of the adrenal cortex", *Journal of Physiology*, Blackwell Publishing Ltd, 15 October, doi: 10.1113/JP271896.

Börner, S., Schwede, F., Schlipp, A., Berisha, F., Calebiro, D., Lohse, M.J. and Nikolaev, V.O. (2011), "FRET measurements of intracellular cAMP concentrations and cAMP analog permeability in intact cells", *Nature Protocols*, Nature Publishing Group, Vol. 6 No. 4, pp. 427–438, doi: 10.1038/nprot.2010.198.

Boulkroun, S., Samson-Couterie, B., Golib Dzib, J.F., Lefebvre, H., Louiset, E., Amar, L., Plouin, P.F., *et al.* (2010), "Adrenal Cortex Remodeling and Functional Zona Glomerulosa Hyperplasia in Primary Aldosteronism", *Hypertension*, Lippincott Williams & Wilkins, Vol. 56 No. 5, pp. 885–892, doi: 10.1161/HYPERTENSIONAHA.110.158543.

Buffolo, F., Tetti, M., Mulatero, P. and Monticone, S. (2022), "Aldosterone as a Mediator of Cardiovascular Damage", *Hypertension*, Lippincott Williams & WilkinsHagerstown, MD, Vol. 79 No. 9, pp. 1899–1911, doi: 10.1161/HYPERTENSIONAHA.122.17964.

Burnay, M.M., Vallotton, M.B., Capponi, A.M. and Rossier, M.F. (1998), "Angiotensin II potentiates adrenocorticotrophic hormone-induced cAMP formation in bovine adrenal glomerulosa cells through a capacitative calcium influx", *The Biochemical Journal*, Biochem J, Vol. 330 (Pt 1) No. Pt 1, pp. 21–27, doi: 10.1042/BJ3300021.

Butt, E., Nolte, C., Schulz, S., Beltman, J., Beavo, J.A., Jastorff, B. and Walter, U. (1992), "Analysis of the functional role of cGMP-dependent protein kinase in intact human platelets using a specific activator 8-para-chlorophenylthio-cGMP", *Biochemical Pharmacology*, Biochem Pharmacol, Vol. 43 No. 12, pp. 2591–2600, doi: 10.1016/0006-2952(92)90148-C.

"Calbryte™ 520 AM | AAT Bioquest". (n.d.). , available at: https://www.aatbio.com/products/calbryte-520-am (accessed 14 October 2025).

Carey, R.M. and Padia, S.H. (2018), "Physiology and Regulation of the Renin–Angiotensin–Aldosterone System", *Textbook of Nephro-Endocrinology*, Academic Press, pp. 1–25, doi: 10.1016/B978-0-12-803247-3.00001-5.

Chen, H.H., Wan, S.H., Iyer, S.R., Cannone, V., Sangaralingham, S.J., Nuetel, J. and Burnett, J.C. (2021), “First-in-Human Study of MANP: A Novel ANP (Atrial Natriuretic Peptide) Analog in Human Hypertension”, *Hypertension*, Lippincott Williams and Wilkins, Vol. 78 No. 6, pp. 1859–1867, doi: 10.1161/HYPERTENSIONAHA.121.17159.

Chen, J., Ding, Q., An, L. and Wang, H. (2022), “Ca2+-stimulated adenylyl cyclases as therapeutic targets for psychiatric and neurodevelopmental disorders”, *Frontiers in Pharmacology*, Frontiers Media S.A., Vol. 13, p. 949384, doi: 10.3389/FPHAR.2022.949384.

Chen, Y., Iyer, S.R., Nikolaev, V.O., Naro, F., Pellegrini, M., Cardarelli, S., Ma, X., *et al.* (2022), “MANP Activation Of The cGMP Inhibits Aldosterone Via PDE2 And CYP11B2 In H295R Cells And In Mice”, *Hypertension (Dallas, Tex. : 1979)*, Hypertension, Vol. 79 No. 8, pp. 1702–1712, doi: 10.1161/HYPERTENSIONAHA.121.18906.

“Competitive ELISA - Creative Diagnostics”. (n.d.). , available at: https://www.creative-diagnostics.com/blog/index.php/competitive-elisa/ (accessed 13 October 2025).

Cooper, D.M.F., Mons, N. and Mons, N. (1995), “Adenylyl cyclases and the interaction between calcium and cAMP signalling”, *Nature*, Vol. 374 No. 6521, pp. 421–424, doi: 10.1038/374421A0.

Corry, D.B. and Tuck, M.L. (1995), “Secondary Aldosteronism”, *Endocrinology and Metabolism Clinics of North America*, Elsevier, Vol. 24 No. 3, pp. 511–530, doi: 10.1016/S0889-8529(18)30029-X.

Currie, K.P.M. (2010), “Inhibition of Ca2+ Channels and Adrenal Catecholamine Release by G Protein Coupled Receptors”, *Cellular and Molecular Neurobiology*, Vol. 30 No. 8, p. 1201, doi: 10.1007/S10571-010-9596-7.

Dinh, H.A., Volkert, M., Secener, A.K., Scholl, U.I. and Stölting, G. (2024), “T- and L-Type Calcium Channels Maintain Calcium Oscillations in the Murine Zona Glomerulosa”, *Hypertension*, Lippincott Williams and Wilkins, Vol. 81 No. 4, pp. 811–822, doi: 10.1161/HYPERTENSIONAHA.123.21798/SUPPL_FILE/HYP_HYPE-2023-21798_SUPP4.PDF.

Dreher, L., Kylies, D., Danser, A.H.J. and Wenzel, U.O. (2025), “Incretin-Based Therapies: A Paradigm Shift in Blood Pressure Management?”, *Hypertension (Dallas, Tex. : 1979)*, Hypertension, Vol. 82 No. 7, pp. 1167–1174, doi: 10.1161/HYPERTENSIONAHA.125.25112.

"DRG Diagnostics GmbH | DRG Aldosterone ELISA". (n.d.). , available at: https://www.drg-diagnostics.de/105-1-DRG+Aldosterone+ELISA.html (accessed 13 October 2025).

Dutt, M., Wehrle, C.J. and Jialal, I. (2023), "Physiology, Adrenal Gland", *StatPearls*, StatPearls Publishing.

Eckel-Mahan, K.L. and Storm, D.R. (2007), "Second messengers: Calcium and cAMP signaling", *Learning and Memory: A Comprehensive Reference*, Elsevier, pp. 427–448, doi: 10.1016/B978-012370509-9.00021-8.

Ferguson, S.S.G., Downey, W.E., Colapietro, A.M., Barak, L.S., Ménard, L. and Caron, M.G. (1996), "Role of β-arrestin in mediating agonist-promoted G protein-coupled receptor internalization", *Science*, American Association for the Advancement of Science, Vol. 271 No. 5247, pp. 363–366, doi: 10.1126/SCIENCE.271.5247.363.

Fernandes-Rosa, F.L., Amar, L., Tissier, F., Bertherat, J., Meatchi, T., Zennaro, M.C. and Boulkroun, S. (2015), "Functional histopathological markers of aldosterone producing adenoma and somatic KCNJ5 mutations", *Molecular and Cellular Endocrinology*, Elsevier, Vol. 408, pp. 220–226, doi: 10.1016/J.MCE.2015.01.020.

Förster, T. (1948), "Zwischenmolekulare Energiewanderung und Fluoreszenz", *Annalen Der Physik*, John Wiley & Sons, Ltd, Vol. 437 No. 1–2, pp. 55–75, doi: 10.1002/ANDP.19484370105.

Förster, Th. and Forster, Th. (1960), "Transfer Mechanisms of Electronic Excitation Energy", *Radiation Research Supplement*, JSTOR, Vol. 2, p. 326, doi: 10.2307/3583604.

Francis, S.H., Busch, J.L. and Corbin, J.D. (2010), "cGMP-Dependent Protein Kinases and cGMP Phosphodiesterases in Nitric Oxide and cGMP Action", *Pharmacological Reviews*, Vol. 62 No. 3, p. 525, doi: 10.1124/PR.110.002907.

Funder, J.W. (2007), "Aldosterone and Mineralocorticoid Receptors", *Encyclopedia of Stress*, Elsevier Inc., pp. 132–135, doi: 10.1016/B978-012373947-6.00024-6.

Furman, B.L. (2007), "Aldosterone", *XPharm: The Comprehensive Pharmacology Reference*, Elsevier Inc., pp. 1–3, doi: 10.1016/B978-008055232-3.61182-1.

Gallo-Payet, N., Grazzini, E., Côté, M., Chouinard, L., Chorvátová, A., Bilodeau, L., Payet, M.D., *et al.* (1996), "Role of Ca2+ in the action of adrenocorticotropin in cultured human adrenal glomerulosa cells", *The Journal of Clinical Investigation*, J Clin Invest, Vol. 98 No. 2, pp. 460–466, doi: 10.1172/JCI118812.

Gambaryan, S., Butt, E., Marcus, K., Glazova, M., Palmetshofer, A., Guillon, G. and Smolenski, A. (2003), “cGMP-dependent protein kinase type II regulates basal level of aldosterone production by zona glomerulosa cells without increasing expression of the steroidogenic acute regulatory protein gene”, *The Journal of Biological Chemistry*, J Biol Chem, Vol. 278 No. 32, pp. 29640–29648, doi: 10.1074/JBC.M302143200.

Gambaryan, S., Butt, E., Tas, P., Smolenski, A., Allolio, B. and Walter, U. (2006), “Regulation of aldosterone production from zona glomerulosa cells by ANG II and cAMP: Evidence for PKA-independent activation of CaMK by cAMP”, *American Journal of Physiology - Endocrinology and Metabolism*, American Physiological Society, Vol. 290 No. 3, pp. 423–433, doi: 10.1152/AJPENDO.00128.2005/ASSET/IMAGES/LARGE/ZH10030644300009.JPEG.

Gambaryan, S., Kuhn, M. and Walter, U. (2005), “Inhibition of agonist-stimulated aldosterone production from adrenal zona glomerulosa cells by ANP is mediated by GC-A”, *BMC Pharmacology*, Springer Science and Business Media LLC, Vol. 5 No. S1, doi: 10.1186/1471-2210-5-s1-p19.

Gambaryan, S., Mohagaonkar, S. and Nikolaev, V.O. (2023), “Regulation of the renin-angiotensin-aldosterone system by cyclic nucleotides and phosphodiesterases”, *Frontiers in Endocrinology*, Front Endocrinol (Lausanne), Vol. 14, doi: 10.3389/FENDO.2023.1239492.

Gambaryan, S., Wagner, C., Smolenski, A., Walter, U., Poller, W., Haase, W., Kurtz, A., *et al.* (1998), “Endogenous or overexpressed cGMP-dependent protein kinases inhibit cAMP-dependent renin release from rat isolated perfused kidney, microdissected glomeruli, and isolated juxtaglomerular cells”, *Proceedings of the National Academy of Sciences of the United States of America*, Proc Natl Acad Sci U S A, Vol. 95 No. 15, pp. 9003–9008, doi: 10.1073/PNAS.95.15.9003.

Ganguly, A. (1992), “Atrial natriuretic peptide-induced inhibition of aldosterone secretion: a quest for mediator(s)”, *Https://Doi.Org/10.1152/Ajpendo.1992.263.2.E181*, American Physiological Society Bethesda, MD , Vol. 263 No. 2 26-2, doi: 10.1152/AJPENDO.1992.263.2.E181.

El Ghorayeb, N., Bourdeau, I. and Lacroix, A. (2016), “Role of ACTH and Other Hormones in the Regulation of Aldosterone Production in Primary Aldosteronism”, *Frontiers in Endocrinology*, Frontiers Media S.A., 27 June, doi: 10.3389/fendo.2016.00072.

Gomez-Sanchez, C.E., Qi, X., Velarde-Miranda, C., Plonczynski, M.W., Parker, C.R., Rainey, W., Satoh, F., *et al.* (2013), "Development of Monoclonal Antibodies against Human CYP11B1 and CYP11B2", *Molecular and Cellular Endocrinology*, Elsevier Ireland Ltd, Vol. 383 No. 0, p. 111, doi: 10.1016/J.MCE.2013.11.022.

Gostimskaya, I. (2022), "CRISPR–Cas9: A History of Its Discovery and Ethical Considerations of Its Use in Genome Editing", *Biochemistry (Moscow)*, Springer, Vol. 87 No. 8, pp. 777–788, doi: 10.1134/S0006297922080090/FIGURES/3.

Guagliardo, N.A., Klein, P.M., Gancayco, C.A., Lu, A., Leng, S., Makarem, R.R., Cho, C., *et al.* (2020), "Angiotensin II induces coordinated calcium bursts in aldosterone-producing adrenal rosettes", *Nature Communications 2020 11:1*, Nature Publishing Group, Vol. 11 No. 1, pp. 1–15, doi: 10.1038/s41467-020-15408-4.

Hanke, C.J., Drewett, J.G., Myers, C.R. and Campbell, W.B. (1998), "Nitric Oxide Inhibits Aldosterone Synthesis by a Guanylyl Cyclase-Independent Effect*This work was supported by grants from the NHLBI (HL-52159 and HL-54717).", *Endocrinology*, Oxford Academic, Vol. 139 No. 10, pp. 4053–4060, doi: 10.1210/ENDO.139.10.6252.

Hanke, C.J., O'Brien, T., Pritchard, K.A. and Campbell, W.B. (2000), "Inhibition of Adrenal Cell Aldosterone Synthesis by Endogenous Nitric Oxide Release", *Hypertension*, Lippincott Williams & Wilkins, Vol. 35 No. 1 II, pp. 324–328, doi: 10.1161/01.HYP.35.1.324.

Hedner, T., Hedner, J., Andersson, O. and Pettersson, A. (1987), *ANP-a Cardiac Hormone and a Putative Central Neurotransmitter*, *European Heart Journal*, Vol. 8.

van der Heijden, C.D.C.C., Bode, M., Riksen, N.P. and Wenzel, U.O. (2022), "The role of the mineralocorticoid receptor in immune cells in cardiovascular disease", *British Journal of Pharmacology*, Br J Pharmacol, Vol. 179 No. 13, pp. 3135–3151, doi: 10.1111/BPH.15782.

Hodgson-Zingman, D.M., Karst, M.L., Zingman, L. V., Heublein, D.M., Darbar, D., Herron, K.J., Ballew, J.D., *et al.* (2008), "Atrial Natriuretic Peptide Frameshift Mutation in Familial Atrial Fibrillation", *New England Journal of Medicine*, New England Journal of Medicine (NEJM/MMS), Vol. 359 No. 2, pp. 158–165, doi: 10.1056/NEJMOA0706300.

Ichiki, T., Usui, M., Kato, M., Funakoshi, Y., Ito, K., Egashira, K. and Takeshita, A. (1998), "Downregulation of angiotensin II type 1 receptor gene transcription by nitric oxide", *Hypertension (Dallas, Tex. : 1979)*, Hypertension, Vol. 31 No. 1 Pt 2, pp. 342–348, doi: 10.1161/01.HYP.31.1.342.

Jabłoństski, A. (1933), “Efficiency of anti-stokes fluorescence in dyes [6]”, *Nature*, Nature Publishing Group, Vol. 131 No. 3319, pp. 839–840, doi: 10.1038/131839B0;KWRD.

Jones-Tabah, J., Mohammad, H., Hadj-Youssef, S., Kim, L.E.H., Martin, R.D., Benaliouad, F., Tanny, J.C., *et al.* (2020), “Dopamine D1 receptor signalling in dyskinetic Parkinsonian rats revealed by fiber photometry using FRET-based biosensors”, *Scientific Reports*, Nature Research, Vol. 10 No. 1, pp. 1–18, doi: 10.1038/S41598-020-71121-8;SUBJMETA=154,1689,1718,2387,340,378,436,631;KWRD=DISEASES+OF+THE+NERVOUS+SYSTEM,MOLECULAR+NEUROSCIENCE,PARKINSON.

KAPLAN, N.M. and BARTER, F.C. (1962), “The effect of ACTH, renin, angiotensin II, and various precursors on biosynthesis of aldosterone by adrenal slices.”, *The Journal of Clinical Investigation*, Vol. 41, pp. 715–724, doi: 10.1172/JCI104530.

Kee, T.R., Khan, S.A., Neidhart, M.B., Masters, B.M., Zhao, V.K., Kim, Y.K., McGill Percy, K.C., *et al.* (2024), “The multifaceted functions of β-arrestins and their therapeutic potential in neurodegenerative diseases”, *Experimental and Molecular Medicine*, Springer Nature, Vol. 56 No. 1, pp. 129–141, doi: 10.1038/S12276-023-01144-4;SUBJMETA.

Kelly, M.P., Nikolaev, V.O., Gobejishvili, L., Lugnier, C., Hesslinger, C., Nickolaus, P., Kass, D.A., *et al.* (2025), “Cyclic nucleotide phosphodiesterases as drug targets”, *Pharmacological Reviews*, p. 100042, doi: 10.1016/j.pharmr.2025.100042.

Klaiber, M., Kruse, M., Völker, K., Schröter, J., Feil, R., Freichel, M., Gerling, A., *et al.* (2010), “Novel insights into the mechanisms mediating the local antihypertrophic effects of cardiac atrial natriuretic peptide: Role of cGMP-dependent protein kinase and RGS2”, *Basic Research in Cardiology*, Dr. Dietrich Steinkopff Verlag GmbH and Co. KG, Vol. 105 No. 5, pp. 583–595, doi: 10.1007/s00395-010-0098-z.

Kojima, I., Kojima, K. and Rasmussen, H. (1985), “Role of calcium and cAMP in the action of adrenocorticotropin on aldosterone secretion.”, *Journal of Biological Chemistry*, Elsevier, Vol. 260 No. 7, pp. 4248–4256, doi: 10.1016/S0021-9258(18)89257-2.

Kovanich, D., Low, T.Y. and Zaccolo, M. (2023), “Using the proteomics toolbox to resolve topology and dynamics 2 of compartmentalized cAMP signalling 3”, *Int. J. Mol. Sci*, Vol. 2023, doi: 10.3390/xxxxx.

Kraft, A.E., Bork, N.I., Subramanian, H., Pavlaki, N., Failla, A. V., Zobiak, B., Conti, M., *et al.* (2024), “Phosphodiesterases 4B and 4D Differentially Regulate cAMP Signaling in

Calcium Handling Microdomains of Mouse Hearts", *Cells*, Cells, Vol. 13 No. 6, doi: 10.3390/CELLS13060476.

Kreklau, E.L., Carlson, E.J. and Drewett, J.G. (1999), "Nitric oxide inhibits human aldosteronogenesis without guanylyl cyclase stimulation", *Molecular and Cellular Endocrinology*, Elsevier, Vol. 153 No. 1–2, pp. 103–111, doi: 10.1016/S0303-7207(99)00075-1.

Kuhn, M. (2016), "Molecular physiology of membrane guanylyl cyclase receptors", *Physiological Reviews*, American Physiological Society, Vol. 96 No. 2, pp. 751–804, doi: 10.1152/physrev.00022.2015.

Lander, E.S. (2016), "The Heroes of CRISPR", *Cell*, Cell Press, Vol. 164 No. 1–2, pp. 18–28, doi: 10.1016/j.cell.2015.12.041.

Lewis, A.E., Aesoy, R. and Bakke, M. (2016), "Role of EPAC in cAMP-Mediated Actions in Adrenocortical Cells", *Frontiers in Endocrinology*, Frontiers Media S.A., Vol. 7, p. 63, doi: 10.3389/FENDO.2016.00063.

Li, S., Dreher, L., Danser, A.H.J. and Wenzel, U.O. (2025), "Combination therapy in preclinical studies and clinical trials: Evidence, gaps and the path ahead", *British Journal of Pharmacology*, Br J Pharmacol, Vol. 182 No. 17, pp. 3971–3974, doi: 10.1111/BPH.70140.

Liao, J., Patel, D., Zhao, Q., Peng, R., Guo, H. and Diwu, Z. (2021), "A Novel Ca2+ Indicator for Long-term Tracking of Intracellular Calcium Flux", *BioTechniques*, Taylor & Francis, Vol. 70 No. 5, doi: 10.2144/BTN-2020-0161.

Lu, H., Cassis, L.A., Kooi, C.W.V. and Daugherty, A. (2016), "Structure and functions of angiotensinogen", *Hypertension Research 2016 39:7*, Nature Publishing Group, Vol. 39 No. 7, pp. 492–500, doi: 10.1038/hr.2016.17.

Lugnier, C. (2006), "Cyclic nucleotide phosphodiesterase (PDE) superfamily: A new target for the development of specific therapeutic agents", *Pharmacology & Therapeutics*, Pergamon, Vol. 109 No. 3, pp. 366–398, doi: 10.1016/J.PHARMTHERA.2005.07.003.

Lymperopoulos, A. (2018), "Arrestins in the Cardiovascular System: An Update", *Progress in Molecular Biology and Translational Science*, Vol. 159, Elsevier B.V., pp. 27–57, doi: 10.1016/bs.pmbts.2018.07.003.

Lymperopoulos, A. and Aukszi, B. (2017), "Angiotensin receptor blocker drugs and inhibition of adrenal beta-arrestin-1-dependent aldosterone production: Implications for heart failure

therapy", *World Journal of Cardiology*, Baishideng Publishing Group Inc., Vol. 9 No. 3, p. 200, doi: 10.4330/WJC.V9.I3.200.

Lymperopoulos, A., Borges, J.I. and Stoicovy, R.A. (2023), "RGS proteins and cardiovascular Angiotensin II Signaling: Novel opportunities for therapeutic targeting", *Biochemical Pharmacology*, Elsevier, Vol. 218, p. 115904, doi: 10.1016/J.BCP.2023.115904.

Lymperopoulos, A., Borges, J.I. and Suster, M.S. (2024), "Angiotensin II-dependent aldosterone production in the adrenal cortex", *Vitamins and Hormones*, Academic Press Inc., Vol. 124, pp. 393–404, doi: 10.1016/bs.vh.2023.05.001.

Lymperopoulos, A., Rengo, G., Zincarelli, C., Kim, J., Soltys, S. and Koch, W.J. (2009), "An adrenal β-arrestin 1-mediated signaling pathway underlies angiotensin II-induced aldosterone production in vitro and in vivo", *Proceedings of the National Academy of Sciences of the United States of America*, Vol. 106 No. 14, pp. 5825–5830, doi: 10.1073/PNAS.0811706106.

Lymperopoulos, A. and Stoicovy, R.A. (2024), "RGS Proteins in Sympathetic Nervous System Regulation: Focus on Adrenal RGS4", *Frontiers in Bioscience - Landmark*, IMR Press Limited, Vol. 29 No. 10, p. 355, doi: 10.31083/J.FBL2910355/2768-6698-29-10-355/FIG2.JPG.

MacFarland, R.T., Zelus, B.D. and Beavo, J.A. (1991), "High concentrations of a cGMP-stimulated phosphodiesterase mediate ANP-induced decreases in cAMP and steroidogenesis in adrenal glomerulosa cells.", *Journal of Biological Chemistry*, Elsevier, Vol. 266 No. 1, pp. 136–142, doi: 10.1016/S0021-9258(18)52413-3.

Mathieu, N.M., Nakagawa, P., Grobe, J.L. and Sigmund, C.D. (2023), "Insights into the Role of Angiotensin-II AT1 Receptor-dependent β-arrestin Signaling in Cardiovascular Disease", *Hypertension (Dallas, Tex. : 1979)*, Lippincott Williams and Wilkins, Vol. 81 No. 1, p. 6, doi: 10.1161/HYPERTENSIONAHA.123.19419.

Megha, R., Wehrle, C.J., Kashyap, S. and Leslie, S.W. (2022), "Anatomy, Abdomen and Pelvis: Adrenal Glands (Suprarenal Glands)", *StatPearls*, StatPearls Publishing.

MICHELS, A. and MICHELS, N. (2014), "Addison Disease: Early Detection and Treatment Principles", *American Family Physician*, Vol. 89 No. 7, pp. 563–568.

Mojica, F.J.M., Ferrer, C., Juez, G. and Rodríguez-Valera, F. (1995), "Long stretches of short tandem repeats are present in the largest replicons of the Archaea Haloferax mediterranei and Haloferax volcanii and could be involved in replicon partitioning", *Molecular*

Microbiology, Mol Microbiol, Vol. 17 No. 1, pp. 85–93, doi: 10.1111/J.1365-2958.1995.MMI_17010085.X.

Mories Álvarez, M.T. (2008), “Primary and secondary hyperaldosteronism. Apparent mineralocorticoid excess syndrome. Pseudohyperaldosteronism. Other mineralocorticoid excess syndrome”, *Medicine*, Ediciones Doyma, S.L., Vol. 10 No. 15, pp. 976–985, doi: 10.1016/s0211-3449(08)73190-4.

Mulrow, P.J. (1999), “Angiotensin II and aldosterone regulation”, *Regulatory Peptides*, Elsevier, Vol. 80 No. 1–2, pp. 27–32, doi: 10.1016/S0167-0115(99)00004-X.

Nakagawa, H., Oberwinkler, H., Nikolaev, V.O., Gaßner, B., Umbenhauer, S., Wagner, H., Saito, Y., *et al.* (2014), “Atrial natriuretic peptide locally counteracts the deleterious effects of cardiomyocyte mineralocorticoid receptor activation”, *Circulation: Heart Failure*, Lippincott Williams and Wilkins, Vol. 7 No. 5, pp. 814–821, doi: 10.1161/CIRCHEARTFAILURE.113.000885.

Natarajan, R., Lanting, L., Bai, W., Bravo, E.L. and Nadler, J. (1997), “The role of nitric oxide in the regulation of aldosterone synthesis by adrenal glomerulosa cells”, *Journal of Steroid Biochemistry and Molecular Biology*, J Steroid Biochem Mol Biol, Vol. 61 No. 1–2, pp. 47–53, doi: 10.1016/S0960-0760(97)00004-6.

Nieman, L.K. and Chanco Turner, M.L. (2006), “Addison’s disease”, *Clinics in Dermatology*, Elsevier, Vol. 24 No. 4, pp. 276–280, doi: 10.1016/J.CLINDERMATOL.2006.04.006.

Nikolaev, V.O., Gambaryan, S., Engelhardt, S., Walter, U. and Lohse, M.J. (2005), “Real-time monitoring of the PDE2 activity of live cells: hormone-stimulated cAMP hydrolysis is faster than hormone-stimulated cAMP synthesis”, *The Journal of Biological Chemistry*, J Biol Chem, Vol. 280 No. 3, pp. 1716–1719, doi: 10.1074/JBC.C400505200.

Parksook, W.W. and Williams, G.H. (2023), “Aldosterone and cardiovascular diseases”, *Cardiovascular Research*, Oxford Academic, Vol. 119 No. 1, pp. 28–44, doi: 10.1093/CVR/CVAC027.

Ramuz, M., Hasan, A., Gruscheski, L., Diakonov, I., Pavlaki, N., Nikolaev, V.O., Harding, S., *et al.* (2019), “A Software Tool for High-Throughput Real-Time Measurement of Intensity-Based Ratio-Metric FRET”, *Cells 2019, Vol. 8, Page 1541*, Multidisciplinary Digital Publishing Institute, Vol. 8 No. 12, p. 1541, doi: 10.3390/CELLS8121541.

Ran, F.A., Hsu, P.D., Wright, J., Agarwala, V., Scott, D.A. and Zhang, F. (2013), “Genome engineering using the CRISPR-Cas9 system”, *Nature Protocols*, Nature Publishing Group, Vol. 8 No. 11, pp. 2281–2308, doi: 10.1038/NPROT.2013.143;SUBJMETA.

Rassi-Cruz, M., Maria, A.G., Faucz, F.R., London, E., Vilela, L.A.P., Santana, L.S., Benedetti, A.F.F., *et al.* (2021), “Phosphodiesterase 2A and 3B variants are associated with primary aldosteronism”, *Endocrine-Related Cancer*, Endocr Relat Cancer, Vol. 28 No. 1, pp. 1–13, doi: 10.1530/ERC-20-0384.

Ren, L., Thai, P., Gopireddy, R.R., Timofeyev, V., Zhang, X.-D., Conti, A.C., Navedo, M.F., *et al.* (2021), “Differential Roles of Calcium-Activated and Calcium-Inhibited Adenylyl Cyclase Isoforms in the Regulation of SAN Automaticity”, *Biophysical Journal*, Elsevier BV, Vol. 120 No. 3, p. 334a, doi: 10.1016/j.bpj.2020.11.2095.

Romero, D.G., Plonczynski, M.W., Gomez-Sanchez, E.P., Yanes, L.L. and Gomez-Sanchez, C.E. (2006), “RGS2 Is Regulated by Angiotensin II and Functions as a Negative Feedback of Aldosterone Production in H295R Human Adrenocortical Cells”, *Endocrinology*, Oxford Academic, Vol. 147 No. 8, pp. 3889–3897, doi: 10.1210/EN.2005-1532.

Romero, D.G., Yanes, L.L., De Rodriguez, A.F., Plonczynski, M.W., Welsh, B.L., Reckelhoff, J.F., Gomez-Sanchez, E.P., *et al.* (2007), “Disabled-2 Is Expressed in Adrenal Zona Glomerulosa and Is Involved in Aldosterone Secretion”, *Endocrinology*, Oxford Academic, Vol. 148 No. 6, pp. 2644–2652, doi: 10.1210/EN.2006-1509.

Ros, O., Zagar, Y., Ribes, S., Baudet, S., Loulier, K., Couvet, S., Ladarre, D., *et al.* (2019), “SponGee: A Genetic Tool for Subcellular and Cell-Specific cGMP Manipulation”, *Cell Reports*, Cell Press, Vol. 27 No. 13, pp. 4003-4012.e6, doi: 10.1016/J.CELREP.2019.05.102.

Ruan, Y., Yu, Y., Wu, M., Jiang, Y., Qiu, Y. and Ruan, S. (2024), “The renin-angiotensin-aldosterone system: An old tree sprouts new shoots”, *Cellular Signalling*, Pergamon, Vol. 124, p. 111426, doi: 10.1016/J.CELLSIG.2024.111426.

Sainz, J.M., Reche, C., Rábano, M.A., Mondillo, C., Patrignani, Z.J., Macarulla, J.M., Pignataro, O.P., *et al.* (2004), “Effects of nitric oxide on aldosterone synthesis and nitric oxide synthase activity in glomerulosa cells from bovine adrenal gland”, *Endocrine*, Endocrine, Vol. 24 No. 1, pp. 61–71, doi: 10.1385/ENDO:24:1:061.

Sassone-Corsi, P. (2012), “The Cyclic AMP Pathway”, *Cold Spring Harbor Perspectives in Biology*, Vol. 4 No. 12, p. a011148, doi: 10.1101/CSHPERSPECT.A011148.

Schieblnger, R.J., Icem, D.C. and Brown, R.D. (1988), *EFFECT OF ATRIAL NATRIUAETIC PEPTIDE ON ACTH, DIBUTYRYL CAMP, ANGIOTENSIN II AND POTASS?.IIM-STIMULATED ALDOSTERONE SECRETION BY RAT ADRENAL GLOMERULGSA CELLS*, *Life Sciences*, Vol. 42.

Seccia, T.M., Caroccia, B., Gomez-Sanchez, E.P., Vanderriele, P.E., Gomez-Sanchez, C.E. and Rossi, G.P. (2017), "Review of Markers of Zona Glomerulosa and Aldosterone-Producing Adenoma Cells", *Hypertension*, Lippincott Williams and Wilkins, 1 November, doi: 10.1161/HYPERTENSIONAHA.117.09991.

Skryabin, E.B., De Jong, K.A., Subramanian, H., Bork, N.I., Froese, A., Skryabin, B. V. and Nikolaev, V.O. (2023), "CRISPR/Cas9 Knock-Out in Primary Neonatal and Adult Cardiomyocytes Reveals Distinct cAMP Dynamics Regulation by Various PDE2A and PDE3A Isoforms", *Cells*, MDPI, Vol. 12 No. 11, p. 1543, doi: 10.3390/CELLS12111543/S1.

Spießberger, B., Bernhard, D., Herrmann, S., Feil, S., Werner, C., Luppa, P.B. and Hofmann, F. (2009), "cGMP-dependent protein kinase II and aldosterone secretion", *The FEBS Journal*, John Wiley & Sons, Ltd, Vol. 276 No. 4, pp. 1007–1013, doi: 10.1111/J.1742-4658.2008.06839.X.

Sprenger, J.U. and Nikolaev, V.O. (2013), "Biophysical techniques for detection of cAMP and cGMP in living cells", *International Journal of Molecular Sciences*, MDPI AG, doi: 10.3390/ijms14048025.

Stowasser, M. and Gordon, R.D. (2004), "Primary aldosteronism - Careful investigation is essential and rewarding", *Molecular and Cellular Endocrinology*, Vol. 217 No. 1–2, pp. 33–39, doi: 10.1016/j.mce.2003.10.006.

Szabó, Á., Szöllősi, J. and Nagy, P. (2022), "Principles of Resonance Energy Transfer", *Current Protocols*, John Wiley & Sons, Ltd, Vol. 2 No. 12, p. e625, doi: 10.1002/CPZ1.625.

Taylor, S.S., Knighton, D.R., Zheng, J., Ten Eyck, L.F. and Sowadski, J.M. (1992), "Structural framework for the protein kinase family.", *Annual Review of Cell Biology*, Vol. 8, pp. 429–462, doi: 10.1146/ANNUREV.CB.08.110192.002241.

Thatcher, S.E. (2017), "A Brief Introduction into the Renin-Angiotensin-Aldosterone System: New and Old Techniques", *Methods in Molecular Biology (Clifton, N.J.)*, Methods Mol Biol, Vol. 1614, pp. 1–19, doi: 10.1007/978-1-4939-7030-8_1.

Verhovez, A., Williams, T.A., Monticone, S., Crudo, V., Burrello, J., Galmozzi, M., Covella, M., *et al.* (2012), *Genomic and Non-Genomic Effects of Aldosterone*, *Current Signal Transduction Therapy*, Vol. 7.

Villela, D., Leonhardt, J., Patel, N., Joseph, J., Kirsch, S., Hallberg, A., Unger, T., *et al.* (2015), "Angiotensin type 2 receptor (AT2R) and receptor Mas: a complex liaison", *Clinical Science (London, England : 1979)*, Clin Sci (Lond), Vol. 128 No. 4, pp. 227–234, doi: 10.1042/CS20130515.

Weir, M.R. and Bakris, G.L. (2008), "Combination Therapy With Renin-Angiotensin-Aldosterone Receptor Blockers for Hypertension: How Far Have We Come?", *The Journal of Clinical Hypertension*, Vol. 10 No. 2, p. 146, doi: 10.1111/J.1751-7176.2008.07439.X.

"Which Controls to Use in ELISA Assays? - Enzo". (n.d.). , available at: https://www.enzo.com/note/which-controls-to-use-in-elisa-assays/ (accessed 13 October 2025).

Whitlock, R., Leon, S.J., Manacsa, H., Askin, N., Rigatto, C., Fatoba, S.T., Farag, Y.M.K., *et al.* (2023), "The association between dual RAAS inhibition and risk of acute kidney injury and hyperkalemia in patients with diabetic kidney disease: a systematic review and meta-analysis", *Nephrology Dialysis Transplantation*, Oxford University Press, Vol. 38 No. 11, p. 2503, doi: 10.1093/NDT/GFAD101.

Wong, S.T., Athos, J., Figueroa, X.A., Pineda, V. V., Schaefer, M.L., Chavkin, C.C., Muglia, L.J., *et al.* (1999), "Calcium-stimulated adenylyl cyclase activity is critical for hippocampus-dependent long-term memory and late phase LTP", *Neuron*, Cell Press, Vol. 23 No. 4, pp. 787–798, doi: 10.1016/S0896-6273(01)80036-2.

Yang, T., He, M., Zhang, H., Barrett, P.Q. and Hu, C. (2020), "L- And T-type calcium channels control aldosterone production from human adrenals", *Journal of Endocrinology*, BioScientifica Ltd., Vol. 244 No. 1, pp. 237–247, doi: 10.1530/JOE-19-0259.

Young, W. and Bancos, I. (2023), "Primary Aldosteronism", *Adrenal Disorders*, Elsevier, pp. 25–27, doi: 10.1016/B978-0-323-79285-1.00102-3.

8 Acknowledgements

I would like to express my profound gratitude to my PhD supervisor Prof. Dr. Viacheslav Nikolaev for providing me with this excellent opportunity and to present this scientific work at various conferences. I am grateful for his guidance and support during my time at the Institute of Experimental cardiovascular research.

I would also like to thank members of my thesis committee, Prof. Dr. Friederike Cuello and Prof. Dr. med Ulrich Wenzel. for their valuable inputs and feedback.

I am grateful to Dr. Stepan Gambaryan and Prof. Dr. Michaela Kuhn for helpful discussions and critical experimental support.

I would like to express my regards to dear colleagues past and present and special thanks to Prof. Dr. Cristina Molina, Dr. Hariharan Subramanian, Dr. Nadja Beck, and Dr. Alexander Foese for their support, advice and useful discussions throughout the PhD thesis.

I thank Ms. Victoria Hänel for her technical expertise and assistance.

I am grateful to my parents, parents-in-laws and brother for believing in me and for their moral support, blessings and constant encouragement.

Special thanks to my husband, Shaurya, for his love, endless patience and motivating me throughout my studies.

Lastly I would like to thank my dear friends Upasana, Aaditya, Hardil and Rajan for all the laughter sessions and fun trips to keep me positive during PhD.

9 Curriculum vitae

“omitted for data protection reasons”

10 Eidesstattliche Erklärung

All the experiments were conducted by me.

PDE2A gRNAs were designed by Dr. Egor Skryabin.

11 Eidesstattliche Versicherung

Ich versichere ausdrücklich, dass ich die Arbeit selbständig und ohne fremde Hilfe, insbesondere ohne entgeltliche Hilfe von Vermittlungs- und Beratungsdiensten, verfasst, andere als die von mir angegebenen Quellen und Hilfsmittel nicht benutzt und die aus den benutzten Werken wörtlich oder inhaltlich entnommenen Stellen einzeln nach Ausgabe (Auflage und Jahr des Erscheinens), Band und Seite des benutzten Werkes kenntlich gemacht habe. Das gilt insbesondere auch für alle Informationen aus Internetquellen.

Soweit beim Verfassen der Dissertation KI-basierte Tools („Chatbots“) verwendet wurden, versichere ich ausdrücklich, den daraus generierten Anteil deutlich kenntlich gemacht zu haben. Die „Stellungnahme des Präsidiums der Deutschen Forschungsgemeinschaft (DFG) zum Einfluss generativer Modelle für die Text- und Bilderstellung auf die Wissenschaften und das Förderhandeln der DFG“ aus September 2023 wurde dabei beachtet.

Ferner versichere ich, dass ich die Dissertation bisher nicht einem Fachvertreter an einer anderen Hochschule zur Überprüfung vorgelegt oder mich anderweitig um Zulassung zur Promotion beworben habe.

Ich erkläre mich damit einverstanden, dass meine Dissertation vom Dekanat der Medizinischen Fakultät mit einer gängigen Software zur Erkennung von Plagiaten überprüft werden kann.

Unterschrift: .....